PONTIFICIA UNIVERSIDAD CATOLICA DE CHILE

SCHOOL OF ENGINEERING

ADVANCED MONITORING OF CONSTRUCTION SAFETY USING UAS AND POSITIONING TECHNOLOGIES

JHONATTAN GUILLERMO TERCERO MARTINEZ RIBON

Thesis submitted to the Office of Graduate Studies in partial fulfillment of the requirements for the Degree of Doctor in Engineering Sciences

Advisor:

LUIS F. ALARCÓN

Santiago de Chile, December 2020

PONTIFICIA UNIVERSIDAD CATOLICA DE CHILE
SCHOOL OF ENGINEERING

ADVANCED MONITORING OF CONSTRUCTION SAFETY USING UAS AND POSITIONING TECHNOLOGIES

JHONATTAN GUILLERMO TERCERO MARTINEZ RIBON

Members of the Committee:

LUIS F. ALARCÓN

CLAUDIO MOURGUES

MIGUEL TORRES

SALVADOR GARCIA

MASOUD GHEISARI

GUSTAVO LAGOS

Thesis submitted to the Office of Graduate Studies in partial fulfillment of the requirements for the Degree Doctor in Engineering Sciences

Santiago de Chile, December, 2020

To my parents Vivian and Zegundo, my sister Monica and my nephew Samuel, who supported and motivated me during all this time.

ACKNOWLEDGMENT

The author would like to acknowledge the University of Florida, Micro Aerial Projects L.L.C, and Triad Drones L.L.C for their assistance in the development of this research. On the other hand, I thank teacher Alarcon and Gheisari that during all this time supported and helped me to achieve this valuable milestone in my life.

TABLE OF CONTENT

LIST OF FIGURES

LIST OF TABLES

ABSTRACT

The high rate of fatalities in the construction domains is one of the major concerns of both practitioners and researchers. The dynamic nature of the construction, the limited number of safety managers, and the difficulty of visiting inaccessible, hard-to-reach, or unsafe locations are some of the factors that adversely affect the capability to properly and frequently monitoring construction sites and, therefore identify hazards. Unmanned aerial systems (UASs) and positioning technologies have become potential tools for enhancing safety-related tasks on construction jobsites. This study aims to develop, assess, and implement customized UASs and positioning sensors for enhancing safety monitoring and hazard identification process on construction jobsites. To accomplish this objective, an exploratory case study was carried out to compare safety managers' risk perception by using UAS-generated visual content and traditional-based visual content. Later, an ultrasound-based positioning system was developed and tested on real construction sites. The main objective of the system was to determine workers' position and calculating their hazard exposure time indoor, especially where UASs cannot operate for collecting visual data. Finally, two UASs were designed, developed, and tested using commercially available open-source software and hardware. The first UAS was equipped with a dual-frequency GNSS (L1/L2) and Post Processed Kinematic (PPK) technology in order to increase the quality and accuracy of the 3D visual representation of construction sites. A second UAS known as iSafeUAS was designed and tested to minimize the potential safety risks associated with UAS deployment for construction-safety related applications. The outcome of this research showed that the systematic use of both UASs and positioning technology on construction sites allows enhancing safety managers' risk perception, reduces time and efforts during the data collection process, increases the amount and quality of the information retrieved, and minimizes the risk associated with the data collection process.

Keywords: Unmanned Aerial Systems (UAS), Risk Perception, Positioning Sensor, Ultrasound-based Positioning System, Post Processed Kinematic (PPK), Construction Safety

RESUMEN

La alta tasa de fatalidad en la industria de la construcción es una de las principales preocupaciones entre los profesionales y los investigadores. La naturaleza dinámica de la construcción, el número limitado de gerentes de seguridad y la dificultad de visitar lugares inaccesibles, de difícil acceso o inseguros son algunos de los factores que afectan negativamente la capacidad de monitorear los sitios de construcción de manera frecuente y, por lo tanto, identificar riesgos. Sistemas aéreos no tripulados (UAS) y las tecnologías de posicionamiento han surgido como herramientas potenciales para mejorar las tareas relacionadas con la seguridad en los sitios de construcción. Este estudio tiene como objetivo el desarrollo, la evaluación y la implementación in situ de UASs personalizados y sensores de posicionamiento para mejorar el monitoreo de seguridad y el proceso de identificación de riesgos en los sitios de trabajo de construcción. Para lograr este objetivo, se realizó un estudio de caso exploratorio para evaluar la percepción de riesgo de los gerentes de seguridad mediante el uso de contenido visual generado por UASs y contenido visual tradicional. Más tarde, se desarrolló y probó un sistema de posicionamiento basado en ultrasonido en un sitio de construcción real. El objetivo principal del sistema fué determinar la posición de los trabajadores y calcular su tiempo de exposición al peligro en un ambiente interior, especialmente donde los UAS no pueden operar para recopilar datos visuales. Finalmente, se diseñaron, desarrollaron y probaron dos UASs utilizando software y hardware de código abierto disponibles comercialmente. El primer UAS fue equipado con un GNSS de doble frecuencia (L1/L2) y tecnología de post procesamiento cinemático (PPK), cuyo objetivo fue aumentar la calidad y precisión de la representación visual en 3D de los sitios de construcción. Un segundo UAS conocido como iSafeUAS fue diseñado y probado para minimizar los riesgos potenciales de seguridad asociados con el despliegue de UASs para aplicaciones relacionadas con la seguridad de la construcción. El resultado de esta investigación mostró que el uso sistemático de UASs y tecnologías de posicionamiento en los sitios de construcción permite mejorar la percepción de riesgo de los gerentes de seguridad, reduce el tiempo y los esfuerzos durante el proceso de

recopilación de datos, aumenta la cantidad y calidad de la información recuperada y minimiza el riesgo asociado con el proceso de recolección de datos.

Palabras claves: Unmanned Aerial Systems (UAS), Risk Perception, Positioning Technology, Ultrasound-based Positioning System, Post processed Kinematic (PPK), Construction Safety

.

CHAPTER 1: INTRODUCTION

1.1 Observed Problem and Research Opportunity

To prevent the occurrence of hazardous situations, safety monitoring and hazard identification play an essential role during the construction stages. Safety managers are usually in charge of jobsites safety monitoring and manage the safety program onsite (Perlman et al. 2014). Despite their relevance, these activities face several issues that difficult their proper implementation. (1) Limited risk perception capabilities of some safety managers that affect hazard identification and assessment (Zuluaga et al. 2016) (2) the difficulty of monitoring systematically and continuously the jobsites (OSHA 2014), (3) the large amount of manual effort required to gather information (Chi and Han 2013) , (4) the low quality and accuracy of jobsites visual representation for safety-related decision-making (Álvares et al. 2018), as well as (5) the fact that some specific locations are not safe or accessible for inspection (Zhou et al. 2018), are some of the factors that hinder the safety monitoring and hazard identification process on construction jobsites.

To overcome these factors, researchers and practitioners have been continually exploring other management plans and technologies that would ultimately enhance the safety monitoring and hazard identification process (Zhou et al. 2015). Mixed and virtual-reality (MR-VR) (Li et al. 2018), building information modeling (BIM) (Zhang et al. 2013), geographic information systems (GIS) (Kumar and Bansal 2019), reality capture and point cloud data (PCD) (Gheisari et al. 2018), eye-tracking (Yousefi 2015), positioning technologies (Cheng et al. 2011) and unmanned aerial systems (UASs) (Albeaino et al. 2019) are some examples of various types of technologies that have been applied for construction safety monitoring-related tasks. Several types of researches claimed that UASs and positioning technologies have become the most promising technologies to guarantee a safer environment by enabling frequent and accurate observation of construction sites conditions (Awolusi et al. 2018; Gheisari and Esmaeili 2019).

UAS is a generic aircraft designed to operate with no human pilot onboard (UVS International, 2018). For safety monitoring-related tasks, UASs can provide real-time information to safety managers concerning ongoing hazardous situations especially outdoors (Melo et al. 2017). In addition, UAS-derived visual content can be processed and transformed into a 3D visual jobsite representation through the Structure from Motion (SfM) technique, enabling safety managers to proactively identify hazardous conditions (Álvares et al. 2018). On the other hand, positioning technologies use sensor and communication tools to locate objects in indoor or outdoor environments, especially in locations where UASs cannot operate, providing a solution to implement safety measurements during construction stages (Cheng and Teizer 2013). Despite the multiples advantages of using such types of technologies on construction sites, no prior studies have implemented both technologies for a systematic and complete indoor and outdoor jobsite safety monitoring. Such integration could offer a complete and detailed visualization of jobsites, as well as reduce the time consuming and the risk associated with the data collection process.

This study aims to develop, assess, and implement UASs and positioning sensors for enhancing safety monitoring and hazard identification process on construction jobsites. In addition, this study fills the technical gaps associated with the proper deployment of these technologies on actives construction sites. The study intends to overcome the aforementioned challenges related to construction safety monitoring and hazard identification through four independent researches, which are described in the dissertation chapters. First, a case study was carried out to investigate how UAS technology and their generated visual contents might affect the current approach of conducting safety planning and monitoring (Chapter 2). According to the findings obtained in Chapter 2 with regards to the impossibility of UAS to fly indoors, an ultrasound-based positioning system was developed with the aim of automatizing workers tracking into these types of environments and overcome the challenges associated with the systematically and continuously

monitoring of jobsites (Chapter 3). Due to the necessity of safety managers to properly visualize the construction site for hazard identification purposes stated in Chapter 2, a customized UAS named MAPM4 intended for enhancing the accuracy and visual representation of the construction jobsites was developed and tested (Chapter 4). Finally and based on the findings obtained in Chapter 2 and 4 with respect to the barriers that face UAs for their deployment over construction sites, a customized UAS named iSafeUAS was developed, programmed, and tested with the aim of mitigating risks associated with the UASs deployment over actives jobsites (Chapter 5).

This research contributes to the body of knowledge in providing construction practitioners and researchers with a comprehensive overview and understanding of technical development, assessment, and onsite implementation of customized UASs and positioning technologies that ultimately enhance safety monitoring and hazard identification process on construction sites.

1.2 Research Background

1.2.1 Construction safety monitoring and hazard identification

The construction industry presents the highest rate of fatal accidents compared with other types of economic activities (Huang 2003). Although the injury rate has decreased since the 1990s, the accident rate in the construction remains 50% higher than other economics sectors (Consejo Económico y Social 2016). Many factors produce accidents and incidents in the construction industry. The high-stress work environment, conflicts of interest between construction stakeholders, a large number of independent contractors, limited learning rates and untrained workers, high employee turnover, and weather conditions are some construction safety-related challenges (Razuri et al. 2007). To avoid safety hazards occurrence, safety monitoring and hazard identification play a decisive role in construction projects. Safety monitoring and hazard identification consist of risk identification and decision-making about safety measures that need to be implemented

during construction stages (Perlman et al. 2014). However, systematic and continuous monitoring of construction sites is not easy to achieve due to the difficulty in visiting different areas simultaneously and the fact that some specific locations are not safe or accessible for inspection (US Bureau of Labor Statistics 2018). These factors limit the possibility that safety managers can directly and frequently observe the workplace (Zhou et al. 2018; Zuluaga et al. 2016). As a result of the manual jobsite monitoring, unsafe acts, and conditions can only be detected after an accident has occurred (Namian et al. 2016). To overcome these challenges, proactive monitoring of the jobsite to collect reliable data for decision-making is essential (Namian et al. 2016). Another factor that directly affects the hazard identification and safety monitoring is the safety manager's risk perception capabilities (Zuluaga et al. 2016). Such capabilities are based on individual skills in anticipating accidents and incidents before they happen. These skills are affected by aspects such as the years of technical experience of safety managers, professional training, and the tools and visual contents used for the safety planning (schedules, 2D plans, imagery, and videos) (Sacks et al. 2013; Zhang et al. 2015).

According to a study conducted by Zhou et al. (2015), one of the gaps in construction safety monitoring and hazard identification is the lack of innovative technologies application. For that reason, there has been significant growth in the number of studies concerning the implementation of innovative technologies applied for construction safety. However, most of those innovative technologies remain in the academic research domain and have still not been successfully implemented in the construction industry (Zhou et al. 2015). Some examples of technologies that researchers have applied to improve the construction safety are mixed and virtual-reality (MR-VR) (Li et al. 2018), building information modeling (BIM) (Zhang et al. 2013), geographic information systems (GIS) (Kumar and Bansal 2019), reality capture and point cloud data (PCD) (Gheisari et al. 2018), eye-tracking (Yousefi 2015), positioning technologies (Cheng et al. 2011) and unmanned aerial systems (UASs) (Albeaino et al. 2019).

1.2.2 UASs for construction safety-related applications

An unmanned aerial system (UAS) is a generic aircraft that does not carry a human operator. UAS additionally includes a ground-based controller and a system of communications. Nowadays, the use of these vehicles has multiplied and extended to various types of applications in the construction domain such as safety monitoring and hazard identification (Irizarry et al. 2012), topography creation (Mancini et al. 2013), progress monitoring (Álvares et al. 2018), as-built data collection (Alizadehsalehi et al., 2018), monitoring of ongoing operations (Ham et al., 2016) and monitoring the current status of civil infrastructure (Álvares and Costa 2018).

For safety monitoring and hazard identification purposes, UASs can provide real-time jobsite information to safety managers, who subsequently could provide immediate feedback in case of a hazardous situation occurrence (Gheisari et al. 2014). Besides, UASs can retrieve jobsite safety violation data in real-time that might have a negative impact on workers' health (Zhou et al. 2018). During ongoing construction activities, UASs could be utilized for visual monitoring of various safety aspects such as lack of guardrails, deficient safety signs, inadequate scaffolding, slab openings, workers without proper personal protective equipment (PPE), or the existence of hazardous wastes (Alizadehsalehi et al. 2018). Additionally, UASs can be deployed to send images and videos of the jobsite to safety managers faster and more efficiently than other types of methods (Gheisari et al. 2014). This visual information could be transformed into 3D models and then used to calculate construction progress levels or perform safety planning-related activities (Howard et al. 2018). Additionally, the use of UAS for construction safety monitoring can reduce the time and cost associated with the data collection process (Tezel and Aziz 2017). The aforementioned UAS-related applications and advantages have captured the attention of researchers and professionals, especially for construction safety applications.

Several studies have investigated the use of UASs for safety monitoring and hazard identification purposes. Irizarry et al. (2012) conducted a usability investigation followed by a heuristic evaluation to use a camera-equipped quadcopter to communicate the real-time feed of the jobsite to the safety managers. Later, Gheisari et al. (2014) used a similar quadcopter platform to provide real-time jobsite information to the safety manager who could then provide immediate feedback to construction workers onsite in case of a hazardous situation. Later on, Irizarry and Costa (2016) conducted an exploratory study to determine the potential applications of UAS-acquired visual images for construction management tasks. Based on a database comprising UAS images and videos of several jobsites, the authors concluded that UAS adoption could be useful for several construction-related applications, including jobsite logistics, progress monitoring, safety condition evaluation, and quality inspection. Kim et al. (2016) developed a survey to identify the users' requirements and the challenges of integrating UASs into construction safety inspection tasks, as well as the factors that affect this technology's performance in this context. The authors recommended using high-quality UAS visualizations and user-friendly interfaces for better implementation. In another study, de Melo et al. (2017) used a case study approach to explore the UAS capability of collecting visual data form the jobsite and assess the compliance with safety regulations. Gheisari et al. (2018) developed and tested an algorithm that relied upon UAS images to automate and ultimately simplify the safety inspection process by making it less time- and labor-intensive. The main objective of the algorithm was to detect openings and guardrails that did not meet the Occupational Safety and Health Administration (OSHA) standards. De Melo and Costa (2019) created a framework to better understand how UAS technology and resilience engineering can be integrated for safety planning and control purposes. After presenting a safety monitoring protocol using UASs, the authors advocated the use of this technology for safety monitoring tasks and concluded that the aerial platforms are capable of enhancing workers' awareness through safety training and providing visual content for safety managers to assist them in the decision-making process. Gheisari and Esmaeili (2019) carried out a survey study on UAS applications for construction safety and

addressed the challenges of using UAS as a construction safety monitoring and control tool on the jobsites. Finally, Melo and Costa (2020) developed a UAS-based safety monitoring protocol to evaluate the potential of using UAS technology for construction safety monitoring applications. More specifically, the authors assessed the compliance of ongoing construction activities with the established safety standards using UAS imagery and a safety checklist. The results showed that UASs could help safety managers in the decision-making process by providing valuable jobsite information as well as improving workers' awareness through safety training.

Despite the advantages of using UAS in the construction domain, several factors were stated in the literature that could affect the usage of UAS technology for safety monitoring and hazard identification on construction jobsites. First, the flight regulation regulations prohibit UAS operations over active sites and populated areas or over people who are not directly involved in the flight mission (US Department of Transportation 2016). The quality of the visual sensors installed on the commercially available platforms that are commonly used in the construction industry is not yet sufficient to capture jobsite visual assets from farther distances. Therefore, UAS flight pilots tend to compromise between the flight regulations, which prevent UAS operation near active sites from one side, and the quality of the UAS-acquired images and videos that would help identify onsite hazardous situations. Those limitations, together with the other ones indicated in the literature, including the high potentials for hazardous situations such as struck-by accidents or worker distraction due to the UAS flights on the jobsites and near or over people; technical limitations (e.g., signal interferences due to the presence of several obstacles and short battery life); the challenging environmental or weather conditions (e.g., snow, rain, wind, sunlight), the difficulty of flying UAS in indoor environments, as well as jobsite obstacles are considered as some of the critical barriers affecting the full usage of UASs for construction safety monitoring and hazard identifications.

1.2.3 Using UAS to generate 3D visual representations of jobsites

The use of UASs, as aerial photogrammetry technology, offers several advantages of accomplishing tasks in an accurate, timely, flexible, and cost-efficient manner (Remondino et al. 2012). As a platform for data collection, UASs can be equipped with several onboard sensors to accomplish their intended tasks. For that reason, UASs have been applied for a wide range of applications from landslide monitoring (Niethammer et al. 2012) or topography mapping in coastal environments (Mancini et al. 2013) to agricultural irrigation precision (Ezenne et al. 2019) or natural disaster assessment (Iqbal et al. 2015). UAS-mediated techniques have also significantly influenced the architecture, engineering, construction, and operation (AECO) domain (Albeaino et al. 2019). Construction industry in particular, incorporated the use of UASs for various types of applications such as site surveying and mapping (Tomaštík et al. 2019), surveying earthwork projects (Hugenholtz et al. 2015; Siebert and Teizer 2014), progress monitoring (Álvares et al. 2018), construction safety management (Gheisari et al. 2018), material handling (Khosiawan et al. 2018), structure and infrastructure inspection (Morgenthal and Hallermann 2014), building inspection (Serrat et al. 2019), and post-disaster building assessment (Ghaffarian and Kerle 2019). The majority of these applications rely mainly on UAS-captured visual contents to accomplish their tasks. While using raw images and videos seem sufficient for some of these applications, others require the use of photogrammetric techniques to process the data and 3D visual representation. A study conducted by Álvares et al. (2018) claimed that the use of UAS-derived images together with the SfM technique could offer a fast-generated comprehensive 3D view of the jobsite that can be observed from different perspectives. At the same time, Mendes et al (2018) and Gheisari et al (2018) created SfM processes and used photos captured by UASs to automate the safety inspection process and optimize time and labor for automatic recognition of guardrails onsite. Martinez et al. (2020) assessed the safety managers' risk perception by comparing UAS-derived visual content (videos, images, and 3D model) and traditional method-derived imagery and videos.

Despite the importance of UASs as a tool for data collection, many factors affect the accuracy and quality of the 3D visual representation of jobsites generated by UAS-derived images and SfM technique. Some of these factors include UAS flight parameters (i.e. flight altitude and angle, percentage of image overlap), environmental effects, ionospheric and tropospheric effects, camera calibration and quality, as well as the adopted georeferencing techniques such as the ground control points (GCPs), real-time kinematic (RTK), and the post-processing kinematic (PPK) (Bolkas 2019; Fazeli et al. 2016). I addition, most of the UASs used in the construction domain are typically equipped with a single-frequency GNSS (L1) device, which limits the absolute attainable positioning accuracy to values ranging between 1 and 25 m. This fact limits the possibility of obtaining accurate point cloud data and their derived 3D models used commonly for decision-making and safety management. Since several construction-related applications require better accuracy and visual quality of the jobsites 3D models, the most commonly used strategy to enhance the accuracy is identifying key features in the point cloud that can be matched to known real-world coordinates via ground control points (GCP) (Bolkas 2019). GCPs are defined as ground targets of known locations that are placed strategically on the earth's surface for georeferencing purposes. However, this traditional georeferencing technique that relies on GCPs is a time-consuming and labor-intensive process (Forlani et al. 2018). Other techniques such as Real-Time Kinematic (RTK) and Post Processing Kinematic and (PPK), which rely on single-frequency GNSS (L1) or double-frequency GNSS (L1/L2) receivers, were found to achieve a positioning accuracy of about 1 to 30 centimeters with no GCPs required, which substantially saves time and cost (Fazeli et al. 2016; Luo et al. 2016). The RTK method simultaneously corrects the positioning coordinates during the flight, whereas PPK technology applies the corrections in the post-flight setting (Tomaštík et al. 2019). In terms of receivers, single-frequency GNSS (L1) is unable to account for the ionospheric and tropospheric effects, encouraging the use of the more robust dual-frequency GNSS (L1/L2) receivers for higher point cloud accuracy (Deng et al. 2011; Fazeli et al. 2016). The aforementioned UAS-related challenges open the necessity of developing and testing different techniques for enhancing the 3D visual

quality and accuracy of the jobsite by implementing UAS with dual-frequency GNSS (L1/L2) and coordinates correction capabilities.

1.2.4 Positioning sensors for safety-related applications

The dynamic nature of construction sites and the presence of multiple teams working onsite are well-known qualities of a typical construction project. Relevant site information such as the location of construction resources (personnel, equipment, and materials) is currently mostly manually monitored and recorded (Cheng and Teizer 2013). Since most of the construction activities are carried out indoors and technologies such as UAS cannot operate in these types of environments, practitioners and researchers are constantly looking for new technologies that ultimately enhance the data collection process intended for construction safety applications. According to a study conducted by Kim et al. (2016), approximately 20% of the accidents in the construction domain occur while workers are moving through the workplace. This aspect highlights the necessity of determining workers' location during their working hours in order to avoid accidents. For this specific scenario, technologies such as positioning sensor could be useful to guarantee a safer jobsite environment and avoid hazardous situation occurrence.

To reduce the efforts associated with jobsite data collection, position technologies offers a faster and reliable manner of retrieving real-time information. A large number of positioning technologies have robust applications for construction safety. Awolusi et al. (2018) stated that the use of positioning technologies would provide a solution to carry out safety measurements proactively during the construction stages. The accurate positioning capabilities of different positioning sensor-based technologies is one of the most important aspects to perform various safety management-related tasks. The accuracy is described as the statistical variation among the estimate or measurement of a quantity and the true value of that quantity. Positioning technologies can be applied for (1) tracking components or materials (Ergen and Akinci 2007), (2) material inventory management (Lu et al. 2011), (3) workers location tracking (Costin et al. 2015) and, (4) safety monitoring (Lin et al.

2013). The most popular positioning technologies include (1) Radio Frequency Identification (RFID), (2) Global Positioning System (GPS), (3) Ultra-wide Band (UWB), (4) Bluetooth of Low Energy (BLE), and (5) Ultrasound technology (UST) (Awolusi et al. 2018). Despite several advantages of using positioning technologies for safety-related applications, limitations such as (1) short-communication range, (2) weather conditions, (3) low-positioning accuracy, (4) high-implementation cost (5) need for a clear line of sight, hindered its full implementation in construction sites. The challenges before mentioned open the opportunity of developing an accurate and reliable positioning system that allows overcoming most of these gaps and ultimately reduce the technical challenges associated with the use of these systems for construction safety monitoring and hazard identifications.

1.3 Hypothesis

This research state the following intuition:

The implementation of UASs and positioning technologies for advanced construction safety monitoring and hazard identification enable safety managers to enhance their risk perception capabilities, improve the systematic and continuous monitoring of jobsites, reduces the manual effort required to collect information, improve the quality and accuracy of visual representation of jobsites and mitigate the risks associated with the data collection process.

1.4 Point of Departure

The main goal of this study is to implement UASs and positioning technologies for enhancing safety monitoring and hazard identification process on construction jobsites. As previously discussed, construction safety monitoring and hazard identification present several challenges that affect their proper implementation. First, safety monitoring relies on manual efforts that are time-consuming to properly inspect jobsites. Besides, jobsites

complexity and their continuously changing environment difficult the systematic and constantly monitoring, especially for some specific locations that are inaccessible, hard-to-reach, or unsafe for safety managers to inspect. Finally, limited capabilities of risk perception of some safety managers affect the hazard identification and assessment. It generally occurs due to the type of visual asset used for this specific task. Therefore, the accuracy of safety managers' hazard recognition heavily relies on the amount and quality of visual information that they use for safety-related decision making.

It is envisioned that the use of UASs and positioning technologies would overcome most of the aforementioned challenges that affect construction safety monitoring and hazard identification. Despite this fact, no previous study stated in the literature has investigated how UASs technology and their generated aerial visual contents might affect the current approach of conducting safety planning and monitoring in construction sites. In addition, UASs deployment over jobsites might represent a potential threat for workers, especially when flying over actives jobsites, limiting the ability of safety managers to properly inspect the construction sites. On the other hand, the visual quality and accuracy of the UAS-derived 3D jobsite representation is affected by factors such as UAS flight parameters, environmental effects, ionospheric and tropospheric effects, camera calibration and quality, as well as the adopted georeferencing techniques such as the ground control points (GCPs), real-time kinematic (RTK), and the post-processing kinematic (PPK). These factors together with the lack of robust GNSS devices such as dual-frequency GNSS (L1/L2) in many commercially available UASs, limit the possibility of obtaining accurate and detailed visual assets needed for construction safety monitoring and hazard identification purposes . Finally, the difficulty of flying UAS at indoor environments and the fact of many construction activities are carried out in these types of scenarios, open the need of implementing other types of technologies that allows a constant and reliable workers' monitoring. Nevertheless, position technologies' accuracy and reliability could be affected by technical, and environmental factors that ultimately impact their performance and deployment for safety-monitoring related tasks. Short-communication range, weather

conditions, low-positioning accuracy, high-implementation cost, need for a clear line of sight, are some challenges that affect positioning technologies implementation. The aforementioned limitations offer construction practitioners and researched the necessity of designing, developing, and testing new UASs and positioning technology that can overcome most of these barriers.

This research contributes to the body of knowledge in providing construction practitioners and researchers with a comprehensive overview and understanding of technical development, assessment, and onsite implementation of customized UASs and positioning sensors for enhancing safety monitoring and hazard identification process on construction jobsites. The outcome of this study could benefit the Architecture, Engineering, and Construction (AEC) industry and the academic field in understanding how the technical development, assessment, and onsite implementation of customized UASs and positioning technology would enhance the construction safety monitoring and hazard identification.

1.5 Research Questions

As a result of the problems observed, the intuitions and the points of departure, the following research questions have been stated:

- Question 1. (Q1) How safety managers' risk perception capabilities could be enhanced by the use of UAS-generated visual content?
- Question 2. (Q2) How to achieve a systematic and continuous safety monitoring of jobsites through positioning technologies?
- Question 3. (Q3) How to reduce the manual effort required to collect information on jobsites, improves the quality and accuracy of its visual representation, and mitigate the risk associated with data collection using UASs?

1.6 Research Methodology

This dissertation aids to enhance the current process of hazard identification and safety monitoring on construction sites through the implementation of UASs and positioning technologies. The dissertation was built to answer the research questions that address the problem noticed and the stated hypothesis. The overall methodology used for this research is shown in Figure 1. The proposed methodology displays all the research questions and, their responses through different research tasks. A case study approach was adopted to respond to each research question. The case study approach consists of a detailed observation of a single individual, group, or event. The use of this methodological approach allows capturing the complexity of a single case and potentially generalize the results to other conditions or circumstances (Yin 2009)

Question 1 was addressed using an exploratory case study approach conducted in a high-rise building construction project located in Santiago de Chile. The case study focused on how UASs and their generated visual asset might affect the current method of conducting safety monitoring and hazard identification. To achieve this goal, the current safety monitoring and hazard identification process was studied and documented. Then, an investigation of how UASs and their generated visual assets could be integrated into the current safety monitoring and hazard identification process was performed. Finally, a risk perception assessment was carried out to assess how visual data generated by the UAS would be useful for safety managers and might affect their risk perception and identification of specific hazardous conditions. The research methods implemented were document review, interviews, process mapping, and visits to the field.

Question 2 was addressed also with a case study approach conducted at an indoor facility located in Colombia. The study proposed the development and assessment of an ultrasound-based positioning system that ultimately enhances the accuracy and reliability for determining workers' locations. The use of such technology allowed safety managers to

continuously determine workers' hazard exposure time during their workday and therefore systematically monitoring the jobsite conditions. To performance this study , two stages were carried out: (1) the ultrasound-based positioning system development and (2) the ultrasound-based positioning system performance assessment on a real construction site. Literature review, visits to the field for data collection, and the Root Mean Square Error (RMSE) analyses-based statistical approach were the methods used for this specific study.

Question 3 was answered by two independents case studies. The first case study was performed in Gainesville, United States. During this study, a customized UAS known as MAPM4 was designed, developed, programmed, and tested using commercially available open-source hardware and software. The study aimed to improve the visual quality and accuracy of the UAS-derived 3D jobsite representation for construction safety purposes. The steps carried out during this study were: (1) UAS design and development, (2) UAS programming, (3) UAS assessment on the field. The latter step was conducted by comparing the customized UAS accuracy with a commercially available UAS. Visits to the field to collect the data and statistical analysis were some of the research methods used during this study. The second case study was carried out in Safety Harbor, United States. A second customized UAS named iSafeUAS that incorporated a super optical RGB camera sensor, and a recovery system was designed, developed, and tested. The iSafeUAS was deployed on a real construction environment to evaluate its potential for safety monitoring and inspection applications. This study aimed to develop a UAS capable of reducing the manual effort required to collect information and reduces the risk associated with data collection. A Three-steps process was implemented in this study: (1) UAS design, development, and programming, (2) technical performance assessment, and (3) UAS application for safety monitoring of a real jobsite. The research methods used for this activity were literature review, visits to the field, and safety managers interviews.

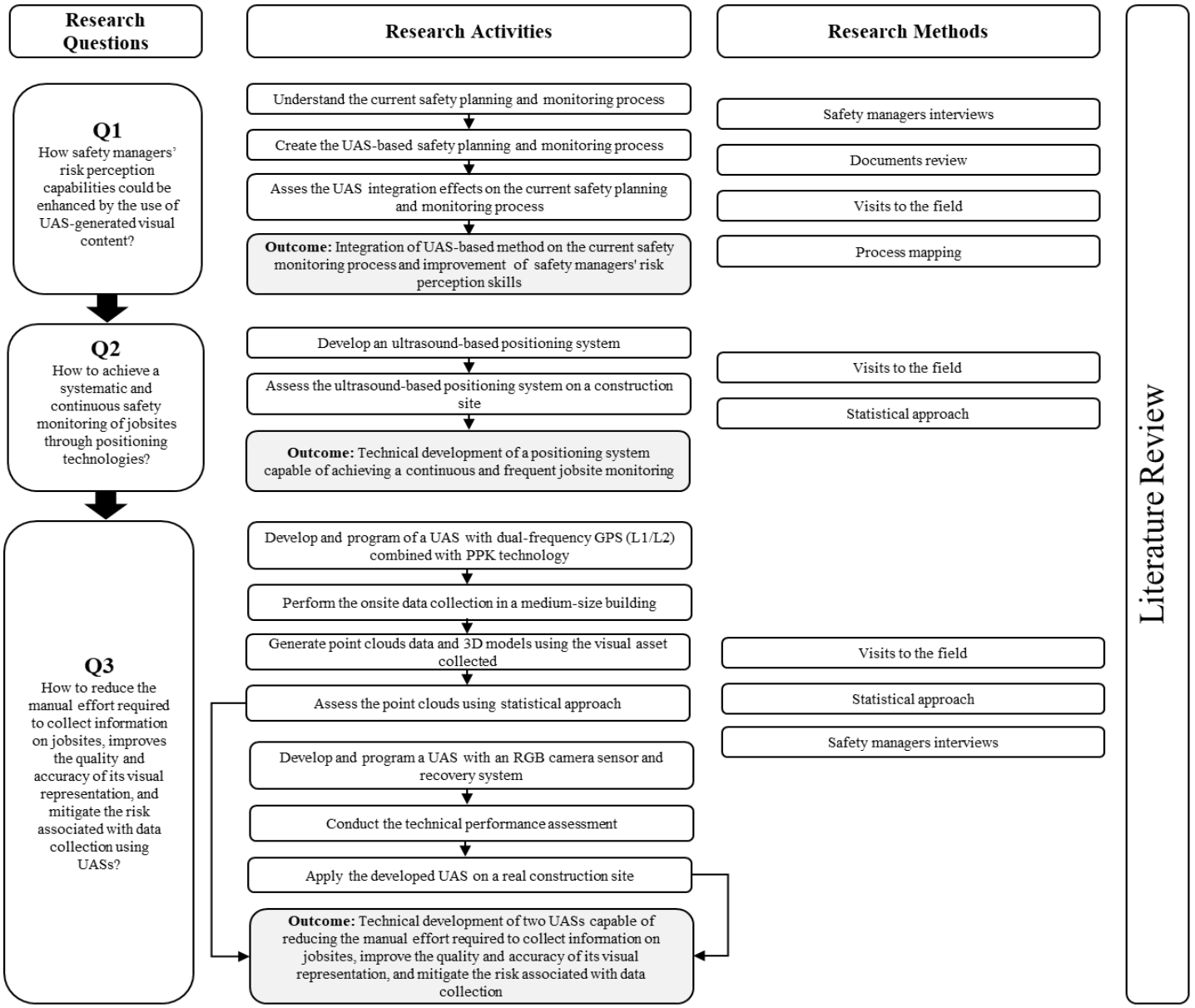

Figure 1. Overall research methodology

1.7 Dissertation organization

The dissertation is organized in a four-paper format. Each paper addressed one of the three research questions. Figure 2 presents the dissertation organization:

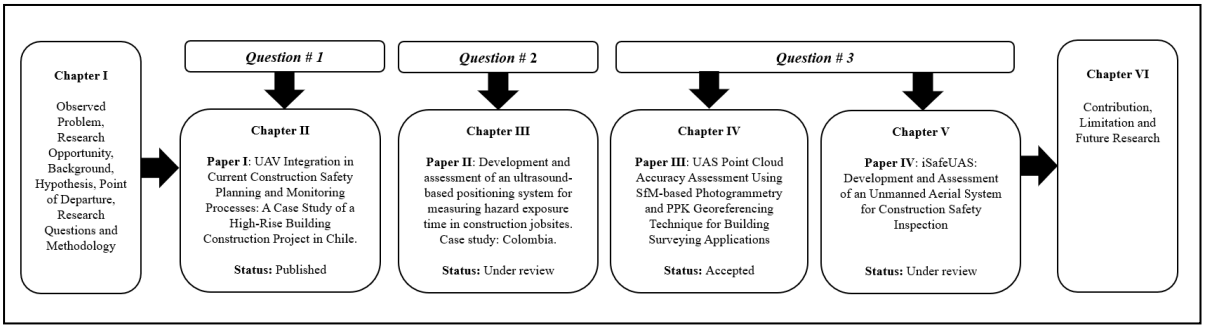

Figure 2. Dissertation organization

Chapter 1 introduce the observed problem, research opportunity, background, hypothesis, point of departure, research questions as well as the methodology.

Chapter 2 (Paper 1) is a manuscript accepted in the ***Journal of Management in Engineering***. The manuscript was published online on March 9, 2020. The manuscript investigates how UAS technology and their generated aerial visual contents might affect the current approach of conducting safety planning and monitoring in a high-rise building construction site in Chile with a limited number of safety managers. The outcomes of this exploratory case study provide initial data and insights on how UASs might be adopted within the current approach of conducting safety planning and monitoring on high-rise building construction sites in Chile.

Chapter 3 (Paper 2) is a manuscript submitted in the ***Journal of Computing in Civil Engineering***. The manuscript introduces the development and assessment of an ultrasound-based positioning system that ultimately enhances the accuracy and reliability of determining workers' locations at active jobsites. The outcomes of this study would benefit construction safety managers and researchers by helping them to understand the

integration of the ultrasound-based positioning system in the current safety monitoring process and recognize the requirements and challenges for such incorporation in safety management-related tasks.

Chapter 4 (Paper 3) is a manuscript accepted in the ***Journal of Computing in Civil Engineering***. The manuscript was accepted on July 15, 2020. This study aims to evaluate the effect of the single-frequency GNSS (L1) and dual-frequency GNSS (L1/L2) together with post-processing kinematic (PPK) technique on the accuracy and visual quality of the UAS-derived 3D jobsite representation. The outcomes of the study would help construction practitioners and researchers to better integrate UAS technology for jobsites 3D model generation and accuracy improvement needed for construction safety purposes

Chapter 5 (Paper 4) is a manuscript submitted for publication in the journal ***Automation in Construction***. This study aims to explore the methods in UAS technical design, development, and assessment that would improve the use of UASs as safety inspection and monitoring tools by minimizing the safety risks associated with their full deployment on construction jobsites. The outcomes of this study aid construction practitioners and researchers in providing a comprehensive overview and understanding of the technical design, development, assessment, and onsite implementation of a customized UAS intended for safety inspection applications.

Chapter 6 gathers a research summary, the research contributions, and limitations, and exposes future lines of research.

Additionally, three conferences papers were developed:

- Using UAV-generated Visual Contents to Assess the Risk Perception of Safety Managers on a Construction Site. This paper was presented at 36th CIB W78 (2019) Conference: ICT in Design, Construction, and Management in Architecture,

Engineering, Construction, and Operations, which was carried out in Northumbria University at Newcastle, United Kingdom.

- Improving Point Cloud Accuracy Using a Customized Unmanned Aerial Vehicle with Dual-Frequency GPS and Post-Processing Kinematic Technology. This paper will be presented in the 2021 European Conference on Computing in Construction and Summer School.

- Development of An Unmanned Aerial System for Construction Safety Inspections. This paper will be presented in the 2021 European Conference on Computing in Construction and Summer School.

1.8 References

Alizadehsalehi, S., Yitmen, I., Celik, T., and Arditi, D. (2018). "The effectiveness of an integrated BIM/UAV model in managing safety on construction sites." *International Journal of Occupational Safety and Ergonomics*, Taylor & Francis, 0(0), 1–16.

Álvares, J. S., and Costa, D. B. (2018). "Literature Review on Visual Construction Progress Monitoring Using Unmanned Aerial Vehicles." *26th Annual Conference of the International Group for Lean Construction*, 669–680.

Álvares, J. S., Costa, D. B., and Melo, R. R. S. de. (2018). "Exploratory study of using unmanned aerial system imagery for construction site 3D mapping." *Construction Innovation*, 18(3), 301–320.

Awolusi, I., Marks, E., Hallowell, M., Ibukun Awolusi, Eric Marks, and Matthew Hallowell. (2018). "Automation in Construction Wearable technology for personalized construction safety monitoring and trending : Review of applicable devices." *Automation in Construction*, Elsevier, 85(July 2016), 96–106.

Cheng, T., and Teizer, J. (2013). "Real-time resource location data collection and visualization technology for construction safety and activity monitoring applications."

Automation in Construction, Elsevier B.V., 34, 3–15.

Chi, S., and Han, S. (2013). "Analyses of systems theory for construction accident prevention with specific reference to OSHA accident reports." *International Journal of Project Management*, Elsevier Ltd and APM IPMA, 31(7), 1027–1041.

Consejo Económico y Social. (2016). *El papel del sector de la construcción en el crecimiento económico: competitividad, cohesión y calidad de vida*. *Informes*.

Costin, A. M., Teizer, J., and Schoner, B. (2015). "RFID and BIM-enabled worker location tracking to support real-time building protocol control and data visualization." *Journal of Information Technology in Construction*, 20(January), 495–517.

Ergen, E., and Akinci, B. (2007). "An Overview of Approaches for Utilizing RFID in Construction Industry." *2007 1st Annual RFID Eurasia*, IEEE, 1–5.

Gheisari, M., and Esmaeili, B. (2019). "Applications and requirements of unmanned aerial systems (UASs) for construction safety." *Safety Science*, 118(May), 230–240.

Gheisari, M., Rashidi, A., and Esmaeili, B. (2018). "Using Unmanned Aerial Systems for Automated Fall Hazard Monitoring." *Proceeding of Construction Research Congress 2018*, (Janicak 1998), 148–157.

Ghueisari, M., Irizarry, J., and Walker, B. N. (2014a). "UAS4SAFETY: The Potential of Unmanned Aerial Systems for Construction Safety Applications." *Construction Research Congress 2014*, (2008), 140–149.

Ghueisari, M., Irizarry, J., Walker, B. N., Jalaei, F., Jrade, A., Gheisari, M., Irizarry, J., and Walker, B. N. (2014b). "UAS4SAFETY: The Potential of Unmanned Aerial Systems for Construction Safety Applications." *Construction Research Congress 2014*, (2008), 140–149.

Ham, Y., Han, K. K., Lin, J. J., and Golparvar-Fard, M. (2016). "Visual monitoring of civil infrastructure systems via camera-equipped Unmanned Aerial Vehicles (UAVs): a review of related works." *Visualization in Engineering*, Visualization in Engineering, 4(1), 1.

Howard, J., Murashov, V., and Branche, C. M. (2018). "Unmanned aerial vehicles in construction and worker safety." *American Journal of Industrial Medicine*, 61(1), 3–

10.

Huang, X. (2003). “The Owner role in construction safety.” UNIVERSITY OF FLORIDA.

Irizarry, J., Gheisari, M., and Walker, B. N. (2012). “Usability Assessment of Drone Technology As Safety Inspection Tools.” *Journal of Information Technology in Construction (ITcon)*, 17(17), 194–212.

Lin, Y., Su, Y., Lo, N., Cheung, W., and Chen, Y. (2013). “Application of Mobile RFID-Based Safety Inspection Management at Construction Jobsite.”

Kim, H., Lee, H. S., Park, M., Chung, B. Y., and Hwang, S. (2016). “Automated hazardous area identification using laborers’ actual and optimal routes.” *Automation in Construction*, Elsevier B.V., 65, 21–32.

Lu, W., Huang, G. Q., and Li, H. (2011). “Scenarios for applying RFID technology in construction project management.” *Automation in Construction*, Elsevier B.V., 20(2), 101–106.

Mancini, F., Dubbini, M., Gattelli, M., Stecchi, F., Fabbri, S., and Gabbianelli, G. (2013). “Using unmanned aerial vehicles (UAV) for high-resolution reconstruction of topography: The structure from motion approach on coastal environments.” *Remote Sensing*, 5(12), 6880–6898.

De Melo, R. R. S., and Costa, D. B. (2019). “Integrating resilience engineering and UAS technology into construction safety planning and control.” *Engineering, Construction and Architectural Management*, 26(11), 2705–2722.

Mendes, C., Costa, D., and Melo, R. (2018). “Evaluating Uas-Image Pattern Recognition System Application For Safety Guardrails Inspection.” (August), 1–3.

Namian, M., Albert, A., Zuluaga, C. M., and Behm, M. (2016). “Role of Safety Training: Impact on Hazard Recognition and Safety Risk Perception.” *Journal of Construction Engineering and Management*, 142(12), 04016073.

Oladinrin, T.O., Ogunsemi, D.R and Aje, I. O. (2012). “Role of Construction Sector in Economic Growth : Empirical Evidence From Nigeria.” *Journal of the Enviroment*, 7(1), 50–60.

Ortiz Coder, P. (2015). “Digitalización automática del patrimonio arqueológico a partir de fotogrametría.” *Virtual Archaeology Review*, 4(8), 46.

Perlman, A., Sacks, R., and Barak, R. (2014). “Hazard recognition and risk perception in

construction.” *Safety Science*, Elsevier Ltd, 64, 13–21.

Razuri, C., Alarcón, L. F., and Diethelm, S. (2007). “Evaluating the Effectiveness of Safety Management Practices and Strategies in Construction Projects.” *15th Annual Conference of the International Group for Lean Construction*, (July), 271–281.

Remondino, F., Barazzetti, L., Nex, F., Scaioni, M., and Sarazzi, D. (2012). “Uav Photogrammetry for Mapping and 3D Modeling – Current Status and Future Perspectives.” *ISPRS - International Archives of the Photogrammetry, Remote Sensing and Spatial Information Sciences*, XXXVIII-1/(June 2014), 25–31.

Sacks, R., Perlman, A., and Barak, R. (2013). “Construction safety training using immersive virtual reality.” *Construction Management and Economics*, 31(9), 1005–1017.

Tezel, A., and Aziz, Z. (2017). “From conventional to it based visual management: A conceptual discussion for lean construction.” *Journal of Information Technology in Construction*, 22(October), 220–246.

US Bureau of Labor Statistic. (2018). “National Census of Fatal Occupational Injuries in 2017.” *Bureau of Labor Statistics US Department of Labor*, (202), 1–14.

UVS International. (2018). “UVS International – Remotely Piloted Systems : Promoting International Cooperation & Coordination.” <https://uvs-international.org/> (Nov. 19, 2018).

Zhang, S., Sulankivi, K., Kiviniemi, M., Romo, I., Eastman, C. M., and Teizer, J. (2015). “BIM-based fall hazard identification and prevention in construction safety planning.” *Safety Science*, 72, 31–45.

Zhou, W., Whyte, J., and Sacks, R. (2012). “Construction safety and digital design: A review.” *Automation in Construction*, Elsevier B.V., 22, 102–111.

Zhou, Z., Goh, Y. M., and Li, Q. (2015). “Overview and analysis of safety management studies in the construction industry.” *Safety Science*, Elsevier Ltd, 72(February), 337–350.

Zhou, Z., Irizarry, J., and Lu, Y. (2018). “A Multidimensional Framework for Unmanned Aerial System Applications in Construction Project Management.” *Journal of*

Management in Engineering, 34(3), : 04018004.

Zuluaga, C. M., Namian, M., and Albert, A. (2016). "Impact of Training Methods on Hazard Recognition and Risk Perception in Construction." *Construction Research Congress 2016*, American Society of Civil Engineers, Reston, VA, 2861–2871.

CHAPTER 2: UAV INTEGRATION IN CURRENT CONSTRUCTION SAFETY PLANNING AND MONITORING PROCESSES: A CASE STUDY OF A HIGH-RISE BUILDING CONSTRUCTION PROJECT IN CHILE

Jhonattan G. Martinez[1]; Masoud Gheisari[2], Ph.D., A.M. ASCE; and Luis F. Alarcón, Ph.D., M. ASCE[3]

2.1 Introduction

In Chile, similar to many other countries, the construction industry is one of the most dangerous ones. A study conducted in Chile by the Superintendencia de Seguridad Social (2017) suggested that during 2017, the rate of accidents in the construction industry was 4.1 per every 100 workers. In the same year, 44 workers died on the job; this represents 20% of all the deaths occurring across different industries. The study found that the leading causes of workers' deaths were falls (36%), struck by objects (8%), electrocution (7%), and caught-in/between (6%). These hazards led to an average of 23.4 working days lost for each accident during the year (Superintendencia de Seguridad Social 2015).

The majority of these construction fatalities and accidents in Chile occur in high-rise building construction projects (Superintendencia de Seguridad Social 2015). The number of multi-story building construction projects have significantly increased since 1990 (Vergara 2017), and they account for roughly 57% of the construction projects in Chile (Instituto Nacional de Estaditica 2017). Based on the occupational safety and health administration requirements in Chile each new construction project must have at least one safety manager who would be responsible for inspection and monitoring, as well as implementing safety measures on site (Camara Chilena de la Construcción 2016). A study conducted by Alarcón et al. (2011) indicated that the majority of the new construction projects in Chile have an average of two safety managers on their site which was identified insufficient for adequately conducting the safety planning and monitoring tasks,

specifically for medium to large size projects. The limited number of safety managers on high-rise building construction projects adversely affect their capability to properly and frequently inspect such construction projects in Chile, where the majority of fatalities and accidents happen. Difficulty in frequently inspecting inaccessible, hard-to-reach, or unsafe locations on such high-rise building construction projects might adversely affect the safety managers' safety perception of the jobsite and might lead to unsafe acts and conditions that can only be detected after an accident has occurred. Therefore, finding ways to conduct a more frequent inspection of these high-rise projects, specifically observing the inaccessible, hard-to-reach, or unsafe locations, is expected to strongly enhance the safety performance in such projects.

One of the emerging technologies that can affect the safety planning and monitoring processes is the unmanned aerial vehicle (UAV). UAVs can be used as a vehicle of various types of sensors (e.g., cameras, motion detectors, heat sensors) and access specifically inaccessible, hard-to-reach, or unsafe locations on the site safely, quickly, and at a low-cost (Gheisari & Irizarry 2015). The recent development in low-cost light-weight UAVs with enhanced battery life, flight control, and autonomous navigation features have significantly increased their application over the last few years (Ham et al. 2016; Liu et al. 2014; Zucchii 2015). It is anticipated that the UAS commercial market will reach to a $30 billion industry by the year 2026 (Cohn et al. 2017).

UAVs can be ideal safety inspection assistants, providing safety managers with another set of eyes on the jobsite, and facilitate their safety inspection and monitoring processes (Gheisari & Esmaeili 2019). More specifically, UAVs might help the limited number of safety managers on high-rise building construction projects in Chile to frequently inspect the inaccessible, hard-to-reach, or unsafe locations on site and enhance their safety perception on the current status of their projects. However, no previous research was conducted on UAVs for safety planning and monitoring purposes in Chile. Furthermore, previous literature on general UAV application for construction safety

purposes has mainly focused on technology or specific hazard identification aspects of safety where little information was collected from users (i.e., safety managers) regarding the integration of UAVs in their current safety planning and monitoring processes. To address this knowledge gap, this study will focus on how safety managers should adopt UAVs and their generated visual contents within their current safety planning and monitoring processes. High-rise building construction projects in Chile, where the majority of fatalities and accidents happen, has been selected as the testbed of this study. It is anticipated that the UAV-captured visual contents combined with 3D models generated by them might provide a more complete and detailed view of the current status of high-rise building projects and can better facilitate safety managers' planning and monitoring process.

2.2 Research Background

2.2.1 Construction safety planning and monitoring

Construction safety management plays two important roles in avoiding accidents: safety planning and safety monitoring. Safety planning identifies hazardous conditions on the jobsite and assesses the probabilities of their occurrence and their severity levels (Perlman et al. 2014). Using the results from the risk assessment, management trains workers to be conscious about preventing hazardous acts and conditions. With safety monitoring, the workers and their environment are monitored to prevent unsafe acts and conditions. A study conducted by McKeown (2012) indicates that the number of unsafe acts and conditions is lower at construction projects that develop proper safety planning and monitoring. On the other hand, the rate of accidents on the jobsites that do not conduct proper and frequent safety planning and monitoring can increase by 40% (Reese 2011).

To prevent construction-related accidents, safety managers need to identify hazardous conditions in the jobsite and assess the probability of occurrence and their severity levels (Perlman et al. 2014). The safety managers are the people designated for

managing and providing oversight of the safety program, and their work play an important role in avoiding accidents (OSHA 2016). As a part of the safety managers' role, they need to observe the jobsite, alert the workers, and prevent unsafe acts and conditions (Woodcock 2014). In the continuously changing environment of construction sites, safety managers play an important role in monitoring the physical conditions and the organization of labor, equipment, subcontractors, and materials (Perlman et al. 2014).

Despite its importance, safety planning is conducted independently of the construction stage, which limits the safety managers' analytical processing of what safety measures are required to prevent accidents (Perlman et al. 2014). On the other hand, safety monitoring is not easy to achieve due to difficulty in visiting various areas simultaneously and the fact that some specific locations are not safe or accessible for inspection (OSHA, 2014). These factors limit the possibility of safety managers' direct and frequent observation of the workplace (Chi & Han, 2013; Zhou et al. 2018; Zuluaga et al. 2016). As a result of the manual jobsite monitoring, unsafe acts and conditions can only be detected after an accident has occurred. Therefore, it is necessary to analyze the jobsite proactively and in-depth to collect the most significant data that can be used for safety planning and monitoring (Namian et al. 2016; Perlman et al. 2014; Zuluaga et al. 2016).

Another factor that directly affects hazard identification and safety monitoring is the safety manager's risk perception capabilities (Zuluaga et al. 2016). These capabilities are based on an individual's skill in anticipating accidents and incidents before they happen. This skill is affected by safety managers' years of technical experience and professional training, and their accessibility and use of proper data for planning from project schedules and 2D drawings to visual contest such as site photos or 3D models (Perlman et al. 2014; Sacks et al. 2013; Zhang et al. 2015). Therefore, the accuracy of the safety managers' hazard recognition heavily relies on their experience and risk perception capabilities and also the visual content they use during the safety planning process (Albert et al. 2014; Bahn 2013).

According to a study conducted by Zhou et al. (2015), one of the gaps in construction safety planning and monitoring processes is the lack of innovative technology applications in safety practices. Regarding technological applications, there has been significant growth in the number of studies concerning the implementation of innovative technologies within construction safety. However, most of these remain in the academic research domain and have still not been successfully implemented in the industry (Zhou et al. 2015). Mixed- and virtual-reality (MR-VR) (Bosché et al. 2016; Eiris et al. 2018; Pham et al. 2018; Sacks et al. 2015), building information modeling (BIM) (Melzner et al. 2013; Kim et al. 2014; Zhang et al. 2015; Ji & Leite 2018), geographic information systems (GIS) (Abune'meh et al. 2016; Bansal 2011; Kumar & Bansal 2019; Manase et al. 2011), radio frequency identification (RFID) sensors (Fang et al. 2016; Lee et al. 2012; Lu et al. 2011; Montaser & Moselhi 2014), reality capture and point cloud data (PCD) (Teizer, 2008; Marks et al. 2013; Wang et al. 2015; Gheisari et al. 2018), and eye-tracking (Dzeng et al. 2016; Hasanzadeh et al. 2017; Jeelani et al. 2018; Yousefi 2015) are some examples of the various types of technologies that have been applied for safety-related applications.

As an MR-VR example, Bosché et al. (2016) combined beams and bricks in the real-world with 3D virtual components to create a sensation of working at elevation in a mixed reality environment for safety training purposes. Ji & Leite (2018) used BIM-based 4D modeling and rule-based checking to determine the tower-crane optimal location and identify potential spatial and capacity conflicts to avoid safety hazards. BIM was also used in other safety-related studies, for example, to develop a scaffolding rule-based system that automatically conducted pro-active management and potential hazard identification (Kim et al., 2014) or to determine fall hazards in the design and planning process using an automatic and customizable safety rule-checking platform (Melzner et al. 2013). In another example, a safety-based GIS database was created to and linked safety information with schedule activities and building model components (Bansal 2011). RFID technology was used in a study to provide real-time, accurate, and robust localization of workers on

jobsites, especially in hard-to-reach areas (Lee et al. 2012). In a reality-capturing-related study, Gheisari et al. (2018) used PCD generated through a photogrammetry process to identify guardrail locations in a safety monitoring process. Moreover, Hasanzadeh et al. (2017) used eye-tracking technology as a tool to study how the construction workers' attentional allocation might be affected by their safety knowledge. Another emerging technology with significant potential to affect the current safety planning and monitoring process is the Unmanned Aerial Vehicle (UAV).

2.2.2 UAVs for construction safety applications

Unmanned Aerial Vehicles (UAV), also known as UAS or drone, is an aerial platform designed to operate with no human pilots on board (UVS International 2018). UAVs are becoming very popular in the construction domain because of their capability to access unreachable or unsafe areas, and accomplishing tasks in a safe and timely manner (Gheisari & Esmaeili 2019). Tuttas et al. (2017) conducted a comparison study between using UAVs and hand-held cameras onsite and concluded that UAVs were more favorable because of their capability of capturing different angles and heights, providing comprehensive coverage of the jobsite current status. Such UAV-based visual data collection procedures can also reduce the time and cost associated with the visual data capture onsite (Tezel & Aziz 2017). UAVs can be integrated throughout different phases of the construction from site mapping and surveying (Ham et al. 2016; Rakha & Gorodetsky, 2018; Samad et al. 2013) and progress monitoring (Álvares et al 2018; Ham et al. 2016; Irizarry & Costa 2016) to structural inspection (Ham et al. 2016; Wierzbicki et al. 2015) and safety monitoring (Irizarry et al. 2012; Jalaei et al. 2014; Rodrigues et al. 2017). UAVs have a significant potential for monitoring acts and conditions such as unprotected edges or openings, activities in the proximity of boom vehicles or cranes, boom vehicles, or cranes in the proximity of overhead power lines (Gheisari & Esmaeili 2019).

Several studies investigated the use of UAVs for safety inspection purposes. All the studies used videos and photos of jobsites captured through a UAV to demonstrate their use mainly for hazard identification purposes. This type of visual data captured by UAVs can reduce the time and cost associated with data collection onsite (Tezel and Aziz 2017). In the earliest study, Irizarry et al. (2012) conducted a usability investigation followed by a heuristic evaluation to use a camera-equipped quadcopter to communicate the real-time feed of the jobsite to the safety managers. The study concluded that UAVs have the potential to be used as a safety inspection assistant to safety managers on the jobsite by providing them with real-time audio and video communication with construction workers onsite. In a follow-up experimental study, Gheisari et al., (2014) used a similar quadcopter platform to provide real-time jobsite information to the safety manager who could then provide immediate feedback to construction workers onsite in case of a hazardous situation. The study concluded that UAVs can be deployed to capture and send visual information to the safety manager faster and more efficiently (Gheisari et al., 2014). In another study, de Melo et al. (2017) used a case study approach to explore the UAV capability of collecting visual data form the jobsite and assess the compliance with safety regulations.

Visual data collected by UAVs were also integrated with building information modeling processes. As an example, Alizadehsalehi et al. (2018) created a methodology to create such integration for safety purposes by proposing a method that uses building information models to detect hazardous conditions and then operating a UAV to monitor those areas onsite. The study concluded that such processes could be utilized for visual monitoring of various safety aspects, such as lack of guardrails, deficient safety signs, inadequate scaffolding, slab openings, workers without proper PPE, or the existence of hazardous wastes (Alizadehsalehi et al. 2018). Several studies on UAVs for safety-related purposes also used photogrammetry technique, which consists of creating 3D models using 2D photos. Photogrammetry process uses image processing algorithms to calculate the exact position of objects and relate them to specific points with X, Y, and Z coordinates to

create a point cloud data (PCD) (Ortiz Coder 2015). 3D mapping developed by UAV photos could offer a fast-generated comprehensive view of the jobsite that can be observed from different perspectives in a 3D environment (Álvares et al. 2018). In two studies, Mendes et al. (2018) and Gheisari et al. (2018) created photogrammetry processes and used photos captured by UAVs to automate the safety inspection process and optimize time and labor for automatic recognition of guardrails onsite. However, neither of these studies collected information from users (i.e., safety managers) to explore how UAVs can be integrated in their current safety planning and monitoring processes. Moreover, there are no previous studies on UAVs for safety planning and monitoring purposes in Chile. This study will specifically focus on how safety managers in high-rise building construction projects in Chile, where the majority of fatalities and accidents happen, could benefit from UAVs in their safety planning and monitoring process and assess how such integration might affect their current process. This integration might help the limited number of safety managers on high-rise building construction projects in Chile to frequently inspect the inaccessible, hard-to-reach, or unsafe locations onsite and enhance their safety perception on the current status of their projects.

2.3 Motivation and Point of Departure

The main goal of this study is to explore how UAV technology and their generated aerial visual contents might affect the current approach of conducting safety planning and monitoring on high-rise building construction sites in Chile. As previously discussed, the majority of construction fatalities and accidents in Chile happens on high-rise building construction projects, and it is envisioned that using UAVs might help the limited number of safety managers on such projects in Chile and facilitate their planning and monitoring process. The specific objective of this study is to understand how safety managers should adopt UAVs and their generated visual contents within their current safety planning and monitoring processes on high-rise building construction sites in Chile and assess how such visual data would be useful for safety managers and how it might affect their risk perception and hazard identification. A case study approach was selected in this paper to

investigate the UAV integration in a high-rise building construction project in Chile with the typical number of safety managers. Despite multiple advantages that using UAVs might have for specific safety planning and monitoring conditions, several limitations were also identified in this case study that will be discussed in this paper.

The primary contribution of this paper is a better understanding of the use of UAVs for construction safety management tasks and their effects on the current safety planning and monitoring processes on the construction jobsites. The specific contribution of this research is to present the complexities of integrating UAVs in the current safety planning and monitoring process of high-rise building construction and provide initial data and insights on how UAVs might be adopted for such projects considering their safety performance and data usefulness. The outcomes of this study could benefit both construction safety professionals and researchers by helping them understand the integration of UAVs in a current safety planning and monitoring process and recognize the requirements and challenges for such integration while getting an understanding of how it would affect safety managers' hazard identification and risk perception.

2.4 Research Methods

A case study strategy was adopted for this research project. The case study approach consists of detailed observation of a case subject to identify practical problems and situations. Using this methodology, it is possible to capture the complexity of a single case and potentially generalize the results to other conditions or circumstances (Johansson 2003; Yin 2009). The outcomes of this exploratory case study provide initial data and insights on how UAVs might be adopted within the current approach of conducting safety planning and monitoring on high-rise building construction sites in Chile.

2.4.1 Case study selection

The study was conducted in a high-rise building construction project in Santiago, Chile (Figure 3). The goal was to select a project that can represent the typical characteristics and limitations of high-rise residential construction projects in Chile. The specific characteristics that were considered to select this project for the case study analysis are as following:

- *A High-rise Building Construction Project in Chile:* As previously indicated, high-rise building projects are the most dominant types of construction projects in Chile (Instituto Nacional de Estaditica 2017) and the majority of fatalities and accidents in Chile occur in such projects (Superintendencia de Seguridad Social 2015). This selected project was a high-rise residential complex that included four 23-story and two six-story buildings on a 16,850 m^2 land.

- *Limited Number of Safety Managers:* The majority of the new construction projects in Chile have an average of two safety managers which was considered insufficient for conducting the safety planning and monitoring properly (Alarcón et al. 2011). A project with two safety managers was deliberately selected to better represent the challenges of safety planning and monitoring with the limited number of safety managers on high-rise building construction projects in Chile. This project also had two safety managers onsite with nine and seven years of construction safety experience who were in charge of the safety planning and monitoring tasks throughout the construction phase of this project.

- *Safety Challenges and UAV Capabilities:* This project and its specific phase of construction were selected because of its safety monitoring complexities and challenges which were due to work at height. As previously indicated, UAVs are a more favorable platform for outdoor applications (Albeaino et al. 2019; Irizarry & Costa 2016) and monitoring the inaccessible, hard-to-reach, or unsafe locations (Gheisari & Esmaeili 2019). The specific phase of the project included activities such

as concrete, formwork, ironwork, and installation of MEP (mechanical, electrical, and plumbing) systems, which were conducted at different levels but mainly in upper levels of the high-rise project. By selecting this phase of the project, UAV was able to provide information quickly from various inaccessible, hard-to-reach, and unsafe spots within different heights where hazards (e.g., fall or struck-by) might be present.

Figure 3. Site visits

It is worth noting that due to the safety challenges that having a flying object might have brought to the jobsite together with other safety-planning and personnel-availability issues, the construction company in charge of the project provided the research team with limited access to the jobsite and their safety personnel for five weeks. The research team visited the project on Fridays to join safety managers' weekly meetings in which they discussed the jobsite's safety status and prepared the safety checklist for the following week. Safety managers were available to facilitate the data collection and help with the case study assessment.

2.4.2 UAV integration

The UAV platform used for the research was a Phantom 4 Pro (Figure 4), and it was selected due to its very high-resolution camera quality, sufficient battery life, and sensors that could allow safe flights in the proximity of objects such as cranes, trucks, scaffolds, and guardrails. This UAV has a camera lens with an 84-degree field-of-view and a 1-inch 20-MP sensor capable of shooting 4K/60 fps video at 100 Mbps (DJI 2017).

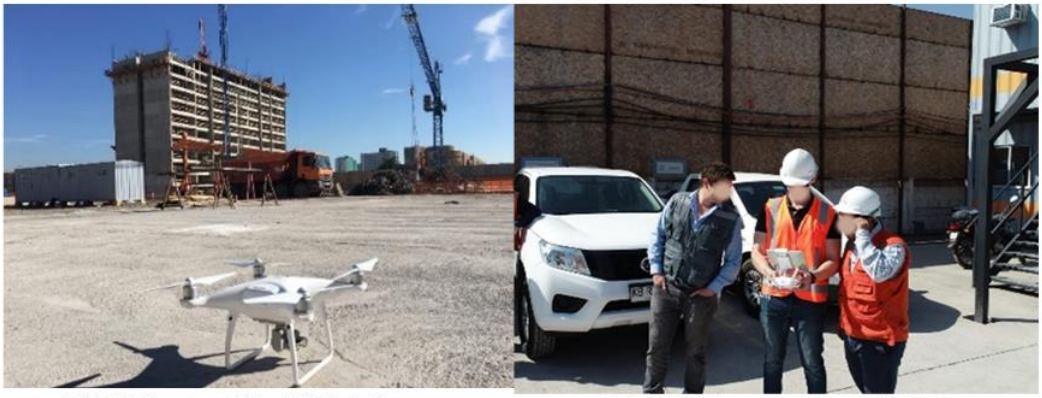

(a) DJI Phantom 4 Pro UAV platform. (b) The pilot conducting the flight.

Figure 4. UAV platform and onsite data collection

Various software packages, such as Drone Deploy® and DJI Go, were used for flight planning and data collection. The flight missions were conducted for five weeks, and the PCD and associated 3D models were generated for each week, utilizing captured aerial visual data and the ground positioning system (GPS) data of each photo. Flight planning was done using the Drone Deploy® app, which was selected due to its ability to conduct flight plans, capture photos automatically, ability to upload the captured content in the cloud, capability of adding plug-ins, cloud-based photogrammetry feature, and software popularity in the construction domain. Different flight paths were used during the data collection phase to consider wind direction changes and to avoid certain jobsite obstacles such as cranes and antennas (Figure 5). It is worth noting that takeoff and landing should

always be against the direction of the wind to increase the airflow under the wings for rotation and to improve UAV control during the flight (Pix4D 2019a). Figure 5(a) shows the flight plan developed for an East to West direction flight with an approximate height of 75 m over ground level covering a five-hectare area. Figure 5(b) indicates the flight plan developed for a Northeast to Southwest flight with an approximate height of 73 m over the ground level covering a four-hectare area.

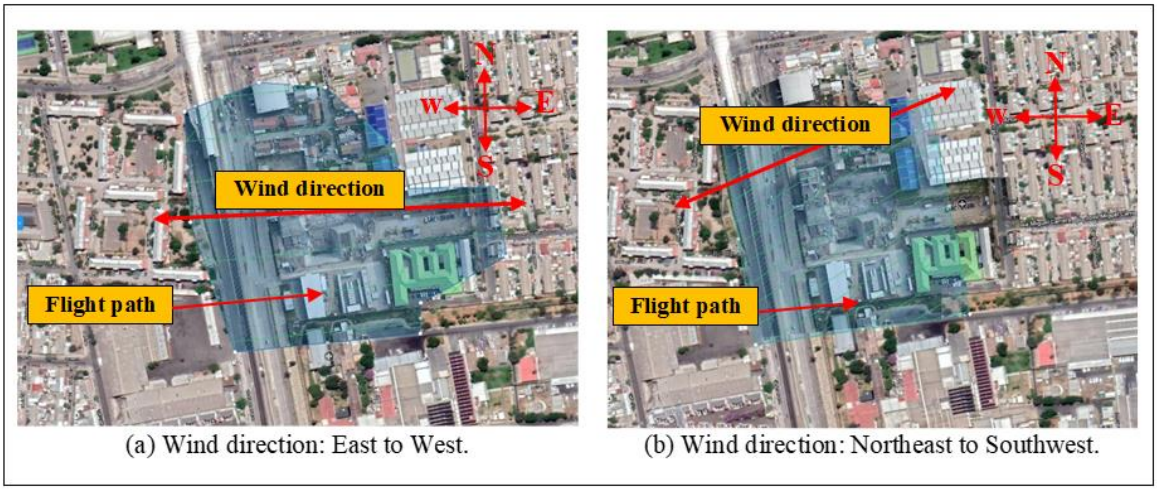

(a) Wind direction: East to West. (b) Wind direction: Northeast to Southwest.

Figure 5. Flight plans for different wind directions

2.4.3 Research Steps

The three research steps required for analyzing this case study project are discussed in this section (See Table 1).

Table 1. Research steps.

Steps	Objectives	Research Methods
I	Understanding the current safety planning and monitoring process	Process Mapping • Project document and visual content review • Interviews • Visits to the field
II	Creating a UAV-based safety planning and monitoring process	Process Mapping • Project document and visual content review • Interviews • Visits to the field
III	Assessing UAV integration effects on current safety planning and monitoring process	Safety Assessment • Identified hazards • Risk perception Data Usefulness Assessment Time

Step I: Understanding the Current Safety Planning and Monitoring Process: The current safety planning and monitoring process mainly consisted of using project data and jobsite information such as plans, schedules, and site photos to determine possible risks and assess their probabilities and consequences. In the current process, the safety managers used their smartphones or regular cameras during their daily safety inspection walks to capture several photos of the jobsite and document safety-related issues. These photos were mainly taken from the ground and did not properly capture the exterior sides of buildings or current activities on the higher levels. To fully illustrate the traditional safety monitoring process conducted in this case study, a process map was developed for this project. Process maps help to visually describe the flow of work to a level of detail necessary to establish opportunities for improvement (Bailey 2015). Together with reviewing the project-related documents and visual contents captured on-site and performing weekly site visits of the project, a series of semi-structured interviews with the two safety managers were conducted during the weekly meetings to better understand the workflow of their safety planning and monitoring process. During those interviews, a series of safety-related questions related to steps within their safety planning and monitoring process, documents and visual contents used for safety analysis purposes, safety metrics and measure, and generated outcome and reports were discussed. Finally, the developed process map was reviewed, refined, and validated by the same safety managers during the last meeting.

Step II: Creating the UAV-based Safety Planning and Monitoring Process: In the UAV-based method, safety managers conducted their safety planning and monitoring using the current project data and jobsite information together with the visual content captured by UAVs (e.g., photos, videos, and generated 3D models). It is envisioned that these UAV-generated visual contents would facilitate safety planning and monitoring by providing a detailed view of outdoor and at-height activities and locations that were previously inaccessible, hard-to-reach, or unsafe for safety managers to inspect. Another

process map was developed in this Step, to better illustrate how UAV-related tasks and generated visual contents can be integrated into the current safety planning and monitoring process. Similar to Step I, the same methods of reviewing the project-related documents and visual contents, visiting the construction site together with a series of weekly semi-structured interviews were used to create the new process map. This process map was also reviewed, modified, and validated by the safety managers during the last week meeting.

Step III: Assessing the UAV Integration Effects on the Current Safety Planning and Monitoring Process: Finally, to assess how the UAV integration within the current safety planning and monitoring process might have affected the safety assessment of the case study project, a few safety-related variables were studied. First, the identified hazards were measured (Carter and Smith 2006; Perlman et al. 2014) and then a detailed risk perception analysis was conducted. The risk perception analysis included metrics such as accident severity, probability, and overall risk level (Perlman et al., 2014):

- Severity: indicates the level of consequence generated by accident. Severity is measured on a scale of No injury (1) to Fatal (5).
- Probability: refers to the possibility that an unwanted event will occur and can produce consequences. Probability is measured on a scale of Infrequent (1) to Frequent (5).
- Risk level: is calculated from the multiplication of Severity and Probability and is illustrated on a scale of Very Low (1) to Very High (5).

To better understand the usefulness of each specific type of the visual content generated by the UAV (e.g., photos, videos, and 3D models) for safety planning and monitoring purposes, their usefulness was measured (Choi et al. 2017; Jebelli et al. 2016) on a scale of Not Useful (1) to Highly Useful (5). These assessments were conducted with the safety managers, mainly at the end of the weekly meetings. Finally, the time factor

was measured to assess how UAV could have affected the number of site visits and total time required to conduct them.

2.5 Results and Discussion

2.5.1 Current safety planning and monitoring process

This section discusses the step-by-step process that safety managers followed in this case study project for their safety planning and monitoring (See Figure 6).

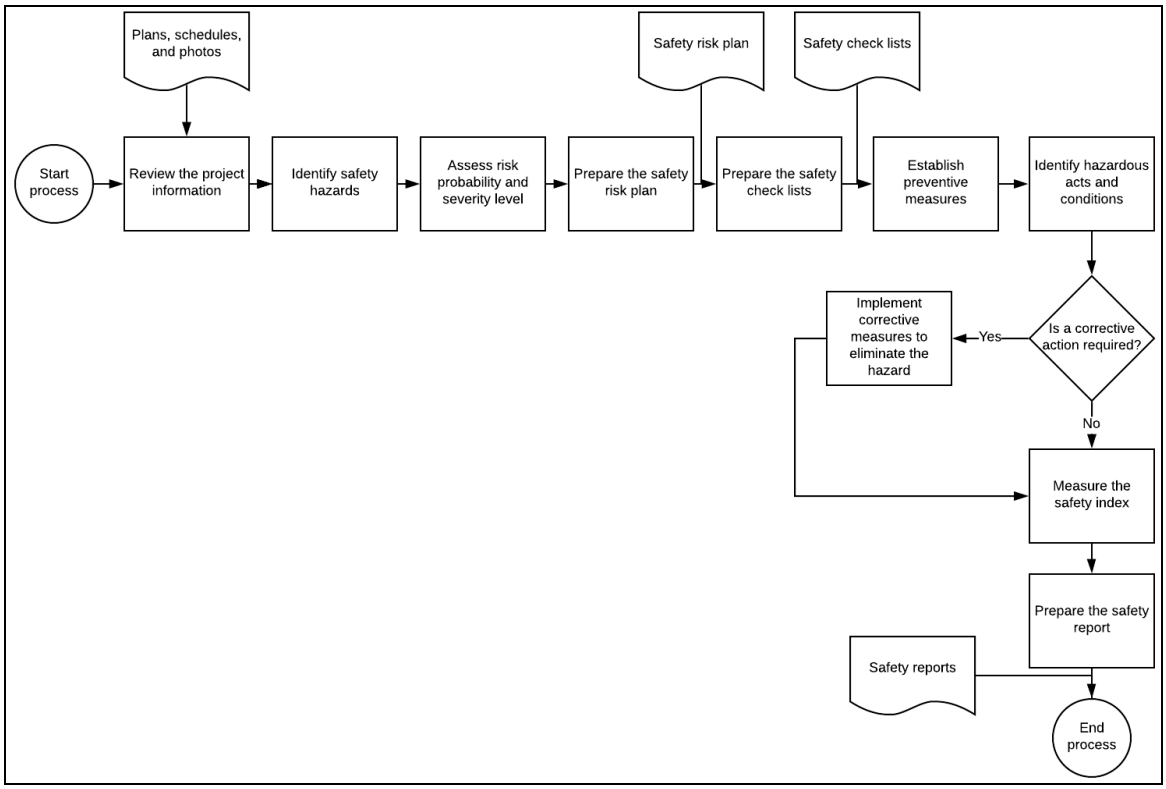

Figure 6. Current safety planning and monitoring process map.

Safety planning and monitoring process in the case study project started with reviewing the project information such as plans, schedules, and photos. The photos used by this method were mainly captured using safety managers' cellphones and cameras to document the current jobsite status. Utilizing this information, safety managers identified possible hazards and assessed their probabilities and severity levels. Then, safety managers

prepared the first version of the safety risk plan. This document frequently got updated as the project activities proceeded or changed due to delays or rescheduling. Using the risks identified in this document, the safety managers were defining safety actions required to prevent hazardous operations and conditions in the form of safety checklists. These lists contained information about potential hazards during the construction stage as well as necessary preventive and corrective measures. To prevent the occurrence of unsafe acts and conditions, the safety manager and the superintendents had to establish preventive measures that included a variety of safety-related activities such as worker training, installing guardrails, and adding safety signs (e.g., danger, warning, caution, and notice signs) in specific areas.

To identify hazardous acts and conditions, the safety managers, together with the superintendents, were reviewing safety monitoring processes on a daily basis. They had one-hour meetings every day to review and discuss the safety challenges of each phase of the project. They were using previously designed checklists to identify and correct any safety violations (e.g., workers exposed to unsafe conditions or unsafe acts that develop on the site). The captured information was also frequently shared with the project managers. The safety managers were also implementing corrective actions to reduce the possible consequences of any identified safety violation. For example, they would stop the construction activities that had safety violations or conducted meetings to discuss the safety violations with individuals or group of workers involved.

Then, the safety managers were assessing the safety index as a measure of safety to evaluate the level of hazards and risks related to work, identify improvement opportunities, implement preventive measures, and communicate the outcomes (Pinto et al. 2011). Ultimately, safety reports were created using all the data collected from the jobsite to all parties involved in the project (e.g., project manager, superintendent) during their weekly safety meetings.

2.5.2 UAV-based safety planning and monitoring process

UAV-based Visual Data Collection and Generation

The visual data collected using UAVs consisted of photos and videos. Different flight parameters such as height, lateral and front lap overlapping percentage, and the ground sample distance (GSD) were considered for the visual data collections during the flights (See Table 2). Building height was between 60 and 66 m during the five weeks of the data collection. There was also a tower crane on the construction site of the project and to properly capture the whole building while flying above the crane, the flight height in this case study project was approximately 75 m over the ground level. The lateral lap refers to the percentage of overlap between different flight legs, and the frontal lap refers to the percentage of overlap between one photo and the next one. These parameters are essential in the photogrammetry process and generating accurate 3D models. Another flight parameter was GSD, which is the distance between the centers of two neighboring pixels in a photo captured from the ground. The lower the value of the GSD gets, the higher the spatial resolution of the photo would be, and more details would be visible in the photo. The GSD is related to the flight height, and the higher the altitude of the flight gets, the larger the GSD value would be (Pix4D 2019a).

Table 2. Flight parameters in the UAV-based visual data collection and generation.

Parameters (Unit)	**Site Visits**				
	#1	**#2**	**#3**	**#4**	**#5**
Building height (m)	60	63	66	66	66
Flight height (m)	76	75	73	73	73
Flight start time (24 h)	12	14	10:30	10:30	10:30
Flight duration, for taking pictures only (min:s)	8:42	10:18	15:03	15:03	15:03
Frontal overlapping (%)	79	79	82	82	82
Lateral overlapping (%)	84	84	82	82	82
GSD resolution (cm/px)	2.3	2.2	2.0	2.0	2.0
Flight speed (m/s)	15	15	15	15	15
Number of photos	122	161	267	267	267
Number of additional vertical photos	15	15	15	15	15
Flight duration, for taking videos only (min:s)	34:34	42:12	45:45	42:23	38:21
Weather conditions	Cloudy	Sunny	Sunny	Sunny	Cloudy

A total of 1,159 photos and around 3.5 h of videos were captured throughout the five site visits and were then used to generate 3D point clouds through the Drone Deploy® application. Around fifteen frontal and vertical photos were also captured each week and added to the photogrammetry process to increase the visual content overlap on the building sides and improve the quality of the generated 3D models. Finally, five 3D models were generated toward the end of each week of the case study project observation (Figure 7). The generated 3D models and the photos and videos captured by the UAV were then provided to the safety managers to use them together with their regular documents and contents to conduct their safety planning and monitoring.

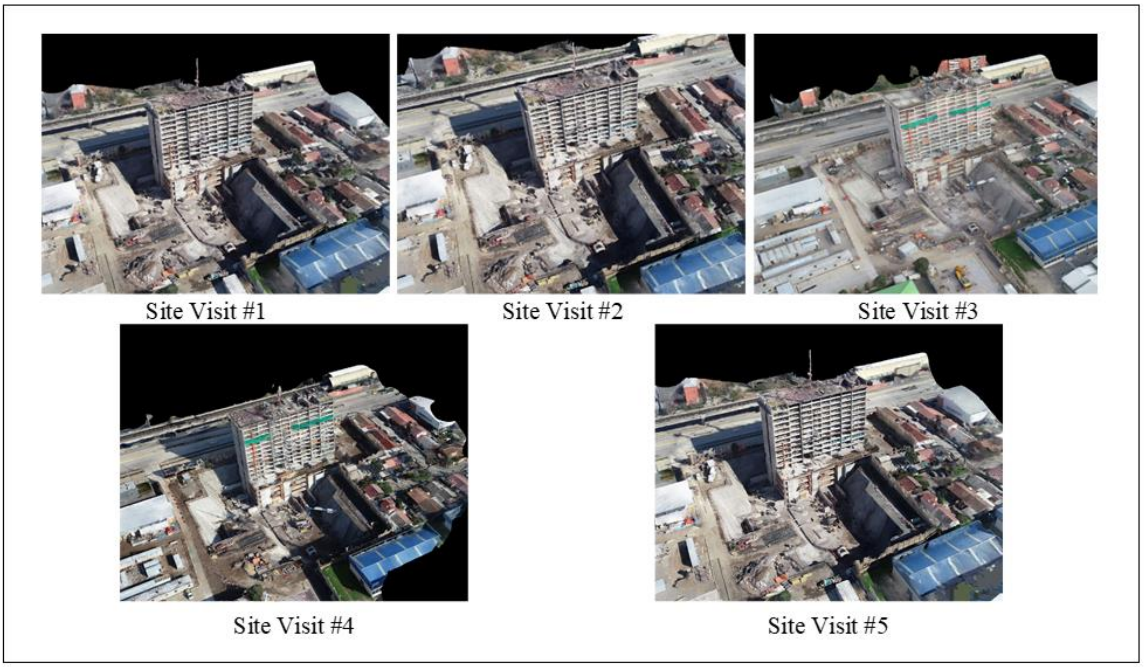

Figure 7. 3D models developed after each site visit.

UAV-based Safety Planning and Monitoring Process Map

This section discusses the new steps required in the case study project to integrate UAVs and their generated visual data within its current safety planning and monitoring process (See Figure 8). The main modifications are the added steps of designing and

conducting UAV flights and collecting and processing the visual data. It is necessary to plan the flight missions to cover all the areas and observe hazardous activities while focusing on activities and locations that might not be properly inspected by the safety managers. Due to UAV battery limitations and weather conditions, currently it is not possible to fly it all the time and every day to do data collections for safety planning and monitoring purposes. Considering the current technical and logistical limitations of using UAVs onsite, it would be ideal to design a proper flight plan (e.g., hourly, daily, or weekly), depending on the construction activities on the jobsite (e.g., indoor vs. outdoor or on-the-ground vs. at-height) or potentials unsafe acts and conditions that might benefit from using UAVs for data collection. In this case study, the weekly collected visual information (e.g., videos, photos, and the generated 3D models) were integrated into the earliest stages of the safety planning and monitoring process to facilitate the hazard identification and safety assessment of the project. The same detailed visual information was also used toward the end of the safety planning and monitoring process to create the safety report.

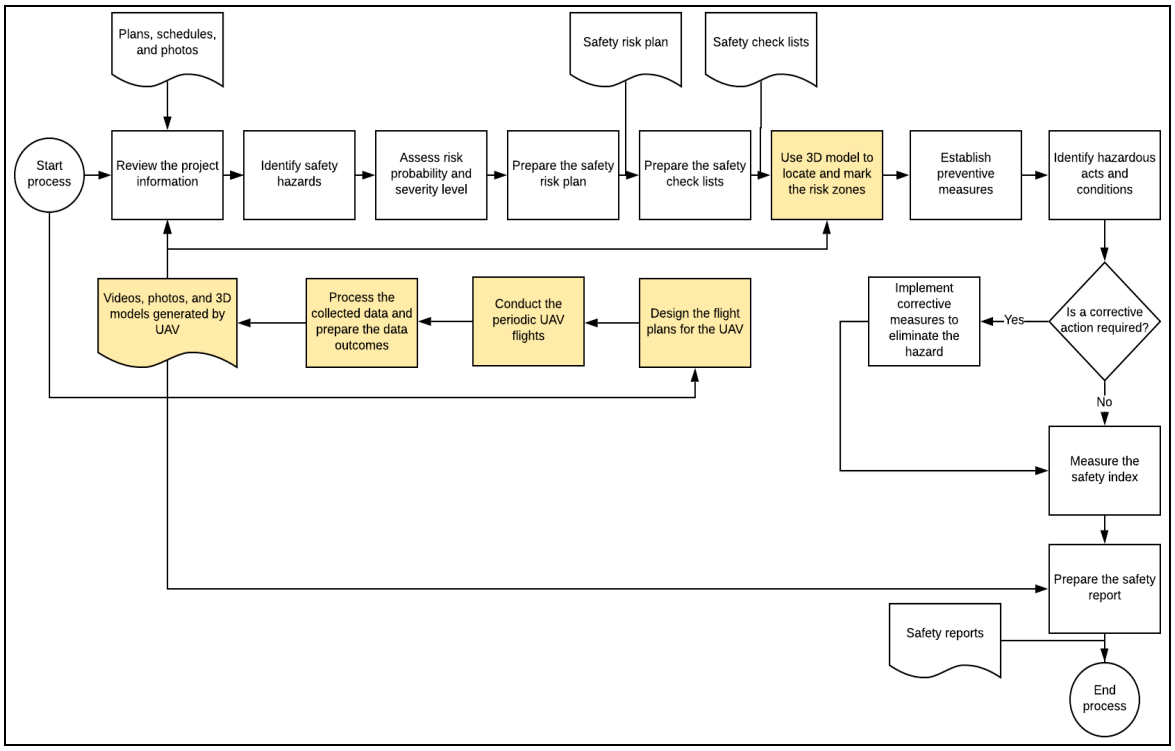

Figure 8. UAV-based safety planning and monitoring process map.

The visual information collected by the UAV facilitated the safety managers' task of hazard identification and assessment. For this purpose, it was necessary to obtain visual data obliquely and vertically to provide proper vertical and horizontal captures of the high-rise buildings onsite with an appropriate amount of detail about the building components, their levels, workers, and equipment onsite. This comprehensive visual information captured by the UAV played an essential role in preparing detailed visual safety risk plans and checklists. Safety risk plans contained visual information of safety actions that had to be implemented to reduce the risk level on the jobsite. The content captured by the UAV allowed the safety managers to prepare a more detailed visual document which highlighted hazardous areas and better communicated the potential safety challenges onsite with the workers. Then the safety checklists, which were designed based on the safety plans, were used to assess the proper implementation of the safety measures documented in the safety risk plans.

Finally, the generated 3D models captured by the UAV provided a comprehensive representation of the overall case study jobsite, which allowed the safety managers to use its 3D modeling flexibility to locate and mark the risk zones. This way, the safety managers were able to not only identify hazardous acts and conditions onsite but also communicate the required preventive measures to other parties (e.g., superintendents, project managers, workers) through simply marking those areas in the 3D model.

2.5.3 UAV Integration effect on current safety planning and monitoring process

Safety Assessment: Identified Hazards and Risk Perception

This section discusses the hazard identification and risk perception factors to illustrate how the UAV integration within the current safety planning and monitoring process affected the safety managers' assessment of the case study project. The actual goal of this section was to assess how visual data generated by the UAV would be useful for

safety managers and might affect their risk perception and identification of specific hazardous conditions.

As it was expected, safety managers were able to identify more hazards using the contents generated by UAVs (Average: 21.2) (See Table 3). It is worth noting that the extra hazards identified using the UAVs were primarily included missing guardrails or safety nets around unprotected edges or openings, loose or unsecured material at height, and lack of proper PPE or safety harnesses which could have been hard to identify through regular safety walks on the high-rise building site. In other words, UAV facilitated safety managers by enhancing their hazard identification under specific hazardous conditions. After identifying more hazards, safety managers' risk perception also slightly changed, and they rated the severity (3.28), probability (3.82), and risk level (3.76) of the identified hazards somewhat higher (Table 3).

Table 3. Number of hazards and risk perception data.

Variables		Site Visit #1		Site Visit #2		Site Visit #3		Site Visit #4		Site Visit #5		Average	
		Regular Process	UAV-based Process	Regular Process	UAV-based Process	Regular Process	UAV-based Process	Regular Process	UAV-based Process	Regular Process	UAV-based Process	Regular Process	UAV-based Process
Identified Hazards (#)		19	22	16	18	22	26	15	19	17	21	17.8	21.2
Risk Perception	Severity	3.3	3.5	2.9	3.1	3.7	3.6	3.2	3.3	2.8	2.9	3.18	3.28
	Probability	3.8	4.1	3.3	3.6	4.1	4.2	3.5	3.7	3.2	3.5	3.58	3.82
	Risk Level	3.7	3.9	3.6	3.7	3.9	3.8	3.4	3.8	3.1	3.6	3.54	3.76

As an example, in week one, the safety managers were able to identify four more hazards that were associated with unprotected edges and openings in the upper three floors of the building. The aerial photos and the 3D model captured and generated using UAVs helped the safety managers to identify and tag missing guardrails or safety nets around four unprotected slabs and openings on the upper levels. The identification of such serious hazards in the UAV-based method also led to higher ratings of severity (3.5), probability (4.1), and risk level (3.9) of identified hazards by the safety managers. Similar increases were noticed in four out of the five weeks of the data collection, except week three. During

week three, the severity and the level of risk were assessed slightly lower using the UAV-based method. This lower assessment occurred because safety managers could visually see in the photos and videos collected by the UAV that specific safety issues, such as inappropriate waste storage and unprotected scaffolding on the lower floors of the building, did not pose a very high potential risk to the current workers and activities that were mainly conducted on the upper levels of the building in that specific week. It is interesting to note that in week three, the visual content captured by the UAV facilitated the safety managers to arrive at a conclusion that the severity and risk level were lower than what they were expecting before.

Focusing on safety hazard types, it was noticed that by using the contents generated by the UAV, the safety managers could better identify specific unsafe conditions in the high-rise building project site:

- *Lack of Guardrails (Fall Hazards):* The 3D models generated by UAV provided a very precise representation of the jobsite status and allowed the safety managers to identify the presence and assess the proper installation of the guardrails through accurate measurements directly in the captured models.
- *Lack of Safety Nets (Fall Hazards):* Safety nets are usually located in hard-to-reach zones (e.g., top of the building) where it is difficult, unsafe, or impossible for safety managers to visually inspect. The visual contents captured by UAVs (especially videos and photos) allowed the safety managers to identify the areas, such as unprotected exterior boundaries of slabs or balconies, that might be needed to be protected by safety nets. They could also inspect the proper installation of current safety nets and their proper coverage of targeted areas.
- *Moving/Falling Objects (Struck-by Hazards):* The aerial photos captured by the UAV allowed the safety managers to better see moving objects (e.g., tower cranes or machinery) or objects with the potential to fall (e.g., loose or unsecured material at height) that might create potential struck-by hazards.

- *Lack of Personal Protective Equipment:* The aerial videos captured by the UAV allowed the safety managers to detect several violations regarding improper or lack of PPE or safety harness on the site (e.g., not wearing hard hats or safety glasses).
- *Evacuation Route:* The aerial photos and the 3D models generated by UAVs also allowed the safety managers to identify areas without proper evacuation routes.

Data Usefulness Assessment

This section discusses the usefulness of each specific type of the visual content generated by the UAV, including photos, videos, and 3D models, for safety planning and monitoring purposes of the case study project (See Table 4). The results showed that safety managers rated videos (4.52) as the most useful data for their safety planning and monitoring activities in this high-rise building construction project, followed by photographs (4.15), and then 3D models (3.22). It is worth noting that, at the beginning, the safety managers were not able to interact and navigate properly within the generated 3D models, but over time they got comfortable using them as a tool for their safety planning and monitoring activities and consequently, the 3D model usefulness rating increased over weeks. Focusing on specific safety planning and monitoring activities, photos were rated very high for preparing safety risk plans (5) and safety checklists (5) and videos for identifying hazardous acts and conditions (5). 3D models were also rated high for preparing safety risk plans (4).

Table 4. Usefulness of UAV-generated visual data.

Activities in the safety planning and monitoring process	Week 1			Week 3			Week 5			Average		
	Video	Photo	3D Model	Video	Photo	3D Model	Video	Photo	3D Model	Video	Photo	3D Model
Review project information	4	4	2	5	5	2	5	5	5	4.67	4.67	3.00
Identify safety risks	4	4	1	4	4	3	5	4	4	4.33	4.00	2.67
Assess probability and severity	4	4	2	4	4	3	5	4	3	4.33	4.00	2.67
Prepare safety risk planning	4	5	2	4	5	4	5	5	5	4.33	5.00	4.00
Prepare check lists	4	5	2	4	5	4	5	5	5	4.33	5.00	3.67
Implement safety measures	4	4	3	4	4	3	5	4	5	4.33	4.00	3.67
Identify hazardous acts and conditions	5	4	3	5	4	4	5	4	5	5.00	4.00	3.67

Measure safety index	4	2	2	5	3	3	5	3	3	4.67	2.67	2.67
Prepare safety reports	4	4	2	5	4	3	5	4	4	4.67	4.00	3.00
Average										4.52	4.15	3.22

Time Assessment

Over the five weeks of data collection, roughly it took safety managers around four hours per week to do their visits, which included visiting the upper floors of the building where the majority of activities were occurring. Using the UAV, safety managers could do a similar site visit within roughly 30 minutes. This means that the use of UAV could allow safety managers to increase the number of site visits and also reduce the total time required to conduct those visits. The UAV also could provide a comprehensive aerial visual content of the upper-level activities which were not possible to inspect through safety managers' regular on-foot site visits. Using the UAV-captured visual data from those locations, the safety managers were also able to identify other unsafe acts and conditions, explicitly associated to guardrails, PPE, and lack of safety nets, that were not visible to inspect in their regular visits. Although the UAV significantly reduced safety managers' site visit duration on the jobsite, its incapability of conducting indoor data collection and cost factor associated with its integration should also be considered for its successful integration. Due to safety concerns and technical incapability of the UAV (e.g., lack of a global navigation satellite system signal for high-precision indoor navigation), no indoor flight was conducted in this case study and only visual content from the indoor environments that was visible from the outdoor flights were captured and used for safety planning and assessment purposes. Using on-ground robots or other UAVs with high-precision indoor navigation capabilities could have been used for such indoor data collection but would have increased UAV-based site visit duration. Furthermore, the time and costs associated with the UAV integration, including its acquisition, insurance, training, maintenance, operation, and data processing, should also be considered for its successful integration.

2.5.4 Lessons learned from the UAV-based safety planning and monitoring process

The research team identified several factors in this case study for successful integration of UAVs and their generated data in the safety planning and monitoring process, which will be discussed in this section. First, it is essential to have a proper flight plan and determine the construction activities, equipment, or buildings that need to be inspected at each phase of the project. Such plans help to capture the most significant and comprehensive amount of data for safety inspection purposes within the time frame of a UAV battery life. Moreover, it is essential to have a UAV with a high-resolution camera to record small-size safety-related items, such as hardhats, safety glasses, guardrails, and safety harnesses. In this case study, a 20 MP high-resolution camera was used, which helped with the proper identification and analysis of those small-size safety-related items in the captured data. A high-resolution camera also allows the UAV not to fly in the proximity of the targeted object (e.g., buildings, workers, machinery) and also improves the safety in the data capture process.

Another critical aspect to consider during the flights is the UAV camera angle while doing the video or photo captures. An area shot with a 90-degree vertical camera position (Figure 9) across the site will allow safety managers to identify the issues that are better visible on the plan view, such as the distribution of workers in the construction area, debris or hazardous materials near work areas, and activities occurring close to the openings and edges. Moreover, if the UAV camera captures information at an oblique or almost horizontal angle (Figure 10), some other safety-related issues can be identified, which are better visible on side views. Examples of such issues are the lack of PPE or safety harness or missing guardrails. It is worth noting that using a UAV could facilitate safety managers by not only providing them access to inspect such inaccessible, hard-to-reach, or unsafe locations onsite but also through providing a more frequent opportunity to conduct such inspections.

(a) Worker distribution on the jobsite.

(b) A worker in close proximity to openings and edges.

Figure 9. UAV captures with a 90-degree vertical camera position.

(a) Lack of guardrails.

(b) Worker without safety rope.

(c) Lack of guardrails.

Figure 10. UAV captures with a horizontal or oblique camera position

Some other critical data collection factors should also be considered during the flights to build an accurate 3D model using the visual data generated by a UAV. It is

recommended to capture high-quality photos that cover the whole jobsite and have proper amounts of horizontal and vertical overlaps. A high-quality 3D model with no missing data allows safety managers to identify hazards appropriately. In this high-rise building project, it was essential to take additional frontal and vertical photos from the building sides, to cover building elevation views that were missing in the autonomous horizontal flights. These additional photos increased the horizontal and vertical visual content overlap and improved the 3D model quality. It is also worth noting that conducting flights at a lower altitude would increase the number of photos captured during flight, which in turn enhance the 3D model quality through the increased number of shared points between photos that are used in the photogrammetry process. Another essential factor to consider during the UAV flight is the weather and environmental condition. If possible, it is recommended to conduct the flights around noontime but while the sky is partly cloudy to get a good light necessary for visual captures and in the meantime minimize the shadows on the site. Shadows can produce inconsistencies such as content gaps and visual distortions in the generated 3D models. Figure 11 shows several examples of visual inconsistencies (e.g., content gap and visual distortions) identified in the generated 3D models. These issues were resolved using various approaches, such as decreasing the UAV data collection speed, increasing the number of photos, or adding additional frontal and vertical photos from sides of the building.

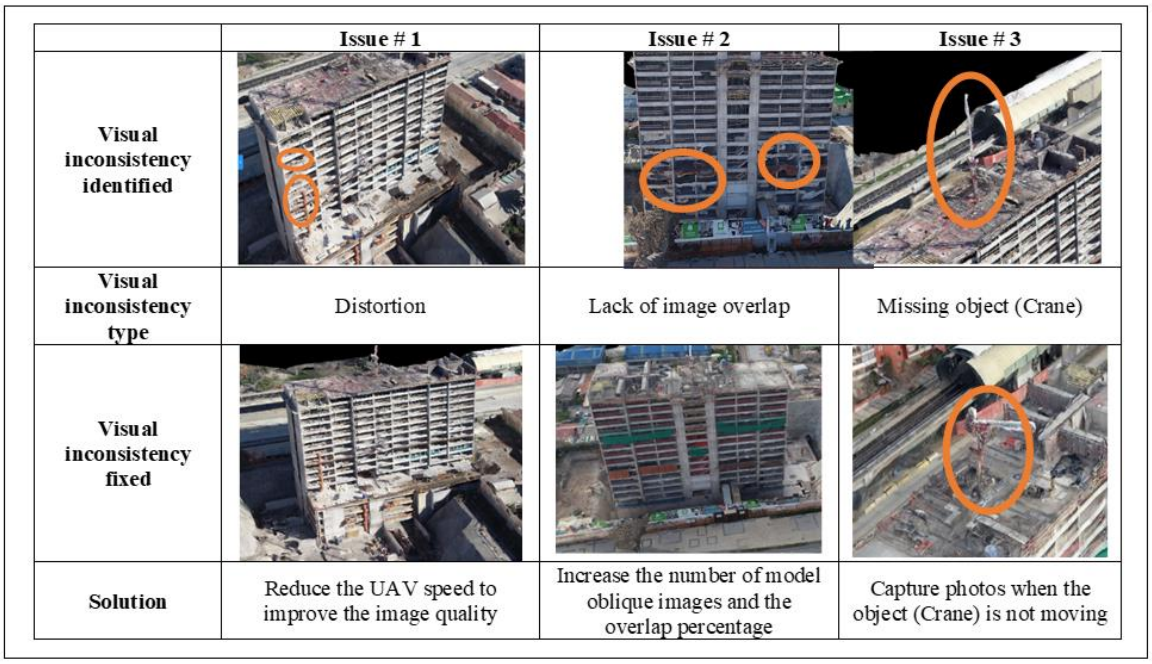

Figure 11. Examples of generated 3D models with visual inconsistencies.

2.6 Limitations for Successful Integration of UAVs

Despite multiple advantages that using UAVs might have for safety planning and monitoring purposes, several limitations were identified in this case study that will be discussed in this section.

- *Aviation regulations:* There are different aviation administrations around the world that would regulate UAV flights in each country. Dirección Aeronautica Nacional (DAN) is the national aeronautical directorate in Chile that regulates UAV flights for commercial applications. Some general flight requirements for commercial applications in Chile (DAN 151, 2015) are as following: (1) the UAV should be registered in the DAN portal, (2) the UAV pilot should be licensed to operate the vehicle for professional purposes, (3) the maximum allowable altitude is 130 m above the ground level, and (4) the horizontal distance between the UAV and the pilot should not be more than 500 m. Some of these factors, including maximum

distance and height, might limit data collection in high-rise construction projects where the UAVs might require flying over the high-rise building height. There is also the possibility of getting a waiver from DAN for such flights. Similar flight agencies also exist in other countries which their regulations should be followed appropriately to use UAVs for safety-related data capture on jobsites.

- *Battery duration:* The UAV used in this case study and the typical types of commercial off-the-shelf UAVs can fly approximately 20–30 minutes, limiting the amount of visual content that can be captured from the jobsite on each flight. For longer flights, customized or more sophisticated UAVs should be considered (Gheisari & Esmaeili 2019). Other alternatives are automated battery charging platforms or a group of low-cost UAVs working collaboratively and covering different areas of the jobsite (Gheisari & Esmaeili 2019).

- *Safety concerns:* UAVs as flying vehicles on the jobsite might create hazardous situations, such as a collision with building elements or moving objects on the site, fall over people, and cause workers' distraction. Integrating technical features, such as sense-and-avoid capabilities, high-precision navigation, or using parachute systems in the UAVs, might minimize the safety concerns associated with their flight. Some human or logistical factors, such as using certified flight pilots with proper training and experience, creating proper flight plans and communicating them properly with all the groups on the jobsite, and developing a specific safety plan for each flight, might also help reduce the safety challenges associated with UAV flights on the jobsite. It should be noted that a better understanding of the UAV operator's cognitive performance and its implications in UAV-integrated tasks would accelerate the successful and safe integration of UAVs in the construction applications (Kim and Irizarry, 2019).

- *Moving objects:* Due to safety measures in this case study project, the UAV was not used while there were large moving objects on the site (e.g., cranes or other large

types of machinery), which limited the amount of visual content captured from the site and missed the specific activities related to those moving objects and their potential safety issues.

- *Indoor data collection:* Due to safety concerns and technical incapability of the UAV, no indoor flight was conducted in this case study. For indoor data collection, UAVs or on-ground robots with high-precision indoor navigation capability could be used.

- *Electromagnetic interferences:* Such interferences are produced by various types of external sources, such as cellphone towers, power lines, or steel structures, which might affect the UAVs compass and GPS signal, and can cause errors or complete data loss. Considering the location of external sources that might cause electromagnetic interferences in the flight plans and avoiding flights in their proximity might reduce such challenges.

- *Camera quality:* The majority of the UAV platforms have a camera that can capture high-quality videos and photos. However, to obtain information about specific types of unsafe acts or conditions (e.g., missing or improper guardrails, wearing proper PPE or safety harnesses), it is necessary to inspect the location from a very close distance. Cameras with very high resolution or zooming capabilities might be ideal for such inspections.

- *Weather conditions:* UAVs are very susceptible to the wind, which adversely affected our data collection in this study a few times. Other weather conditions, such as rain and snow, would also completely stop UAV operation.

2.7 Summary and Conclusion

This case study focused on how UAV technology and their generated aerial visual contents might affect the current approach of conducting safety planning and monitoring

on high-rise building construction sites in Chile. First, the current safety planning and monitoring process in a high-rise construction site was studied, followed by investigating how UAV-related tasks and generated visual contents could be integrated into this current process. Then a few safety variables (e.g., risk perception and hazard identification) were studied to assess how such UAV integration might have affected the current safety planning and monitoring process. Data usefulness was also assessed to better understand the usefulness of each specific type of visual content generated by the UAV for safety planning and monitoring purposes. Finally, time was measured to understand UAV could affect the number of site visits and total time required to conduct them.

The case study provided the details of the new steps required in a high-rise building construction project to integrate UAVs and their generated visual data within its current safety planning and monitoring process. The main added steps were related to designing and conducting UAV flights and collecting and processing visual data. The aerial visual contents and 3D models generated in the UAV-based method provided a detailed and comprehensive view of the site and associated safety challenges in it. The collected visual information was mainly integrated into the earliest stages of the safety planning and monitoring process and facilitated the hazard identification and safety assessment of the project. It also helped the safety managers to create the safety report toward the end of the safety planning and monitoring process. The aerial visual contents and 3D models were embedded in these safety reports and the enhanced their quality to better represent and communicate of the identified safety challenges. In general, the case study results showed that the adoption of UAV technology as a tool for safety planning and monitoring in high-rise building construction projects enhances identification and assessment of hazards, especially in outdoor at-height acts and conditions. Some examples of such acts and conditions were missing guardrails or safety nets around unprotected edges or openings, loose or unsecured material at height, and lack of proper personal protective equipment or safety harnesses. The identification of such severe hazardous conditions also led to a higher rating of severity assessment, probability of occurrence, and risk level by the safety

managers. The results also showed that the safety managers considered the aerial videos provided by the UAV as the most useful type of data for their safety planning and monitoring tasks, followed by photos and 3D models. It was also noticed that using the UAV, safety managers could significantly reduce the total time required to conduct their site visit walkthroughs and consequently increase the number of their visits.

Despite several advantages that using UAV platforms might have for safety planning and monitoring purposes, several technical challenges need to be considered for their successful implementation for safety planning and monitoring process of high-rise construction projects. Some examples of such limitations are aviation regulations (e.g., maximum distance or height limits), limited battery duration, safety concerns of having a flying vehicle onsite, electromagnetic interferences, indoor flight capabilities, and weather conditions.

This case study presented the complexities of integrating UAVs in current safety planning and monitoring process of high-rise building construction in Chile. Although using UAVs for safety monitoring and planning purposes is at early stages of development and implementation in Chile, however the outcomes of the study showed that UAVs might have significant impact on the safety planning and monitoring process of high-rise building construction projects by helping the limited number of safety managers to properly and frequently inspect such construction projects where the majority of fatalities and accidents happen. This effort needs to be followed by further studies on the technical, legal, financial, safety, as well as hardware and software development aspects of UAVs for their successful implementation for safety planning and monitoring on the construction jobsites.

2.8 Data Availability Statement

Some or all data, models, or code generated or used during the study are available from the corresponding author by request (3D models, photos, and videos).

2.9 References

Abune'meh, M., El Meouche, R., Hijaze, I., Mebarki, A., & Shahrour, I. (2016). Optimal construction site layout based on risk spatial variability. *Automation in Construction*, *70*, 167–177. https://doi.org/10.1016/j.autcon.2016.06.014

Alarcón, L. F., Acuña, D., & Diethelm, S. (2011). Using empirical data to identify effective safety management strategies in construction companies. *19th Annual Conference of the International Group for Lean Construction 2011, IGLC 2011*, 1–10.

Albeaino, G., Gheisari, M., & Franz, B. W. (2019). A systematic review of unmanned aerial vehicle application areas and technologies in the AEC domain. *Journal of Information Technology in Construction*, *24*(July), 381–405.

Albert, A., Hallowell, M. R., & Kleiner, B. M. (2014). Enhancing Construction Hazard Recognition and Communication with Energy-Based Cognitive Mnemonics and Safety Meeting Maturity Model: Multiple Baseline Study. *Journal of Construction Engineering and Management*, *140*(2), 04013042. https://doi.org/10.1061/(ASCE)CO.1943-7862.0000790

Alizadehsalehi, S., Yitmen, I., Celik, T., & Arditi, D. (2018). The effectiveness of an integrated BIM/UAV model in managing safety on construction sites. *International Journal of Occupational Safety and Ergonomics*, *0*(0), 1–16. https://doi.org/10.1080/10803548.2018.1504487

Álvares, J. S., Costa, D. B., & Melo, R. R. S. de. (2018). Exploratory study of using unmanned aerial system imagery for construction site 3D mapping. *Construction Innovation*, *18*(3), 301–320. https://doi.org/10.1108/CI-05-2017-0049

Bahn, S. (2013). Workplace hazard identification and management: The case of an underground mining operation. *Safety Science*, *57*, 129–137. https://doi.org/10.1016/j.ssci.2013.01.010

Bailey, M. L. (2015). What is it ? Why Use It ? What does it do ? How do I do it ? *Process Mapping LEIT 564: Performance Technology and Training Margaret L. Bailey,*

Ph.D. Northern Illinois University, 1–3.

Bansal, V. K. (2011). Application of geographic information systems in construction safety planning. *International Journal of Project Management*, *29*(1), 66–77. https://doi.org/10.1016/j.ijproman.2010.01.007

Bosché, F., Abdel-Wahab, M., & Carozza, L. (2016). Towards a Mixed Reality System for Construction Trade Training. *Journal of Computing in Civil Engineering*, *30*(2), 1–12. https://doi.org/10.1061/(ASCE)CP.1943-5487.0000479

Camara Chilena de la Construcción. (2016). Manual para el inicio de la obra de construcción.

Carter, G., & Smith, S. D. (2006). Safety Hazard Identification on Construction Projects. *Journal of Construction Engineering and Management*, *132*(2), 197–205. https://doi.org/10.1061/(ASCE)0733-9364(2006)132:2(197)

Chi, S., & Han, S. (2013). Analyses of systems theory for construction accident prevention with specific reference to OSHA accident reports. *International Journal of Project Management*, *31*(7), 1027–1041. https://doi.org/10.1016/j.ijproman.2012.12.004

Cohn, P., Green, A., Langstaff, M., & Roller, M. (2017). Commercial Drone are Here: The Future of Unmanned Aerial Systems. *McKinsey&Company*, (December), 1–11.

De Melo, R. R. S., Costa, D. B., Álvares, J., & Irizarry, J. (2017). Applicability of unmanned aerial system (UAS) for safety inspection on construction sites. *Safety Science*, *98*, 174–185. https://doi.org/10.1016/j.ssci.2017.06.008

DJI. (2017). Phantom 4 Pro/Pro+ User Manual. https://doi.org/10.1007/SpringerReference_28001

Eiris, R., Gheisari, M., & Esmaeili, B. (2018). PARS: Using Augmented 360-Degree Panoramas of Reality for Construction Safety Training. *International Journal of Environmental Research and Public Health*, *15*(11), 2452. https://doi.org/10.3390/ijerph15112452

Fang, Y., Cho, Y. K., & Chen, J. (2016). A framework for real-time pro-active safety assistance for mobile crane lifting operations. *Automation in Construction*, *72*, 367–379. https://doi.org/10.1016/j.autcon.2016.08.025

Gheisari, M., & Esmaeili, B. (2019). Applications and requirements of unmanned aerial systems (UASs) for construction safety. *Safety Science*, *118*(May), 230–240. https://doi.org/10.1016/j.ssci.2019.05.015

Gheisari, M., & Irizarry, J. (2015). A User-centered Approach to Investigate Unmanned Aerial System (UAS) Requirements for a Department of Transportation Applications. *Conference on Autonomous and Robotic Construction of Infrastructure*, (January), 85.

Gheisari, M., Rashidi, A., & Esmaeili, B. (2018). Using Unmanned Aerial Systems for Automated Fall Hazard Monitoring. *Proceeding of Construction Research Congress 2018*, (Janicak 1998), 148–157. https://doi.org/10.1213/01.ANE.0000149897.87025.A8

Ghueisari, M., Irizarry, J., Walker, B. N., Jalaei, F., Jrade, A., Gheisari, M., … Walker, B. N. (2014). UAS4SAFETY: The Potential of Unmanned Aerial Systems for Construction Safety Applications. *Construction Research Congress 2014*, (2008), 140–149. https://doi.org/10.1061/9780784413517.176

Ham, Y., Han, K. K., Lin, J. J., & Golparvar-Fard, M. (2016). Visual monitoring of civil infrastructure systems via camera-equipped Unmanned Aerial Vehicles (UAVs): a review of related works. *Visualization in Engineering*, *4*(1), 1. https://doi.org/10.1186/s40327-015-0029-z

Hasanzadeh, S., Esmaeili, B., & Dodd, M. D. (2017). Measuring the Impacts of Safety Knowledge on Construction Workers' Attentional Allocation and Hazard Detection Using Remote Eye-Tracking Technology. *Journal of Management in Engineering*, *33*(5), 04017024. https://doi.org/10.1061/(asce)me.1943-5479.0000526

Instituto Nacional de Estaditica. (2017). Informe Anual de Edificación en Chile. https://doi.org/10.1016/j.aqpro.2013.07.003

Irizarry, J., & Costa, D. B. (2016). Exploratory Study of Potential Applications of Unmanned Aerial Systems for Construction Management Tasks. *Journal of Management In*, *32*(February), 1–8. https://doi.org/10.1061/(ASCE)ME

Irizarry, J., Gheisari, M., & Walker, B. N. (2012). Usability Assessment of Drone

Technology As Safety Inspection Tools. *Journal of Information Technology in Construction (ITcon)*, *17*(17), 194–212. Retrieved from http://www.itcon.org/2012/12

Jannadi, O. A., & Almishari, S. (2003). Risk Assessment in Construction. *Journal of Construction Engineering and Management*, *129*(5), 492–500. https://doi.org/10.1061/(asce)0733-9364(2003)129:5(492)

Ji, Y., & Leite, F. (2018). Automated tower crane planning: leveraging 4-dimensional BIM and rule-based checking. *Automation in Construction*, *93*, 78–90. https://doi.org/10.1016/j.autcon.2018.05.003

Kim, K., & Teizer, J. (2014). Automatic design and planning of scaffolding systems using building information modeling. *Advanced Engineering Informatics*, *28*(1), 66–80. https://doi.org/10.1016/j.aei.2013.12.002

Kumar, S., & Bansal, V. K. (2019). Use of GIS in locating TFs safely on a construction site in hilly regions. *International Journal of Construction Management*, *19*(4), 341–353. https://doi.org/10.1080/15623599.2018.1435153

Lee, H., Asce, M., Lee, K., Park, M., Asce, M., Baek, Y., … Asce, A. M. (2012). *RFID-Based Real-Time Locating System for Construction Safety Management*. (June), 366–378.

Lee, K.-P., Lee, H.-S., Park, M.-S., Kim, H.-S., & Baek, Y.-J. (2012). Development of Real-Time Locating System for Construction Safety Management. *Korean Journal of Construction Engineering and Management*, *11*(2), 106–115. https://doi.org/10.6106/kjcem.2010.11.2.106

Liu, P., Chen, A. Y., Huang, Y. N., Han, J. Y., Lai, J. S., Kang, S. C., … Tsai, M. H. (2014). A review of rotorcraft unmanned aerial vehicle (UAV) developments and applications in civil engineering. *Smart Structures and Systems*, *13*(6), 1065–1094. https://doi.org/10.12989/sss.2014.13.6.1065

Lu, W., Huang, G. Q., & Li, H. (2011). Scenarios for applying RFID technology in construction project management. *Automation in Construction*, *20*(2), 101–106. https://doi.org/10.1016/j.autcon.2010.09.007

Manase, D., Heesom, D., Oloke, D., Proverbs, D., Young, C., & Luckhurst, D. (2011). A

gis analytical approach for exploiting construction health and safety information. *Electronic Journal of Information Technology in Construction*, *16*, 335–356.

Marks, E. D., Cheng, T., Teizer, J., & Ph, D. (2013). <*QCO000248.pdf*>. *139*(August), 1006–1014. https://doi.org/10.1061/(ASCE)CO

McKeown, C. (2012). Accident/incident prevention techniques. *Ergonomics*, *55*(12), 1622–1623. https://doi.org/10.1080/00140139.2012.740841

Melzner, J., Zhang, S., Teizer, J., & Bargstädt, H.-J. (2013). A case study on automated safety compliance checking to assist fall protection design and planning in building information models. *Construction Management and Economics*, *31*(6), 661–674. https://doi.org/10.1080/01446193.2013.780662

Mendes, C., Costa, D., & Melo, R. (2018). *Evaluating Uas-Image Pattern Recognition System Application For Safety Guardrails Inspection*. (August), 1–3.

Montaser, A., & Moselhi, O. (2014). Automation in Construction RFID indoor location identi fi cation for construction projects. *Automation in Construction*, *39*, 167–179. https://doi.org/10.1016/j.autcon.2013.06.012

Namian, M., Albert, A., Zuluaga, C. M., & Behm, M. (2016). Role of Safety Training: Impact on Hazard Recognition and Safety Risk Perception. *Journal of Construction Engineering and Management*, *142*(12), 04016073. https://doi.org/10.1061/(ASCE)CO.1943-7862.0001198

Ortiz Coder, P. (2015). Digitalización automática del patrimonio arqueológico a partir de fotogrametría. *Virtual Archaeology Review*, *4*(8), 46. https://doi.org/10.4995/var.2013.4287

OSHA(Occupational Safety and Health Administration). (2016). Competent person. Retrieved August 3, 2019, from https://www.osha.gov/SLTC/competentperson/

Osha. (2014). *Compendio del sector de la construcción*. Retrieved from https://www.osha.gov/Publications/osha3530.pdf

Perlman, A., Sacks, R., & Barak, R. (2014). Hazard recognition and risk perception in construction. *Safety Science*, *64*, 13–21. https://doi.org/10.1016/j.ssci.2013.11.019

Pham, H. C., Dao, N. N., Pedro, A., Le, Q. T., Hussain, R., Cho, S., & Park, C. S. (2018).

Virtual field trip for mobile construction safety education using 360-degree panoramic virtual reality. *International Journal of Engineering Education*, *34*(4), 1174–1191.

Pinto, A., Nunes, I. L., & Ribeiro, R. A. (2011). Occupational risk assessment in construction industry - Overview and reflection. *Safety Science*, *49*(5), 616–624. https://doi.org/10.1016/j.ssci.2011.01.003

Pix4D. (2019). Image acquisition for mapping. Retrieved February 14, 2019, from https://support.pix4d.com/hc/en-us/articles/115002471546-Image-acquisition

Rakha, T., & Gorodetsky, A. (2018). Review of Unmanned Aerial System (UAS) applications in the built environment: Towards automated building inspection procedures using drones. *Automation in Construction*, *93*, 252–264. https://doi.org/10.1016/J.AUTCON.2018.05.002

Reese, C. D. (2011). *Accident/Incident Prevention Techniques*. https://doi.org/10.1201/b11390

Rolf Johansson. (2003). Case study methodology. Retrieved February 3, 2019, from https://www.researchgate.net/publication/236143987_Case_study_methodology

Sacks, R., Perlman, A., & Barak, R. (2013). Construction safety training using immersive virtual reality. *Construction Management and Economics*, *31*(9), 1005–1017. https://doi.org/10.1080/01446193.2013.828844

Sacks, R., Whyte, J., Swissa, D., Raviv, G., Zhou, W., & Shapira, A. (2015). Safety by design: dialogues between designers and builders using virtual reality. *Construction Management and Economics*, *33*(1), 55–72. https://doi.org/10.1080/01446193.2015.1029504

Samad, A. M., Kamarulzaman, N., Hamdani, M. A., Mastor, T. A., & Hashim, K. A. (2013). The potential of Unmanned Aerial Vehicle (UAV) for civilian and mapping application. *Proceedings - 2013 IEEE 3rd International Conference on System Engineering and Technology, ICSET 2013*, 313–318. https://doi.org/10.1109/ICSEngT.2013.6650191

Superintendencia de Seguridad Social. (2015). Informe Anual: Estadísticas de Seguridad

Social. https://doi.org/FUT ORTIZ/T4

Teizer, J. (2008). 3D range imaging camera sensing for active safety in construction. *Electronic Journal of Information Technology in Construction*, *13*(April), 103–117.

Tezel, A., & Aziz, Z. (2017). From conventional to it based visual management: A conceptual discussion for lean construction. *Journal of Information Technology in Construction*, *22*(October), 220–246.

Tuttas, S., Braun, A., Borrmann, A., & Stilla, U. (2017). Acquisition and Consecutive Registration of Photogrammetric Point Clouds for Construction Progress Monitoring Using a 4D BIM. *Photogrammetrie, Fernerkundung, Geoinformation*, *85*(1), 3–15. https://doi.org/10.1007/s41064-016-0002-z

UVS International. (2018). UVS International – Remotely Piloted Systems : Promoting International Cooperation & Coordination. Retrieved November 19, 2018, from https://uvs-international.org/

Vergara, J. (2017). Verticalización. La edificación en altura en la Región Metropolitana de Santiago (1990-2014). *Revista INVI*, *32*(90), 9–49. Retrieved from http://revistainvi.uchile.cl/index.php/INVI/article/view/1095/1343

Wang, J., Zhang, S., & Teizer, J. (2015). Geotechnical and safety protective equipment planning using range point cloud data and rule checking in building information modeling. *Automation in Construction*, *49*, 250–261. https://doi.org/10.1016/j.autcon.2014.09.002

Wierzbicki, D., Kedzierski, M., & Fryskowska, A. (2015). Assesment of the influence of UAV image quality on the orthophoto production. *International Archives of the Photogrammetry, Remote Sensing and Spatial Information Sciences - ISPRS Archives*, *40*(1W4), 1–8. https://doi.org/10.5194/isprsarchives-XL-1-W4-1-2015

Woodcock, K. (2014). Model of safety inspection. *Safety Science*, *62*, 145–156. https://doi.org/10.1016/j.ssci.2013.08.021

Yin, R. K. (2009). Case study research : design and methods. In *Applied social research methods series ;* https://doi.org/10.1097/FCH.0b013e31822dda9e

Zhang, S., Sulankivi, K., Kiviniemi, M., Romo, I., Eastman, C. M., & Teizer, J. (2015).

BIM-based fall hazard identification and prevention in construction safety planning. *Safety Science*, *72*, 31–45. https://doi.org/10.1016/j.ssci.2014.08.001

Zhou, Z., Goh, Y. M., & Li, Q. (2015). Overview and analysis of safety management studies in the construction industry. *Safety Science*, *72*(February), 337–350. https://doi.org/10.1016/j.ssci.2014.10.006

Zhou, Z., Irizarry, J., & Lu, Y. (2018). A Multidimensional Framework for Unmanned Aerial System Applications in Construction Project Management. *Journal of Management in Engineering*, *34*(3), : 04018004. https://doi.org/10.1061/(ASCE)ME.1943-5479.0000597

Zucchii, M. (2015). *Drones: A Gateway Technology to Full Site Automation*.

Zuluaga, C. M., Namian, M., & Albert, A. (2016). Impact of Training Methods on Hazard Recognition and Risk Perception in Construction. *Construction Research Congress 2016*, 2861–2871. https://doi.org/10.1061/9780784479827.285

CHAPTER 3: DEVELOPMENT AND ASSESSMENT OF AN ULTRASOUND-BASED POSITIONING SYSTEM FOR MEASURING HAZARD EXPOSURE TIME AT CONSTRUCTION JOBSITES. CASE STUDY: COLOMBIA

Jhonattan G. Martinez[1], Luis F. Alarcón, Ph.D.., M. ASCE[2] and Roberto M. Luna[3]

3.1 Introduction

A construction site is a diverse, dynamic, and constantly changing place (Teo et al. 2005). As a result, workers face many safety hazards on a daily basis, which produce several consequences such as injuries, illness, disabilities, or even death (US Bureau of Labor Statistics 2018). These factors, together with the frequency and nature of the construction tasks, rank the construction industry one of the most dangerous working environments (Yang et al. 2012). During 2018, 573 people died in the private industry in Colombia; 101 of them passed away in construction environments, which represents 17.2% of the total (Fasecolda 2018). In the same year, 82,470 accidents occurred in construction-related tasks, which represents 12.8% of the private industry total accidents (Fasecolda 2018). To avoid hazard occurrence, safety managers and professionals regularly monitor construction sites (Woodcock 2014). Based on site observation, preventive and corrective actions are carried out to avoid the occurrence of hazardous situations (Perlman et al. 2014). Safety managers walk the jobsite on a daily basis to identify and mitigate unsafe situations. Nevertheless, jobsite monitoring primarily relies on manual efforts, which are time-consuming and error-prone (Park et al. 2016). In addition, the reduced number of safety managers and the dynamic nature, complexity, and size of construction jobsites affect the overall performance and lead to injuries and fatalities among construction workers (Zhou et al. 2018). In addition, the traditional approach for measuring safety indicators relies on manual data collection efforts, and it is error-prone; as a result, data are collected with low frequency or only when an accident occurs (Hinze et al. 2013).

The traditional approach is costly and generally results in data sets that are too small for successful safety management of construction jobsites (Teizer and Vela 2009). To overcome limitations of manual data collection methods, researchers and practitioners are continually exploring other management plans and technologies that would ultimately mitigate construction-related safety hazards. Mixed- and virtual-reality (MR-VR) (Bosché et al. 2016; Eiris et al. 2018; Sacks et al. 2015), building information modeling (BIM) (Kim et al. 2014; Zhang et al. 2015; Ji & Leite 2018), geographic information systems (GIS) (Abune'meh et al. 2016; Bansal 2011; Kumar & Bansal 2019), reality capture and point cloud data (PCD) (Marks et al. 2013; Wang et al. 2015; Gheisari et al. 2018), eye-tracking technology (Dzeng et al. 2016; Hasanzadeh et al. 2017; Jeelani et al. 2018) and positioning technology (Fang et al. 2016; Lee et al. 2012; Montaser & Moselhi 2014) are some examples of various technologies that have been applied for construction safety-related tasks. Positioning technologies have become one of the most promising types of technology, as they allow frequent and accurate observation of construction workplace conditions (Park et al. 2016).

Among positioning technologies, a good number have robust applications for construction safety. Authors such as Awolusi et al. (2018) have claimed that the use of positioning technologies would provide a solution to carry out safety measurements proactively during the construction stages. The accurate positioning capabilities of different positioning sensor-based technologies are one of the most important aspects to conduct some safety management tasks, such as hazard identification and accident forewarning systems (Zhang et al. 2017). The accuracy is defined as the statistical variation among the estimates or measurements of a quantity and the true value of that quantity (Awolusi et al. 2018). For instance, the positioning accuracy is how much the estimated position diverges from the actual position. Based on different construction site conditions and safety management requirements, positioning technologies can be used for (1) tracking components or materials in an uncontrolled and dynamic construction environment (Ergen and Akinci 2007), (2) material inventory management (Lu et al.

2011), (3) workers' location tracking (Costin et al. 2015) and (4) safety monitoring (Lin et al. 2013). The most popular positioning technologies include (1) radio frequency identification (RFID), (2) global positioning system (GPS), (3) ultrawide band (UWB), (4) Bluetooth of low energy (BLE), and (5) ultrasound technology (UST) (Awolusi et al. 2018). In recent years, RFID has been used as a communication technology. It utilizes radio waves for reading electronic tags from a distance automatically (Nath et al. 2006). RFID technology consists of two elements: a communication tag installed into the object to be identified and a reader that is capable of detecting a tag's unique transmitted frequency and its identification. RFID is considered one of the most common positioning system used (Awolusi et al. 2018). However, RFID's attainable accuracy ranges from 3 to 10 m, which renders it suboptimal for safety-related applications. Compared with other positioning technologies, RFID provides noncontact data transfers between tags and readers, without the need for a strictly obstacle-free or line-of-sight reading (Lin et al. 2013). Nevertheless, limitations such as signal interference due to metal or liquid surfaces and the high implementation cost affect proper implementation of this technology (Michael and Mccathie 2005). GPS is a satellite-based navigation system composed of receivers that use satellite information for calculating the user's exact position through triangulation (Ni 2016). The position is determined by measuring the distance from a set of satellites to the GPS receiver, the duration of the GPS signal travel from the satellite, and the speed of light (Zito et al. 1995). GPS typically has better accuracy than RFID technology, offering an absolute attainable positioning accuracy ranging between 1 m and 10 m. Advantages such as easy installation, real-time data transfer, and affordability make this technology widely used in several industries (Pradhananga and Teizer 2013). Despite its multiples advantages for positioning tasks, factors such as the need for a clear line of sight and several calibration points to determine an accurate position of the object, poor performance in indoor environments as well as its high implementation cost compared with other positioning technologies might affect its proper application for safety-related tasks (Nasr et al. 2013). BLE is a low-cost and low-energy-consumption device designed for short-range wireless communication between devices (Cho et al. 2015). This system can be connected

to several types of devices, including cellphones, laptops, or other technological gadgets, providing positioning accuracy up to 2 m. The main disadvantages of BLE are its short-communication range and the low rate of data transfers (Mackensen et al. 2012). The UWB approach is a network of different receivers and tags communicating with each other over a large bandwidth greater than 500 MHz. The tags are in charge of broadcasting UWB radio pulses, which activate the system to locate their 3D position coordinates (Shahi et al. 2012). In contrast to other technologies, UWB is less prone to signal interference and easily passes through obstructions due to it being capable of transmitting data over a large bandwidth. Some researchers report an accuracy range between 0.1 m and 2 m under laboratory conditions. However, drawbacks such as its very short-range signal and signal interference due to metal objects affect its positioning accuracy (Wierzbicki et al. 2015). Finally, UST relies on the measurement of the distance between stationary beacons and the mobile unit. To measure the distance between the transmitter (a mobile unit that is represented by a user) and a static receiver's network, the principle of measuring the time of the received signal (TOA - Time of Arrival) is employed. On the other hand, the location of the mobile unit is determined by applying the principle of trilateration. Based on several studies conducted in different test environments, the attainable accuracy of this technology was established to be between 1 and 2 cm (Ilkovicova 2016). Nevertheless, factors such as changing weather conditions (temperature) and the need for a clear line of sight might affect its reliability in terms of accuracy levels.

Several types of methods based on the aforementioned positioning technologies have been tested and used in jobsite environments. In early studies, Giretti et al. (2009) discussed a UWB-based-safety method for real-time monitoring of workers and machinery in an outdoor environment. The positioning system was interfaced with software that allows identifying and recording hazardous situations. At the same time, Jang and Skibniewski (2009) developed an embedded positioning sensor system intended to track construction assets by combining RFID and UST. The results obtained showed a positioning error of 5 cm using the trilateration approach. Later, Pyeon et al. (2010)

investigated the feasibility of a Wi-Fi-based indoor positioning system for tracking workers' locations, vehicles, and materials. The system uses a fingerprint method of received signal strength indication (RSSI) from each access point (AP). The research was conducted in a shield tunnel, reaching an accuracy of 5 m on-site. Carbonari et al. (2011) developed and tested a prototype UWB-based positioning system for proactive safety management and real-time alerting to prevent hazards produced by possible falling objects at construction sites. Based on the results obtained in both lab and construction site testing, the reachable accuracy of the UWB-based positioning system was up to 1 m. Lee et al. (2012) created an RFID-based real-time locating system capable of providing accurate and robust positioning on construction jobsites, where the availability of the RFID signal is difficult to maintain due to moving objects. Wu et al. (2013) tailored an approach using an RFID sensor network for tracking struck-by-falling object accidents; this network is based on real-time information for avoiding hazardous situations. Riaz et al. (2014) developed an integrated system based on wireless sensor technology and BIM, intending to improve the visualization for effective workers' safety monitoring in confined spaces on construction jobsites. Costin et al. (2015) presented a method for integrating RFID technology and BIM for tracking construction workers in real time. The combination of these technologies into one system generated valuable data that were used for real-time resource tracking, zone safety violation, and data analysis.

Golovina et al. (2016) presented a GPS based-method for recording, identifying, and analyzing interactive hazards near-miss situations between workers-on-foot and heavy construction equipment. The data were collected by GPS to automatically calculate a hazard index, which is presented as a heat map. At the same time, Park et al. (2016) combined BLE and building information modeling (BIM) for monitoring workers' locations, recognition and registration of potential hazards, real-time detection of unsafe incidents, and reporting and sharing of the detected events with the relevant participants in real time. The system is composed of BLE sensors and a cloud-based communication network capable of communicating with positioning devices for gathering all the relevant

information and sharing it in real time with stakeholders. At the same time, Kim et al. (2016) developed an RFID-based system that is capable of automatically identifying hazard in workers' movement paths through worker location tracking. The system utilizes real-time tracking to detect unknown hazards that were not previously identified and to reduce the duration that such hazards remain with any safety corrective. On the other hand, signal interference due to the presence of several jobsite obstacles was stated as a limitation in this study. Nowotarski et al. (2017) used BLE technology in a building environment to examine and perform range tests on these devices with the aim of improving construction safety-related tasks. Later, Kim and Han (2018) developed an RFID-based real-time locating system capable of improving the accuracy of real-time location tracking at construction jobsites. In addition, the research introduced an algorithm intended to mitigate the tracking error caused by the multipath effect.

More recently, Siddiqui et al. (2019) applied a wireless UWB RTLS approach for tracking construction equipment on a congested construction site for a high-rise building. The wireless UWB system performance was analyzed using pose estimation methods. The developed system shows that it can be used under harsh construction site conditions. At the same time, Pittokopiti and Grammenos (2019) implemented a low-cost, battery-powered Ultra-Wideband (UWB)-based collision avoidance system that can detect potential crash between vehicles and workers on real-time for construction safety application. The main advantage of this system is that it does not require fixed infrastructure. Recently, Jo et al. (2019) created a robust construction safety system based on a UWB-based proximity warning system and GPS technology to avoid hazards due to being caught in between heavy machinery on construction jobsites. Despite the advantages of this safety system, the author stated that its accuracy might be affected by environmental factors such as temperature and humidity. Table 5 presents the level of accuracy of each positioning system and their drawbacks regarding their implementation:

Table 5. Positioning sensors (accuracy levels and their drawbacks)

		Limitations						
Positioning approach	Level of accuracy	Signal interference	High-implementation cost	Require a clear line of sight	Short communication range	Weather conditions (Temperature)	Low positioning accuracy
Radio frequency identification (RFID)	3 m to 10 m	■	■	■				■
Global positioning system (GPS)	1 m to 25 m		■	■				
Bluetooth of low energy (BLE)	Up to 2 m				■			
Ultrawide band (UWB)	0.1 m to 2 m	■			■			
Ultrasound technology (UST)	0.01 m to 0.05 m			■		■		

To summarize, the limitations reported in the previous research discussed above include several factors that could affect the usage of positioning technologies for safety monitoring-related applications on construction jobsites. First, authors repeatedly indicated that signal interference affects the positioning sensor reliability and accuracy. This interference is particularly generated by metal object or surfaces, which can be present at almost all construction sites. In addition, metal objects are known to produce multipath reflection of the positioning sensor signal. Second, the implementation cost of some positioning sensors has hindered their proper implementation in the construction industry. Proper monitoring of a jobsite requires the installation of many sensors on workers and the site, increasing the implementation cost of the positioning technology. Third, most of the positioning sensors investigated require a clear line of sight between the transmitter and receivers to determine the locations of objects. In general, jobsites present several obstacles that might affect this requirement, such as concrete walls, cranes, and building structures. Fourth, a short-communication range between receivers and transmitters plays a vital role in the positioning sensor precision and accuracy. Since a construction site is a dynamic and changing environment, it is required that positioning technology be capable of adapting to this condition. Unfortunately, most of the positioning technology discussed previously offer a short-communication range that results in difficulty tracking construction workers

in this type of environment. Finally, weather conditions, especially the temperature, might affect the positioning sensor reliability. High temperature can cause a systematic deviation in the signal frequency, affecting the positioning sensor accuracy. This specific aspect might be a disadvantage for the application of some types of positioning technologies in outdoor construction environments.

3.2 Research Problem and Objectives

While the application of various positioning technologies has demonstrated their potential as a tool to support safety management tasks, several limitations affect their full implementation in the construction domain. Limitations stated by different authors previously presented such as (1) short-communication range, (2) weather conditions, (3) low positioning accuracy, (4) high implementation cost, and (5) the need for a clear line of sight represent some implementation-related limitations that affect positioning technologies for safety-related applications. The limitations mentioned above highlight the necessity of implementing an accurate and reliable positioning system that allows overcoming most of these gaps. Propelled by the abovementioned gaps, this study introduces the development and assessment of an ultrasound-based positioning system that ultimately enhances the accuracy and reliability of determining workers' locations at active jobsites. This study aims to develop and assess an ultrasound-based positioning system to determine workers' hazard exposure time and their proximity to hazardous areas. To accomplish this objective, two stages were carried out:

a) An ultrasound-based positioning system was developed using open-source hardware known as the Mavelmind Robotics® Indoor Navigation System, and software packages capable of registering and analyzing the data log were generated.
b) A performance assessment of the developed system was conducted in an indoor construction environment to determine its accuracy, reliability, and usefulness for safety-related applications.

The outcomes of this study would benefit construction safety managers and researchers by helping them to understand the integration of the ultrasound-based positioning system in the current safety monitoring process and recognize the requirements and challenges for such incorporation in safety management-related tasks. The scope of this study was limited to safety hazards associated with physical jobsite conditions. The risks associated with human factors and psychological, organizational, and physical variables were not contemplated in this study.

3.3 Research Methods

The research was conducted as an attempt to assess the implementation of an ultrasound-based positioning system in a real construction environment. To accomplish this goal, two stages were carried out: (1) the ultrasound-based positioning system development and (2) the ultrasound-based positioning system performance assessment on a real construction jobsite. The first stage consisted of developing the ultrasound-based positioning system using a well-known off-the-shelf system known as Mavelmind Robotics® Indoor Navigation. Then, to enable the system deployment, a set of field experiments were conducted to validate its accuracy and usefulness for measuring hazard exposure times. Figure 12 shows the methodology used for the case study.

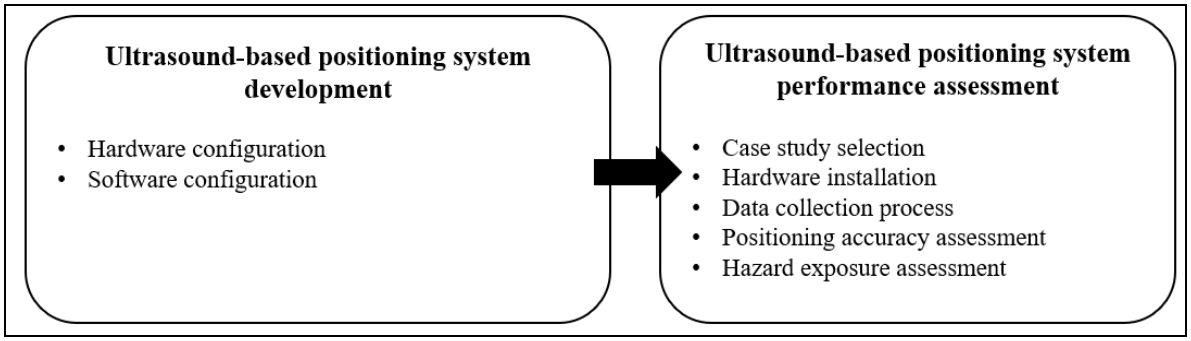

Figure 12. Research methodology steps

This section will further discuss each step of the research methodology process.

3.4 Ultrasound-Based Positioning System Development

In the first stage of the study, an ultrasound-based positioning system was developed using a commercially available technology known as the Mavelmind Robotics® Indoor Navigation System. Hardware components such as stationaries beacons, mobiles beacons, and a modem/router were configured and tuned through a ground station (laptop Asus VivoBook Pro 510U). Subsequently, the beacons and the modem/router were connected using open-source software known as Mavelmind Robotics® Robo Manager version 6.160. The data recorded (position along X, Y, and Z) through this software were then exported and analyzed in Microsoft® Excel. The stages carried out to accomplish this task were the following:

3.4.1 Hardware configuration

Mavelmind Robotics® Indoor Navigation was the hardware selected for this research. This off-the-shelf system has an attainable accuracy ranging of 0.02 m under lab conditions. Its high level of accuracy, low implementation cost, low energy consumption, and reliability in terms of signal strength under controlled conditions were some of the factors considered when selecting this hardware (Amsters et al. 2019). During the research, six (6) stationary ultrasonic beacons, one (1) mobile beacon and one (1) modem/router linked to each one via a radio interface were used. These components together are capable of providing a theoretical total coverage area of up to 1.000 m^2 (Marvelmind 2019). Moreover, based on the technical features established on the operation manual, the distance between the two nearest beacons needs to be up to 30 m at maximum. The mobile beacon's position (X, Y, and Z) is calculated based on the propagation delay of the ultrasonic pulses between stationary beacons and the mobile beacon through a trilateration-based method. This approach consists of calculating the object's absolute or relative position based on simultaneous range measurement from at least three stations located at know places (Shchekotov 2014; Thomas and Ros 2005). Despite their reliability and high level of accuracy, ultrasound-based positioning systems are significantly affected by not only the

multipath effect but also the temperature (Ilkovicova 2016). For that reason, this technology is more suitable for indoor environments. The maximum update rate for tracking a single beacon is 433 MHz. The description of each system component is as follows:

1. *Stationary Beacons (Figure 13a):* These beacons are responsible for measuring the distances between other beacons using ultrasonic pulses. For the proper operation of the system, an unobstructed line of sight is required between the three fixed and mobile beacons. Each beacon includes an internal 1000 mAh LiPo battery providing at least two days of power. The weight of each beacon is 54 grams, and its size is 55 mm x 55 mm x 65 mm. The beacons are equipped with a full-size 165-mm antenna that provides a connection with the router.

2. *Mobile beacon (Figure 13a):* The location of this beacon is calculated based on the propagation delay of ultrasonic pulses. Similar to the stationary beacons, the mobile beacon is equipped with a full-size antenna that provides a connection with the router.

3. *Modem/router (Figure 13b):* the modem/router is the central controller of the ultrasound-based positioning system. This device is capable of broadcasting ultrasonic pulses up to 45 MHz to calculate the positions of mobile beacons. A single router can support up to 30 mobile beacons at the same time. The router is equipped with a full-size 165-mm antenna that provides the connection with both stationaries and mobile beacons. The router is connected by a USB cable to the ground station and then synchronized with the Mavelmind Robotics® Robo Manager Software. The device weighs 42 grams in total.

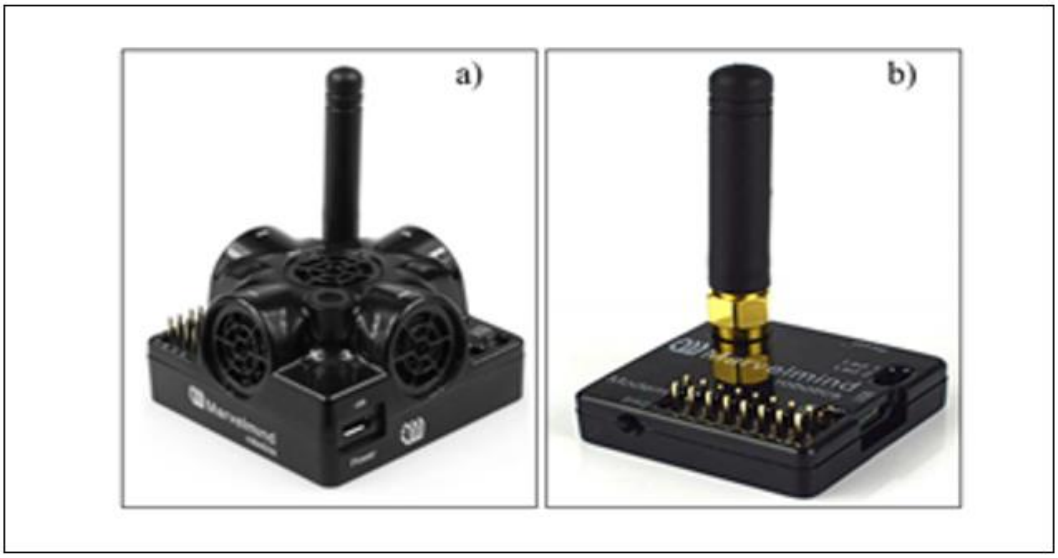

Figure 13. Ultrasound-based positioning components: (a) mobile/stationary beacon; (b) modem/router

The technical features of this system are summarized in Table 6:

Table 6. Ultrasound-based positioning system components and characteristics

NAME	MODEL MANUFACTURER	CHARACTERISTICS
STATIONARY BEACONS AND MOBILE BEACON (X5)	Mavelmind Robotics ® 433 MHz	• Weight: 54 g • Size: 55 x 55 x 65 mm • Internal battery: 1000 mAh LiPo • Battery lifetime: 2 days approximately. • Distance reached: Up to 50 m in lab conditions • Differential precision: 0.02 m • Radio interface: 433 MHz
MODEM (X1)	Mavelmind Robotics ® 433 MHz	• Weight: 13.6 g • Size: 35 mm x 35 mm x 10.6 mm • Distance reached: Up to 50 m in lab conditions

3.4.2 Software configuration

Two types of software were adopted for the ultrasound-based positioning system development. First, Mavelmind Robotics® Robo Manager version 6.160 was used as a central platform to connect the stationary and mobile beacons to the router. Features such as its compatibility with the ultrasound-based positioning hardware and its ease of use were factors considered when selecting this software. The software technical features allow

calculating the cartesian position of mobile and stationary beacons in real time along the X-, Y-, and Z-axes. In addition, the software can provide visual tracking locations of both stationary and mobile beacons by categorizing them using two different colors: blue (mobile beacons) and green (stationary beacons). The positioning coordinates obtained by this software can be exported as comma-separated values (CVS) to a database and subsequently used to calculate construction safety indexes (CSIs). Microsoft® Excel was selected as data base software to analyze the positioning data set. Figure 14 presents the system configuration:

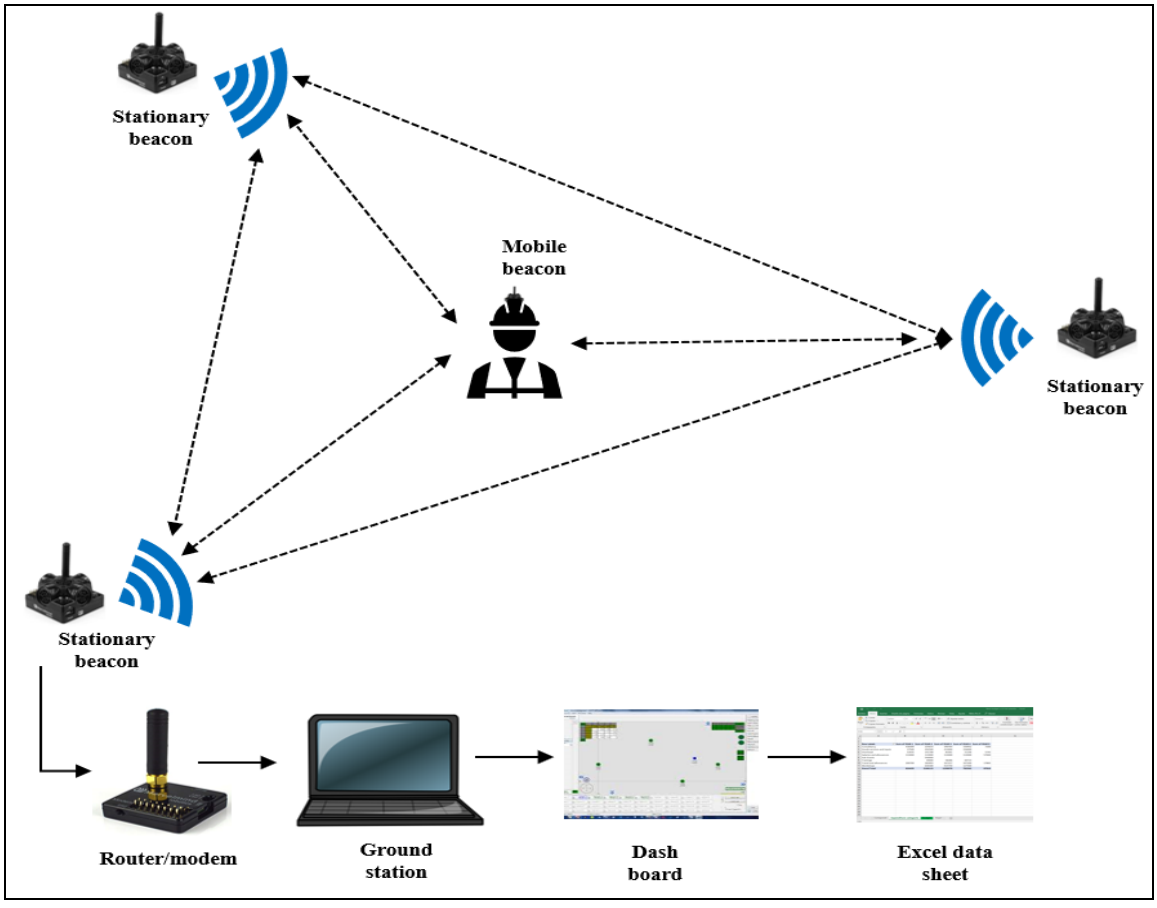

Figure 14. Software system configuration

3.5 Ultrasound-Based Positioning System Performance Assessment

3.5.1 Case study description

To further validate the ultrasound-based positioning system performance, a real construction site was selected for conducting a field experiment. The construction site consisted of one indoor facility located at the Popular University of Cesar, Colombia (10°30'03.5"N 73°16'10.4"W). The jobsite included seven (7) rooms with a 180 m^2 total area, divided using concrete walls. Ongoing construction activities at the time of data collection mainly included (1) demolition, (2) building concrete walls, and (3) debris movement. Based on the research conducted by Ilkovicova (2016), this type of construction area tends to block signal lines of sight, causing interference and signal degradation.

3.5.2 Hardware installation

A total of six (6) stationary beacons were set up on the jobsite walls. To guarantee reliable signal communication between the router and the mobile beacon, three stationary beacons were placed on the walls of the selected area at a height of 2 m above ground level (AGL). The positioning coordinates (X, Y) and the identification number (1, 2, 3, 4, 5 and 6) of each stationary beacon installed on the jobsite are presented in Table 7. For this specific construction site, it was not required to determine the mobile beacon's position along the Z-axis due to its entire surface being located at the same height AGL. In addition, a mobile beacon was installed on a worker's hard hat to track the worker's position during the experiment.

Table 7. Stationary beacons' positioning coordinates

	Stationary beacon cartesian position (m)	
Beacon number	X	Y
1	0.00	0,00
2	4.00	0.00
3	4.00	-5.00
4	7.00	-12.00
5	11.00	-5.00
6	11.00	-12.00

Moreover, to perform both the positioning accuracy assessment and the hazard exposure assessment, two jobsite areas considered by the safety manager in charge as potentially hazardous were selected. The presence of several items that could lead to worker accidents was the main reason to select these two hazardous areas for conducting the experiment. Prior to beginning the data collection process, the actual cartesian positions (X, Y) of each hazardous area were measured and then demarked by measuring tape. Figure 15 present the jobsite layout and locations of the stationary beacons and hazardous areas:

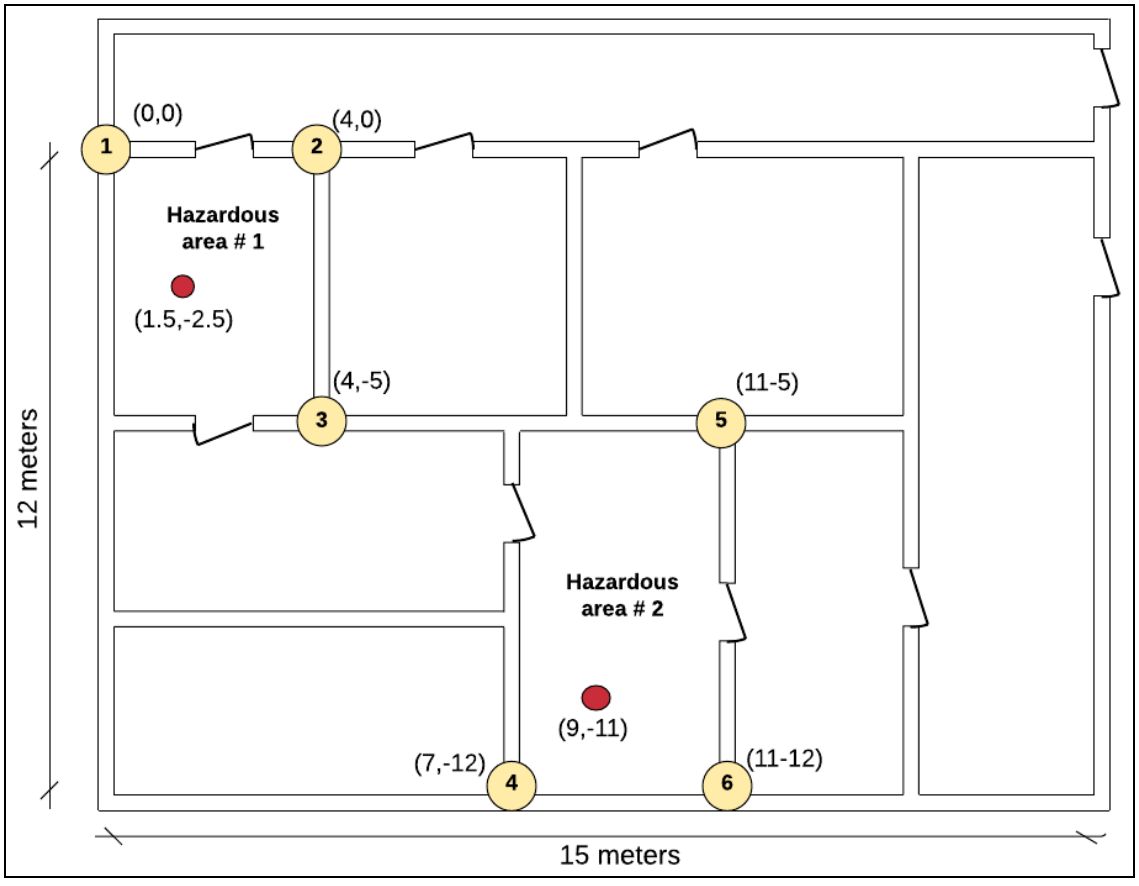

Figure 15. Jobsite layout

The characteristics of each hazardous areas (Table 8) are described as follows:

- *Hazardous area # 1:* In this specific area, construction activities such as floor demolition and installation of MEP (mechanical, electrical, and plumbing) were conducted during the field experiment. These types of construction tasks could lead to tripping and struck-by hazards among workers (Figure 16a and 16b).
- *Hazardous area # 2:* In this area, construction activities such as wall demolition and roof girder installation were carried out. The development of these construction activities could produce tripping and fall hazards among workers (Figure 16c and 16d).

Table 8. Hazardous areas positioning coordinates

	Stationary beacon cartesian position (m)	
Hazardous area	X	Y
1	1.50	-2.50
2	9.00	-11.00

Figure 16. Jobsite hazardous areas: (a) Hazardous area # 1 (frontal); (b) Hazardous area # 1 (side); (c) Hazardous area # 2 (frontal); (b) Hazardous area # 2 (side)

3.5.3 Data collection process

The data collection process was performed in two stages. The first stage was carried out on January 20th, 2020. The indoor and outdoor temperatures during the first data collection period (10 am - 3 pm) were 36°C and 31°C respectively. To accomplish the data collection, one (1) mobile beacon was placed forty times in hazardous areas # 1 and # 2 to determine its estimated position using the ultrasound-based positioning system. Later, the positioning data recorded were exported to Microsoft® Excel and then analyzed to calculate the system positioning error using the approach described in section 3.5.4. The second data collection process was performed on January 21st, 2020. For the data collection period, the indoor and outdoor temperatures (8 am - 6 pm) were 29°C and 31°C, respectively. During this process, a worker's hard hat was equipped with a mobile beacon in order to track the worker's movement across the jobsite. During approximately one working day (eight hours), the mobile beacon's position was recorded, and then the data log generated (log time and positioning) was exported and analyzed to calculate the overall time that the worker was in hazardous areas # 1 and # 2.

3.5.4 Positioning accuracy assessment

The accuracy assessment of the ultrasound-based positioning system was evaluated through statistical analysis. The analysis consisted of assessing the positioning accuracy along the *X*- and *Y*-axes or, in other words, the planimetric accuracy. This process was carried out by retrieving the position of the mobile beacon and comparing this to its actual location. To accomplish this, two jobsite locations were selected (see Figure 15) and then their positions measured. The actual positioning coordinates of each location are shown in Figure 15 (red circles). The comparative analysis was performed using the mean absolute error (*MAE*), standard deviation (*SD*), root mean square error (*RMSE*) and modular error (*ME*) (Cuartero et al. 2010). The last is one of the most common approaches used for assessing coordinate positioning accuracy (Rempel 2016). MAE was calculated by computing the sum of the actual positioning values (d_{ai}) minus the observed positioning

coordinate positions (d_{oi}) and then dividing by the total number of iterations. The difference, or error, between the actual (d_{ai}) and observed (d_{oi}) position is known as e_i. The standard deviation (*SD*) indicates the dispersion of observed positioning coordinate values concerning their actual positions. It was calculated by computing the square root of the sum of the square of e_i minus $\bar{e_i}$ (average of all the e_i) divided by total number of interactions. On the other hand, the RMSE represents the square root of the differences between predicted values (d_{ai}) and observed values (d_{oi}). The ME was used for calculating the magnitude of the error, which is a vector with two cartesian components (*X* and *Y*). This magnitude is equivalent to the square root of the sum of the square of $RMSE_x$ and $RMSE_y$, corresponding to the magnitude of the error along X and Y.

$$MAE = \frac{1}{n}\sum_{i=1}^{n}|d_{ai} - d_{oi}| = \frac{1}{n}\sum_{i=1}^{n}|e_i| \quad (1)$$

$$SD = \sqrt{\frac{\sum_{i=1}^{n}|e_i - \bar{e_i}|^2}{n-1}} \quad (2)$$

$$RMSE = \sqrt{\frac{\sum_{i=1}^{n}(e_i - \bar{e_i})^2}{n}} \quad (3)$$

$$ME = \sqrt{(RMSE_x)^2 + (RMSE_y)^2} \quad (4)$$

3.5.5 Hazard exposure assessment

A study conducted by Mitropoulos et al. (2005) defined exposure to hazards when workers are near potentially hazardous zones. Exposure to hazards produces the potential for an accident but does not automatically lead to one. For instance, a worker near an unprotected edge will not necessarily fall. Based on this statement, the time for which a worker is exposed to hazards during the workday is called the hazard exposure time. For this research, a worker's location was determined through the ultrasound-based positioning system in order to calculate their hazard exposure time. The data log generated (X and Y positions and time of the event) were recorded and then analyzed to determine the amount of time for which the worker was exposed to hazardous areas # 1 and # 2. The hazard exposure time was calculated by dividing the number of hours for which the worker was

within the coordinates pertaining to hazardous areas by the total duration of the experiment. The following formula was used to perform this calculation:

$$\%\ Hazard\ exposure\ time = \frac{Time\ into\ hazardous\ area\ \#\ 1\ and\ \#\ 2}{Total\ time\ recorded} \times 100\% \qquad (5)$$

In addition, the percentage of time that the ultrasound-based positioning system was unable to establish the worker's position while moving along the jobsite was calculated. To determinate this time, the following equation was employed:

$$\%\ positioning\ time\ no\ calculated = \frac{Positiong\ \ time\ no\ calculated\ by\ the\ system}{Total\ time\ recorded} \times 100 \qquad (6)$$

3.6 Results and Discussion

The planimetric accuracy of the ultrasound-based positioning system was analyzed using the formulas discussed in section 3.5.4. Tables 9 and 10 present the results of the accuracy assessment in meters (m) for each hazardous area. The actual position column represents the previously determined locations of hazardous areas #1 and #2. The observed position column indicates the locations of hazardous area #1 and #2 established by the ultrasound-based positioning system. Finally, the difference column presents the absolute values of the differences between the actual and observed positions along the X- and Y-axes.

Table 9. Accuracy assessment results (hazardous area # 1)

	Actual position (m)		Observed position (m)		Difference (m)	
N	X	Y	X	Y	d (x)	d(y)
1	1,50	-2,50	1,52	-2,57	0,02	0,07
2	1,50	-2,50	1,56	-2,51	0,06	0,01
3	1,50	-2,50	1,45	-2,52	0,05	0,02
4	1,50	-2,50	1,55	-2,57	0,05	0,07

	Actual position (m)		Observed position (m)		Difference (m)	
N	X	Y	X	Y	d (x)	d(y)
5	1,50	-2,50	1,52	-2,51	0,02	0,01
6	1,50	-2,50	1,55	-2,51	0,05	0,01
7	1,50	-2,50	1,60	-2,65	0,10	0,15
8	1,50	-2,50	1,56	-2,51	0,06	0,01
9	1,50	-2,50	1,45	-2,47	0,05	0,03
10	1,50	-2,50	1,57	-2,55	0,07	0,05
11	1,50	-2,50	1,43	-2,51	0,07	0,01
12	1,50	-2,50	1,54	-2,60	0,04	0,10
13	1,50	-2,50	1,45	-2,55	0,05	0,05
14	1,50	-2,50	1,48	-2,56	0,02	0,06
15	1,50	-2,50	1,45	-2,70	0,05	0,20
16	1,50	-2,50	1,48	-2,55	0,02	0,05
17	1,50	-2,50	1,47	-2,60	0,03	0,10
18	1,50	-2,50	1,55	-2,57	0,05	0,07
19	1,50	-2,50	1,45	-2,54	0,05	0,04
20	1,50	-2,50	1,51	-2,45	0,01	0,05
			MAE		0,05	0,06
			SD		0,02	0,05
			$RMSE_X$ and $RMSE_Y$		0,05	0,08
			ME		0.09	

Table 10. Accuracy assessment results (hazardous area # 2)

	Actual position (m)		Observed position (m)		Difference (m)	
N	X	Y	X	Y	d (x)	d(y)
1	9,00	-11,00	9,01	-11,05	0,01	0,05
2	9,00	-11,00	9,05	-11,05	0,05	0,05
3	9,00	-11,00	9,06	-11,10	0,06	0,10
4	9,00	-11,00	8,95	-10,95	0,05	0,05
5	9,00	-11,00	8,95	-10,97	0,05	0,03
6	9,00	-11,00	8,95	-11,07	0,05	0,07
7	9,00	-11,00	8,99	-11,03	0,01	0,03
8	9,00	-11,00	9,05	-11,05	0,05	0,05
9	9,00	-11,00	8,94	-11,04	0,06	0,04
10	9,00	-11,00	9,06	-10,80	0,06	0,20
11	9,00	-11,00	9,06	-10,97	0,06	0,03
12	9,00	-11,00	8,97	-11,07	0,03	0,07
13	9,00	-11,00	8,95	-11,05	0,05	0,05
14	9,00	-11,00	8,99	-10,94	0,01	0,06
15	9,00	-11,00	8,93	-10,97	0,07	0,03
16	9,00	-11,00	8,95	-11,04	0,05	0,04

	Actual position (m)		Observed position (m)		Difference (m)	
N	X	Y	X	Y	d (x)	d(y)
17	9,00	-11,00	8,95	-10,90	0,05	0,10
18	9,00	-11,00	8,99	-10,92	0,01	0,08
19	9,00	-11,00	8,95	-11,03	0,05	0,03
20	9,00	-11,00	8,99	-10,95	0,01	0,05
MAE					0,04	0,06
SD					0,02	0,04
$RMSE_X$ and $RMSE_Y$					0,05	0,07
ME					0.09	

In addition, the average results for hazardous areas # 1 and 2 are presented in Table 11.

Table 11. Average results for hazardous areas #1 and 2

	d (x) (m)	d (y) (m)	SD_x (m)	SD_y (m)	RME_x (m)	RME_y (m)	ME (m)
Hazardous area # 1	0,05	0,06	0,02	0,05	0,05	0,08	0,09
Hazardous area # 2	0,04	0,06	0,02	0,04	0,05	0,07	0,09
Average	0,04	0,06	0,02	0,04	0,05	0,07	0,09

After reviewing the planimetric error analysis, the following observations can be stated:

- *Positioning accuracy assessment:* The results of the MAE analysis revealed that the ultrasound-based positioning system was more accurate along the X-axis compared to the Y-axis. This finding can be concluded based on the results obtained for the SD, which disclosed that the dispersion of the observed values along the X-axis was less than that along the Y-axis. Moreover, similar results were obtained for $RMSE_x$ and $RMSE_y$, which indicated a lower level of accuracy along the Y-axis. Despite the $RMSE_x$ and $RMSE_y$ results being different for each hazardous area, the ME results were similar. The ME error results show that the ultrasound-based positioning system total accuracy obtained during the experiment (0.09 m) was less than its attainable accuracy (0.02 m). The accuracy reached during the experiment (0.09 m) was 350% lower than the attainable accuracy. Many factors could have affected the overall accuracy of the ultrasound-based positioning system during the experiment. For instance, factors such as signal interference due to the presence of

several jobsite obstacles, such as debris or scaffolds, as well as the high temperature during the data collection process could have affected the overall accuracy. However, the ultrasound-based positioning accuracy level obtained during the experiment would be useful for tracking workers indoors, particularly if the data are compared with the attainable accuracy of other positioning technologies previously discussed. Further research is warranted to determine the effects of jobsite obstacles and the temperature on the ultrasound-based positioning system accuracy.

- *Hazard exposure assessment:* The result obtained though the hazard exposure assessment (see Figure 17) showed that the worker was exposed to both hazardous areas # 1 and # 2 for a total of 4 hours and 23 minutes during the workday (8 am – 12 pm and 2 pm to 6 pm). This finding indicates a hazard exposure of 54.79% during this period. In the first half of the workday, the worker spent 3 hours and 3 minutes in these two areas (38.12%), while during the second half, the worker spent 1 hour and 20 minutes in total (21.67%). During this experiment, the presence of several obstacles located in the hazardous areas did not affect the ultrasound-based positioning system's reliability. In fact, the system could determine the worker's position within the hazardous areas all of the time with no signal interference. In contrast, the ultrasound-based positioning system was not capable of retrieving the worker's position for approximately 3 hours and 37 minutes. During this time, the mobile beacon mounted on the worker's hard hat was not capable of broadcasting the worker's real-time position to the stationary beacons. The main reason behind this issue was the signal interference occurred due to the concrete walls that separate the hazardous areas of other jobsite locations. This finding confirms the need for a clear line of sight between the mobile and stationary beacons.

- *Positioning reliability assessment:* Based on the data log recorded by the positioning accuracy assessment, the ultrasound-based positioning system was capable of determining the position of the mobile beacon during the entire data collection process. This result indicates that the system has a reliability of 100% when the mobile beacon positioning is obtained by at least three stationary beacons and these are located at fixed positions. Similar results were obtained during the hazard exposure assessment. For this specific scenario, the mobile beacon mounted on a worker's hard hat was moved around the jobsite. During this time, the ultrasound-based positioning system established the worker's position without any interference or lag. Therefore, it can be concluded that the system had 100% reliability for this type of scenario. However, the mobile beacon's position could not be determined in certain jobsite areas where stationary beacons were not installed. This result indicates that the system is not capable of establishing positions of objects without a clear line-of-sight between the mobile and stationary beacons (Zhang et al. 2017). Further research that measures the positioning reliability at other types of jobsites is required.

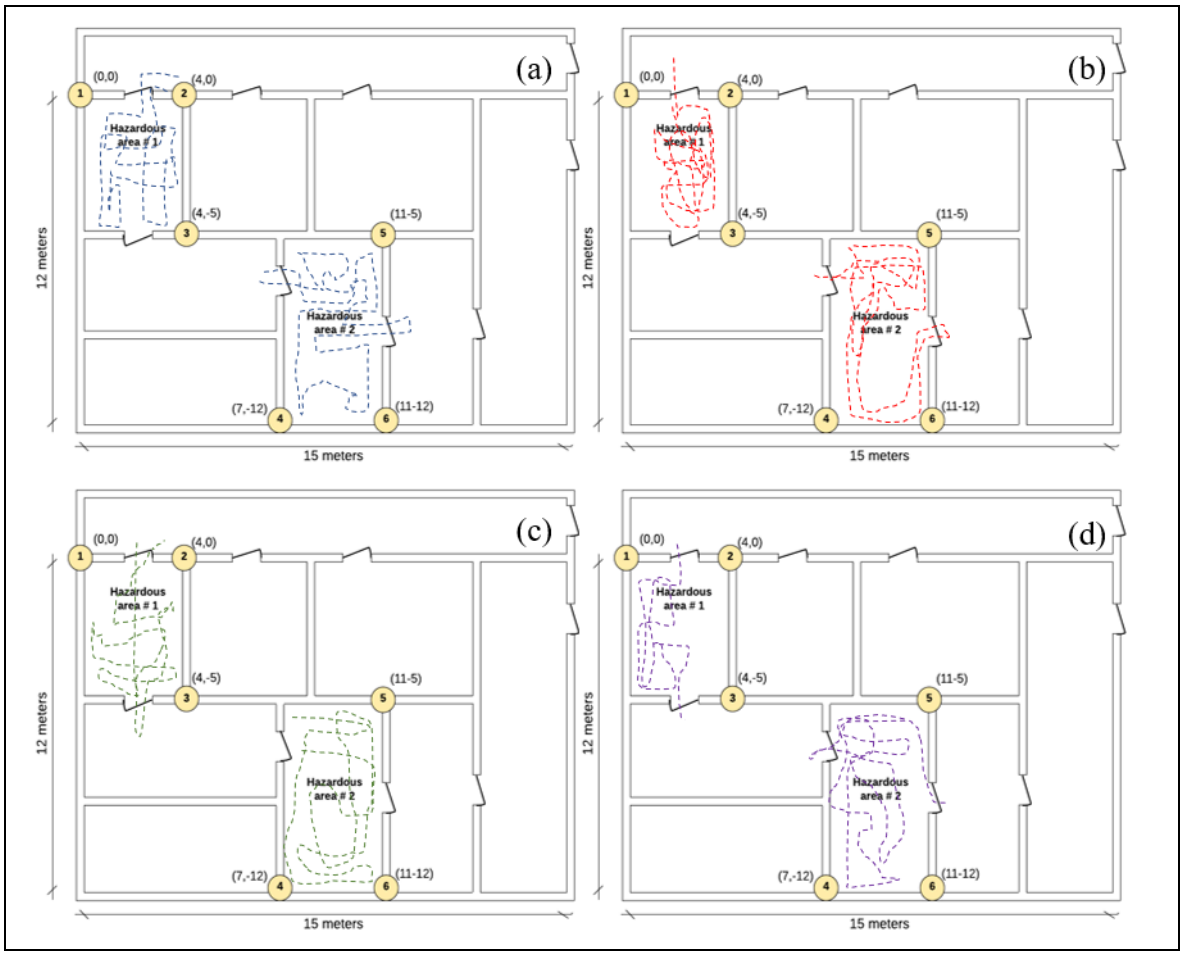

Figure 17. Worker hazard exposure time: (a) worker exposure to hazardous areas # 1 and #2 (8 am to 10 am); (b) worker exposure to hazardous areas # 1 and #2 (10 am to 12 pm); (c) worker exposure to hazardous areas # 1 and #2 (2 pm to 4 pm); (b) worker exposure to

3.7 Limitations and Conclusion

In this study, an ultrasound-based positioning system was developed, and then its performance was assessed at a real construction jobsite. For this purpose, a well-known off-the-shelf indoor navigation system known as Mavelmind Robotics® Indoor Navigation was used as the hardware. This system includes stationaries beacons, mobile beacons, and a router/modem that together can estimate the positions of objects. To connect the beacons to the modem/router and visualize the positions of objects, an open-source software package known as Mavelmind Robotics® Robo Manager version 6.160 was used. The data

log generated through this open-source software were exported and analyzed in Microsoft® Excel. The performance of the developed system was assessed at a real construction site to determine its accuracy level and usefulness in measuring workers' hazard exposure times. The level of accuracy was determined by comparing the actual and observed positions of the mobile beacon and then analyzing the data through statistical approaches.

The results revealed that the ultrasound-based positioning system total accuracy obtained during the experiment (0.09 m) was lower than its attainable accuracy (0.02 m). In other words, the overall accuracy reached during the experiment was 350% lower than its attainable accuracy. Factors such as signal interference due to the presence of several jobsite obstacles, such as debris or scaffolds, as well as the high temperature during the data collection process could have affected the overall accuracy. However, such a level of accuracy might be useful for many safety-related tasks, especially if it is compared with the accuracies of other commercially available positioning sensors. Regarding the hazard exposure assessment, an ultrasound-based positioning system could retrieve the worker's position while he stayed within the hazardous areas. Nevertheless, the position of the worker outside these areas could not be calculated. This finding indicates the need for a clear line of sight between mobile and stationary beacons for calculating the positions of mobile objects.

Construction safety managers and professionals might benefit from the study outcomes by better understanding of the developing and testing of an ultrasound-based positioning system to determine workers' hazard exposure times and their proximity to hazardous areas. However, this research has some limitations that need to be stated. First, due to the limited number of stationary beacons installed on the jobsite, it was not possible to determine the worker's position outside of hazardous areas # 1 and # 2. Further research is warranted to assess the developed system using more stationary beacons on the jobsite. Second, despite it being well known that temperature plays a vital role in determining the

reliability of ultrasound-based positioning systems, it was not possible to calculate its numerical impact on the results obtained during the accuracy assessment stage. Further research needs to be conducted to establish the quantitative effect of the temperature on the developed system's accuracy. Finally, since only one worker was being tracking during the hazard exposure assessment, it was not possible to determine the effects in terms of accuracy of tracking more than one mobile beacon at a time. Future studies must also be conducted to establish the possible effect in terms of accuracy of tracking more than one mobile beacon.

3.8 References

Abune'meh, M., El Meouche, R., Hijaze, I., Mebarki, A., and Shahrour, I. (2016). "Optimal construction site layout based on risk spatial variability." *Automation in Construction*, Elsevier B.V., 70, 167–177.

Amsters, R., Stevens, N., and Slaets, P. (2019). "Evaluation of Low-Cost / High-Accuracy Indoor Positioning Systems Evaluation of Low-Cost / High-Accuracy Indoor Positioning Systems time and the known layout of the lego track for the first set." (October).

Awolusi, I., Marks, E., Hallowell, M., Ibukun Awolusi, Eric Marks, and Matthew Hallowell. (2018). "Automation in Construction Wearable technology for personalized construction safety monitoring and trending: Review of applicable devices." *Automation in Construction*, Elsevier, 85(July 2016), 96–106.

Bansal, V. K. (2011). "Application of geographic information systems in construction safety planning." *International Journal of Project Management*, 29(1), 66–77.

Bosché, F., Abdel-Wahab, M., and Carozza, L. (2016). "Towards a Mixed Reality System for Construction Trade Training." *Journal of Computing in Civil Engineering*, 30(2), 1–12.

Carbonari, A., Giretti, A., and Naticchia, B. (2011). "Automation in Construction A proactive system for real-time safety management in construction sites." 20, 686–698.

Cho, K., Park, W., Hong, M., Park, G., Cho, W., Jihoon, J., and Han, K. (2015). "Analysis

of latency performance of bluetooth low energy (BLE) networks." *Sensors (Switzerland)*, 15(1), 59–78.

Costin, A. M., Teizer, J., and Schoner, B. (2015). "RFID and BIM-enabled worker location tracking to support real-time building protocol control and data visualization." *Journal of Information Technology in Construction*, 20(January), 495–517.

Cuartero, A., Armesto, J., Rodríguez, P. G., and Arias, P. (2010). "Error analysis of terrestrial laser scanning data by means of Spherical statistics and 3D graphs." *Sensors (Switzerland)*, 10(11), 10128–10145.

Eiris, R., Gheisari, M., and Esmaeili, B. (2018). "PARS: Using Augmented 360-Degree Panoramas of Reality for Construction Safety Training." *International Journal of Environmental Research and Public Health*, 15(11), 2452.

Ergen, E., and Akinci, B. (2007). "An Overview of Approaches for Utilizing RFID in Construction Industry." *2007 1st Annual RFID Eurasia*, IEEE, 1–5.

Fang, Y., Cho, Y. K., and Chen, J. (2016). "A framework for real-time pro-active safety assistance for mobile crane lifting operations." *Automation in Construction*, Elsevier B.V., 72, 367–379.

Fasecolda. (2018). "Datos Riesgos Laborales." *2018*, <https://sistemas.fasecolda.com/rldatos/Reportes/xClaseGrupoActividad.aspx> (Nov. 18, 2019).

Giretti, A., Carbonari, A., Naticchia, B., and De Grassi, M. (2009). "Design and first development of an automated real-time safety management system for construction sites." *Journal of Civil Engineering and Management*, 15(4), 325–336.

Golovina, O., Teizer, J., and Pradhananga, N. (2016). "Automation in Construction Heat map generation for predictive safety planning : Preventing struck-by and near miss interactions between workers-on-foot and construction equipment." *Automation in Construction*, Elsevier B.V., 71, 99–115.

Hinze, J., Thurman, S., and Wehle, A. (2013). "Leading indicators of construction safety performance." *Safety Science*, Elsevier Ltd, 51(1), 23–28.

Ilkovicova, L. (2016). "Positioning System in Indoor Environment Using Ultrasound

Technology.” *16th International Multidisciplinary Scientific GeoConference SGEM2016, Informatics, Geoinformatics and Remote Sensing*.

Jang, W., and Skibniewski, M. J. (2009). “Embedded System for Construction Asset Tracking Combining Radio and Ultrasound Signals.” (August), 221–230.

Ji, Y., and Leite, F. (2018). “Automated tower crane planning: leveraging 4-dimensional BIM and rule-based checking.” *Automation in Construction*, 93, 78–90.

Jo, B. W., Lee, Y. S., Khan, R. M. A., Kim, J. H., and Kim, D. K. (2019). “Robust Construction Safety System (RCSS) for collision accidents prevention on construction sites.” *Sensors (Switzerland)*, 19(4).

Kim, H., and Han, S. (2018). “Accuracy improvement of real-time location tracking for construction workers.” *Sustainability (Switzerland)*, 10(5), 1–16.

Kim, H., Lee, H. S., Park, M., Chung, B. Y., and Hwang, S. (2016). “Automated hazardous area identification using laborers’ actual and optimal routes.” *Automation in Construction*, Elsevier B.V., 65, 21–32.

Kumar, S., and Bansal, V. K. (2019). “Use of GIS in locating TFs safely on a construction site in hilly regions.” *International Journal of Construction Management*, Taylor & Francis, 19(4), 341–353.

Lee, H., Asce, M., Lee, K., Park, M., Asce, M., Baek, Y., Lee, S., and Asce, A. M. (2012). “RFID-Based Real-Time Locating System for Construction Safety Management.” (June), 366–378.

Lin, Y., Su, Y., Lo, N., Cheung, W., and Chen, Y. (2013). “Application of Mobile RFID-Based Safety Inspection Management at Construction Jobsite.”

Lu, W., Huang, G. Q., and Li, H. (2011). “Scenarios for applying RFID technology in construction project management.” *Automation in Construction*, Elsevier B.V., 20(2), 101–106.

Mackensen, E., Lai, M., and Wendt, T. M. (2012). “Performance analysis of an Bluetooth Low Energy sensor system.” *2012 IEEE 1st International Symposium on Wireless Systems - Within the Conferences on Intelligent Data Acquisition and Advanced Computing Systems, IDAACS-SWS 2012*, IEEE, (September), 62–66.

Manase, D., Heesom, D., Oloke, D., Proverbs, D., Young, C., and Luckhurst, D. (2011). "A gis analytical approach for exploiting construction health and safety information." *Electronic Journal of Information Technology in Construction*, 16, 335–356.

Marks, E. D., Cheng, T., Teizer, J., and Ph, D. (2013). "<QCO000248.pdf>." 139(August), 1006–1014.

Marvelmind. (2019). "Indoor Navigation System Operating Manual." <www.marvelmind.com> (Nov. 19, 2019).

Michael, K., and Mccathie, L. (2005). "The pros and cons of RFID." *Strategic Direction*, 21(5), 24–26.

Mitropoulos, P., Abdelhamid, T. S., and Howell, G. A. (2005). "Systems Model of Construction Accident Causation." 131(7), 816–826.

Montaser, A., and Moselhi, O. (2014). "Automation in Construction RFID indoor location identi fi cation for construction projects." *Automation in Construction*, Elsevier B.V., 39, 167–179.

Nasr, E., Shehab, T., and Vlad, A. (2013). "Tracking Systems in Construction : Applications and Comparisons." *49th ASC Annual International Conference Proceedings*, 1–9.

Nath, B., Reynolds, F., and Want, R. (2006). "RFID technology and applications." *Pervasive computing*, 9780521880, 1–218.

Ni, D. (2016). "Traffic Sensing Technologies." *Traffic Flow Theory*, Elsevier, 3–17.

Nowotarski, P., Pasławski, J., and Mielcarek, D. (2017). "ScienceDirect ScienceDirect Accuracy of BLE systems in the H & S improvement aspects in construction." *Procedia Engineering*, Elsevier B.V., 208, 98–105.

Park, J., Kim, K., and Cho, Y. (2016). "A Framework of Automated Construction Safety Monitoring using Cloud-enabled BIM and BLE Mobile Tracking Sensors." *Journal of Construction Engineering and Management*, 143(2), 1–12.

Perlman, A., Sacks, R., and Barak, R. (2014). "Hazard recognition and risk perception in construction." *Safety Science*, Elsevier Ltd, 64, 13–21.

Pham, H. C., Dao, N. N., Pedro, A., Le, Q. T., Hussain, R., Cho, S., and Park, C. S. (2018).

"Virtual field trip for mobile construction safety education using 360-degree panoramic virtual reality." *International Journal of Engineering Education*, 34(4), 1174–1191.

Pittokopiti, M., and Grammenos, R. (2019). "Infrastructureless UWB based collision avoidance system for the safety of construction workers." *2019 26th International Conference on Telecommunications, ICT 2019*, Institute of Electrical and Electronics Engineers Inc., 490–495.

Pradhananga, N., and Teizer, J. (2013). "Automatic spatio-temporal analysis of construction site equipment operations using GPS data." *Automation in Construction*, 29, 107–122.

Pyeon, M., Choi, C., Heo, J., Mok, E., Jeong, S., Xia, L., and Woo, S. (2010). "Application of WiFi-based indoor positioning system for labor tracking at construction sites: A case study in Guangzhou MTR." *Automation in Construction*, Elsevier B.V., 20(1), 3–13.

Riaz, Z., Arslan, M., Kiani, A. K., and Azhar, S. (2014). "Automation in Construction CoSMoS : A BIM and wireless sensor based integrated solution for worker safety in con fi ned spaces." 45, 96–106.

Sacks, R., Whyte, J., Swissa, D., Raviv, G., Zhou, W., and Shapira, A. (2015). "Safety by design: dialogues between designers and builders using virtual reality." *Construction Management and Economics*, Routledge, 33(1), 55–72.

Shahi, A., Aryan, A., West, J. S., Haas, C. T., and Haas, R. C. G. (2012). "Deterioration of UWB positioning during construction." *Automation in Construction*, Elsevier B.V., 24, 72–80.

Shchekotov, M. (2014). "Indoor Localization Method Based on Wi-Fi Trilateration Technique." *Proceeding of the 16Th Conference of Fruct Association*, 177–179.

Siddiqui, H., Vahdatikhaki, F., and Hammad, A. (2019). "Case study on application of wireless ultra-wideband technology for tracking equipment on a congested site." *Journal of Information Technology in Construction*, 24(October 2017), 167–187.

Teizer, J. (2008). "3D range imaging camera sensing for active safety in construction."

Electronic Journal of Information Technology in Construction, 13(April), 103–117.

Teizer, J., and Vela, P. A. (2009). "Personnel tracking on construction sites using video cameras." *Advanced Engineering Informatics*, Elsevier Ltd, 23(4), 452–462.

Teo, E. A. L., Ling, F. Y. Y., and Chong, A. F. W. (2005). "Framework for project managers to manage construction safety." *International Journal of Project Management*, 23(4), 329–341.

Thomas, F., and Ros, L. (2005). "Revisiting trilateration for robot localization." *IEEE Transactions on Robotics*, 21(1), 93–101.

US Bureau of Labor Statistic. (2018). "National Census of Fatal Occupational Injuries in 2017." *Bureau of Labor Statistics US Department of Labor*, (202), 1–14.

Wang, J., Zhang, S., and Teizer, J. (2015). "Geotechnical and safety protective equipment planning using range point cloud data and rule checking in building information modeling." *Automation in Construction*, Elsevier B.V., 49, 250–261.

Wierzbicki, D., Kedzierski, M., and Fryskowska, A. (2015). "Assesment of the influence of UAV image quality on the orthophoto production." *International Archives of the Photogrammetry, Remote Sensing and Spatial Information Sciences - ISPRS Archives*, 1–8.

Woodcock, K. (2014). "Model of safety inspection." *Safety Science*, Elsevier, 62, 145–156.

Wu, W., Yang, H., Li, Q., and Chew, D. (2013). "An integrated information management model for proactive prevention of struck-by-falling-object accidents on construction sites." *Automation in Construction*, Elsevier B.V., 34, 67–74.

Yang, H., Chew, D. A. S., Wu, W., Zhou, Z., and Li, Q. (2012). "Design and implementation of an identification system in construction site safety for proactive accident prevention." *Accident Analysis and Prevention*, Elsevier Ltd, 48, 193–203.

Zhang, M., Cao, T., and Zhao, X. (2017). "Applying sensor-based technology to improve construction safety management." *Sensors (Switzerland)*, 17(8).

Zhang, S., Sulankivi, K., Kiviniemi, M., Romo, I., Eastman, C. M., and Teizer, J. (2015). "BIM-based fall hazard identification and prevention in construction safety planning." *Safety Science*, 72, 31–45.

Zhou, Z., Goh, Y. M., and Li, Q. (2015). "Overview and analysis of safety management studies in the construction industry." *Safety Science*, Elsevier Ltd, 72(February), 337–350.

Zhou, Z., Irizarry, J., and Lu, Y. (2018). "A Multidimensional Framework for Unmanned Aerial System Applications in Construction Project Management." *Journal of Management in Engineering*, 34(3), 04018004.

Zito, R., D'Este, G., and Taylor, M. A. P. (1995). "Global positioning systems in the time domain: How useful a tool for intelligent vehicle-highway systems?" *Transportation Research Part C*, Pergamon, 3(4), 193–209.

CHAPTER 4: UAS POINT CLOUD ACCURACY ASSESSMENT USING SFM-BASED PHOTOGRAMMETRY AND PPK GEOREFERENCING TECHNIQUE FOR BUILDING SURVEYING APPLICATIONS

Jhonattan G. Martinez[1]*, Gilles Albeaino[2], Masoud Gheisari, Ph.D., A.M.ASCE[3], Walter Volkmann[4], and Luis F. Alarcón, Ph.D., M.ASCE[5]

4.1 Introduction and Background

Remote sensing is defined as the non-contact acquisition of information pertaining to the physical characteristics of objects (Xiang et al. 2018). This technology has been successfully applied in several industries, including forestry, ecology, urban planning, land-use restoration, and landslides monitoring (Iizuka et al. 2018; Ruggles et al. 2016). Conventional remote sensing data collection is mainly accomplished using spaceborne, terrestrial, and airborne equipment which utilizes several technologies such as Global Navigation Satellite System (GNSS), differential global navigation satellite systems (DGNSS), Light Detection and Ranging (LiDAR), aerial and terrestrial laser scanners, as well as thermal sensors (Vetrella et al. 2019). However, several factors, such as the high costs and time, atmospheric effects, resolution of the derived product, and deficiency in surveying topographically complex areas, hinder the full deployment of these surveying technologies (Xiang et al. 2018). As a result, Unmanned Aerial Systems (UASs) have emerged as an efficient data collection alternative that has been widely applied for remote sensing applications (Niethammer et al. 2012). The use of UASs, or drones, as an aerial photogrammetry technology offers the advantages of accomplishing tasks in an accurate, timely, flexible, and cost-efficient manner (Remondino et al. 2012). These devices are defined as aerial platforms that operate with no pilot onboard (UVS International 2018).

As a platform for data collection, UASs can be equipped with several onboard sensors to accomplish their intended tasks.These sensors recently witnessed tremendous technical improvements in terms of size and accuracy, a factor that paved the way for

integrating UAS technology in a wide range of industries (Harwin and Lucieer 2012). UASs have been applied for a wide range of applications from landslide monitoring (Niethammer et al. 2012) or topography mapping in coastal environments (Mancini et al. 2013) to agricultural irrigation precision (Ezenne et al. 2019) or natural disaster assessment (Iqbal et al. 2015). UAS-mediated techniques have also significantly influenced the architecture, engineering, construction, and operation (AECO) domain (Albeaino et al. 2019). Construction, in particular, incorporated the use of UASs for various types of applications such as site surveying and mapping (Remondino et al. 2012; Tomaštík et al. 2019), surveying earthwork projects (Hugenholtz et al. 2015; Siebert and Teizer 2014), progress monitoring (Álvares et al. 2018; Vacanas et al. 2015), construction safety management (Costa et al. 2016; Gheisari et al. 2018), material handling (Hubbard et al. 2015; Khosiawan et al. 2018), structure and infrastructure inspection (Eschmann et al. 2013; Morgenthal and Hallermann 2014), building inspection (Liu et al. 2016; Serrat et al. 2019), and post-disaster building assessment (Adams et al. 2014; Ghaffarian and Kerle 2019). The majority of these applications rely mainly on UAS-captured visual contents to accomplish their tasks. While using raw images and videos seem sufficient for some of these applications, others require the use of photogrammetric techniques to process the data and generate PCDs.

With the aim of processing the data collected using UAS imagery, researchers primarily used Structure from Motion (SfM), which is an imaging technique that relies on 2D images to generate 3D PCDs (Carrivick et al. 2016). In contrast to classic photogrammetric methods, SfM applies algorithms to identify matching features in a set of overlapping digital images in terms of orientation, camera location, and position (Martínez-Carricondo et al. 2018). Several researchers combined UAS technology with the SfM technique in their applications. For example, Scaioni et al. (2009) combined SfM and UASs to survey and generate a digital replica of the highest part of the Milano cathedral dome for reconstruction purposes. Koutsoudis et al. (2014) also created a digital model of a monument using SfM and dense multi-view algorithms to evaluate the quality of the

generated 3D data. Barbosa et al. (2017) studied several UAS flight plans to conduct more efficiently the collection of visual assets and obtain high-quality SfM-derived products in construction jobsites. A more recent study presented an SfM-based 3D reconstruction framework capable of providing real-time feedback about the data captured for the accurate reconstruction of building facades (Daftry et al. 2015). Other studies integrated the SfM technique with UAS-acquired visualizations for the damage assessment of structures in the post-disaster setting (Mohammadi and Wood 2018) as well as for the visualization and monitoring of cultural heritage sites in coastal areas (Papakonstantinou et al. 2019).

While some research areas do not require a high degree of PCD accuracy, specific construction-related applications such as building damage assessment, crack detection and quantification, or construction progress monitoring, hugely rely on the accuracy of the model for a successful deployment (Bolkas 2019; Siebert and Teizer 2014). Several researchers studied the factors affecting the accuracy of SfM-driven 3D PCD (Álvares et al. 2018; Ishida 2017). Some of these factors include UAS flight parameters (i.e. flight altitude and angle, percentage of image overlap), environmental effects, ionospheric and tropospheric effects, camera calibration and quality, as well as the adopted georeferencing techniques such as the ground control points (GCPs), real-time kinematic (RTK), and the post-processing kinematic (PPK) (Bolkas 2019; Fazeli et al. 2016; Martínez-Carricondo et al. 2018; Sanz-Ablanedo et al. 2018).

Commercially available off-the-shelf UASs are typically equipped with a single-frequency GNSS (L1) device, which limits the absolute attainable positioning accuracy to values ranging between 1 and 25 m (Yao and Clark 2000). Since several construction-related applications require a better accuracy, the most commonly used strategy to enhance the accuracy is identifying key features in the PCD that can be matched to known real-world coordinates via GCPs (Bolkas 2019). GCPs are defined as ground targets of known locations that are placed strategically on the earth's surface for georeferencing purposes.

However, this traditional georeferencing technique that relies on GCPs is a time-consuming and labor-intensive process (Forlani et al. 2018). Other techniques such as RTK and PPK, which rely on single frequency GNSS (L1) or double-frequency GNSS (L1/L2) receivers, were found to achieve a positioning accuracy of about 1 to 30 cm with no GCPs required, which substantially saves time and cost (Fazeli et al. 2016; Luo et al. 2016; Bolkas 2019; Tomaštík et al. 2019). The RTK method simultaneously corrects the positioning coordinates during the flight, whereas PPK technology applies the corrections in the post-flight setting (Tomaštík et al. 2019). In terms of receivers, single-frequency GNSSs (L1) are unable to account for the ionospheric and tropospheric effects, encouraging the use of the more robust dual-frequency GNSS (L1/L2) receivers for higher PCD accuracy (Deng et al. 2011; Fazeli et al. 2016). This study aims to evaluate the effect of the single-frequency GNSS (L1) and dual-frequency GNSS (L1/L2) together with post-processing kinematic (PPK) technique on the accuracy of the UAS-generated PCDs. This paper first discusses the customization of an open-source UAS platform equipped with a dual-frequency GNSS (L1/L2) that is capable of georeferencing the captured data using PPK technology. Then a comprehensive accuracy assessment was conducted through a building surveying application.

4.2 Motivation and Research Approach

There is an increased interest and need among construction researchers and professionals to enhance the accuracy of the UAS-generated PCDs and improve this technology's integration in construction. High-accuracy visualizations are required for a variety of construction applications such as structural and infrastructural inspection, site surveying and mapping, building maintenance, and post-disaster assessment. The specific aim of this study is to evaluate the effect of the single-frequency GNSS (L1) and dual-frequency GNSS (L1/L2) together with post-processing kinematic (PPK) technique on the accuracy of the UAS-generated PCDs for building surveying application. Despite the wide implementation and popularity of this technique in other fields such as forestry, surveying, and mapping, evaluating the effects of the dual-frequency GNSS (L1/L2) combined with

PPK technology on the accuracies of the generated PCDs for AECO-related applications is still new, and has not been fully explored yet. More specifically, no prior papers have used the planimetric (X and Y), altimetric (Z), and overall PCD accuracy errors together with the time required for PCD generation as assessment metrics to perform comparative evaluations for UAS-PPK building surveying types of applications. The main contribution of this study is that it assesses the effects of various UAS technical configurations and flight parameters on the accuracy of the UAS-generated PCD data for building surveying types of applications. Experimental assessment conditions were as following:

- *UAS Configurations and Conditions*:
    - A UAS platform, named as MAPM4, with a dual-frequency GNSS (L1/L2) was customized. The data collection was conducted using the MAPM4 Platform, and then the collected data was processed with and without the use of PPK technology.
    - A popular off-the-shelf UAS platform, DJI® Phantom 4 Pro, with a single-frequency GNSS (L1) was used as the typical UAS platform used in the construction industry.
- *Benchmark:* The PCDs assessment were based on benchmark GCPs coordinates surveyed using a dual-frequency terrestrial GNSS (L1/L2) and on actual field measurements conducted on-site
- *Flight Parameters and Image Combination:* Ground sampling distance (GSD) and camera angle were considered in the experimental assessment to better understand their effects on the generated PCD accuracies.
- *Assessment Metrics:* Planimetric (*X* and *Y*), altimetric (*Z*), and overall PCD accuracy error assessment together with the total time for the PCD generation.

The outcomes of the study will help construction practitioners and researchers better integrate UAS technology for PCD generation and accuracy improvement needed for a variety of applications in the AECO industry.

4.3 Methods

In this experimental study, a comparative analysis was performed on a medium-sized building, serving as a test environment, in an attempt to assess the effects of the dual-frequency GNSS (L1/L2) combined with PPK technology on the accuracies of the generated PCD. This objective was achieved through the following four steps (See Figure 18):

(1) *UAS Development and Programming*: A UAS platform, named as MAPM4, with a dual-frequency GNSS (L1/L2) was designed, assembled, and programed using commercially available software and hardware and an open-source ground control station.
(2) *Onsite Data Collection:* Flights were performed using the previously developed MAPM4 platform and a DJI® Phantom 4 Pro (a popular single-frequency GNSS (L1) UAS platform). Installed and surveyed Ground Control Points (GCPs) on the test location was used as the benchmark. And several flights were planned considering specific flight parameters (e.g., GCD, camera angle).
(3) *PCD Generation:* The collected datasets were processed through a SfM-based image processing technique to generate the PCDs.
(4) *PCD Accuracy Assessment:* Finally, the generated PCDs were assessed against the benchmark GCPs, and on-site field measurements.

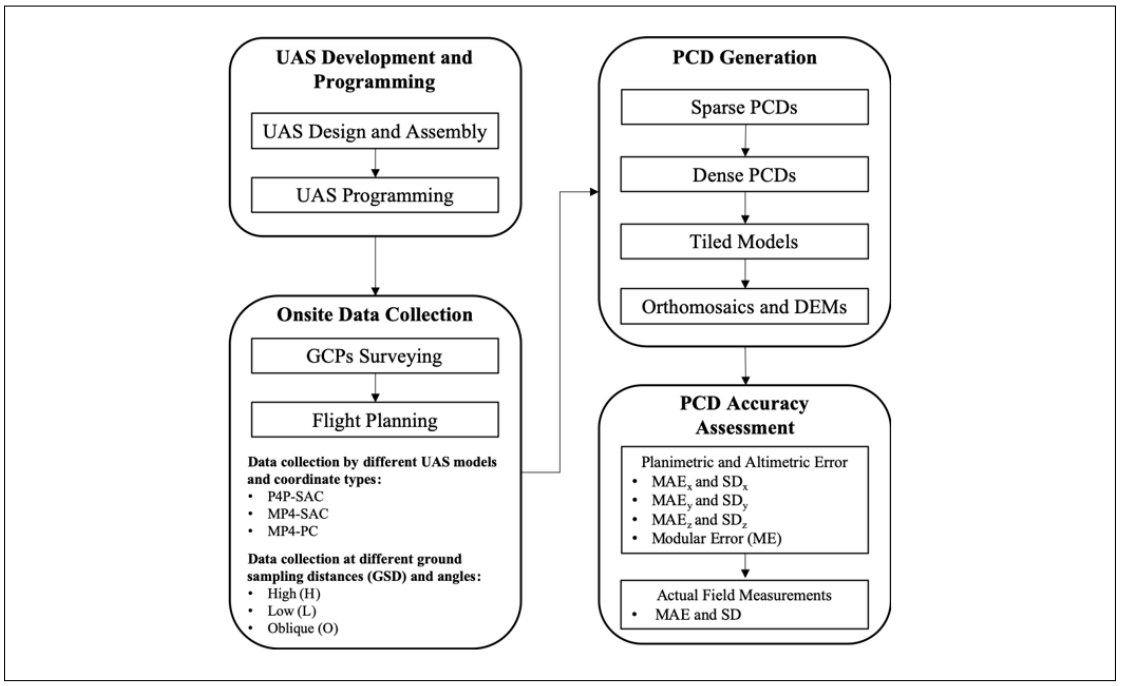

Figure 18. Research Steps of the Study

This section will further discuss each step of the research methodology process.

4.3.1 UAS development and programming

In the first step of the study, MAPM4, a UAS platform with a dual-frequency GNSS (L1/L2), was designed and developed. The use of a customized platform presents several advantages over the readily available off-the-shelf UAS platforms. While there are several commercial UASs that might have dual-frequency GNSS (L1/L2) and PPK georeferencing capabilities, a customized UAS platform with these technical capabilities would have a considerably lower cost to build. Furthermore, unlike the off-the-shelf UASs platforms, customizing an open-source UAS platform would make customization, mounting and changing different types of sensors, as well as integrating various programming processes possible. The opportunity to repair or adopt several types of payloads, or integrate enhanced versions of originally mounted sensors, will increase the return-on-investment as well as the operational life of the customized UAS platform. In

this study, the open-source programming feature offered the ability to adjust several technical aspects that could be otherwise impossible to modify with off-the-shelf UASs. For example, configuring the camera mid-exposure pulse, which is defined as the midpoint of exposure of the camera position (Blankenberg 1992) was not possible in readily-available UASs but was necessary to ensure that the imagery is accurately time-stamped during the flight mission (Mian et al. 2015). This exact time of camera exposure is known as the event marking process (Blankenberg 1992). However, it should be noted that customizing a UAS platform is a complicated and time-consuming process that requires advanced technical knowledge, which might not be a viable option for general users in the AECO industry. The following subsections further discuss the design, assembly, and programming details of the customized MAPM4 platform.

UAS Design and Assembly

In this step, the MAPM4 UAS platform with a dual-frequency GNSS (L1/L2) was designed and assembled using commercially available software and hardware. The adopted UAS configuration was a quadcopter rotary-wing. A quadcopter is a vehicle that is lifted by four engines and propellers. Advantages of such type of platforms include their flexibility in vertical take-off and landing, safe deployment (ensuring a controlled return despite multiple engine failures due to the rotors' redundancy), stability (withstanding environmental conditions that could be otherwise challenging to other platform types such as the fixed-wing), and maneuverability (Albeaino et al. 2019). On the other hand, their drawbacks include their limited coverage of photogrammetric areas, payload capacity, and flying endurance (Albeaino et al. 2019; Siebert and Teizer 2014). However, rotary-wing vehicles have been shown to be popular and effective for small to medium-sized constructions and vertical types of projects (Albeaino et al. 2019).

Table 12 summarizes the details of the UAS parts, components, and their features. The MAPM4, including its payloads, weights 4.6 kg. The aerial platform can be operated at a maximum speed of 20 m/s for a single flight duration of 25 min. It is capable of

attaining a maximum altitude of 3,500 meters above ground level (AGL) and covering 2 hectares/minute of mapping area.

Table 12. MAPM4 Components and Characteristics

UAS Parts	Components	Model Manufacturer	Characteristics
Body	Frame (x1)	Foxtech ® Hover 1 Quadcopter	Size: Unfolded (640mm x 640mm x 280mm) and folded (285mm x 285mm x 175mm) Weight: 596 g
	Motors (x4)	Tiger Motor ® MN4014	Power: 750 W Diameter: 44.7 mm Weight:171 g (Total)
	Propellers (x4)	APC MR® 16x5.5MRPseries	Pitch size: 152.4 mm Weight: 120 g (Total)
	Electronic speed controllers (x4)	XRotor® COB/30901001	Current peak: 40 A Weight: 104 g (Total)
	Batteries (x2)	TATTU® 6S1P	Power: 7000 mA Cells: 6 in each Weight: 1.815 kg (Total)
Navigation System	Automatic pilot system (x1)	Pixhawk® 2.1 series	Processor: 32-bit STM32F427 Cortex-M4F® core with FPU RAM: 256 kB RAM Flash memory: 2 MB Co-processor: 32-bit STM32F103 failsafe co-processor IMU included: Accelerometers, gyroscopes, compass, and magnetometers. Weight: 250 g
	Single-frequency GNSS (L1) (x1)	Hex Technology® Here 2 GNSS	Navigational update rate: 10 Hz Size: 94 mm x 94 mm x 43 mm Sensitivity: 167 dBm Receiver type: L1 Operating voltage: 5V Power consumption: 500 mA at 12V IMU included: Compass, gyroscopes, and accelerometer Weight: 136 g
	Dual-frequency GNSS (L1/L2)	V-Map® system	Navigation update rate: 20 Hz Size: 80mm x 67mm x 25.5mm Sensitivity: >59 dB Operating voltage: 6V to 36V Power consumption: 500mA at 12V Weights: 138 g
Data Communication and Collection	Radio transmitting system (x1)	RFdesign ® RFD900	Air antenna 1: 900 MHz 2 dBi Monopole Air antenna 2: 900 MHz 2 dBi Right angle Monopole Ground antenna 1: 900 MHz 3 dBi Dipole Ground antenna 2: 900 MHz 3 dBi Dipole RFD air modem: RFD900 Plus Weight: 140 g
	Radio controller and First-Person View (x1)	FrSky® Taranis Q X7	Operating voltage Range: 6~15V Operating current: 210mA Number of channels: 16 Weight: 719 g in total
	RGB camera (x1)	Sony® Alpha 6000	Focal length: 50 mm, a resolution of Camera resolution: 24.3 MP, video-recording capabilities: 11 FPS

UAS Parts	Components	Model Manufacturer	Characteristics
	Video transmitter (x1)	Immersion RC® TX5G6R	Weight: 342 g Video resolution: 729 px Power: 600mW Frequency: 5.8 GHz Link range: 1.5 km Weight: 100 g

UAS Body: The utilized carbon-fiber frame was a Foxtech® Hover 1 Quadcopter Frame, which has a total weight of 596 g, an unfolded size of 640 mm x 640 mm x 280 mm, and folded size of 285 mm x 285 mm x 175 mm. The MAPM4 was equipped with a power system that is driven by two Tattu® 7000 mAh lithium-poly batteries. An XRotor® motor was installed at each of the four arms of the platform and was characterized by a maximum continuous power of 750 W, a diameter of 44.7 mm, and a weight of 171 g. The motors were connected to the power system through four XRotor® electronic speed controllers having each a peak current of 40 A and a weight of 26 g. These speed controllers regulate the speed of the motors based on the flight controller's commands. Finally, plastic APC MR® propellers having a pitch size of 152.4 mm were mounted on the four motors.

UAS Navigation System: The Cube flight controller, formerly identified as Pixhawk 2.1®, was the autopilot system used on the MAPM4. The role of the autopilot system is to autonomously operate the UAV with minimum human involvement (Chao et al. 2010). This flight controller is specifically designed for manufacturers of UAS systems with an open-source hardware design (ArduPilot 2019). The flight controller incorporates a total of three redundant sets of Inertial Measurement Units (IMUs) composed of several gyroscopes, accelerometers, barometers, and magnetometers. While such sensors allow the UAS to be navigated effectively, their redundant number ensures a reliable and safe UAS operation. A Hex Technology® Here-2 GNSS 72-channel GNSS was combined with the controller system for the navigation of the MAPM4. Initially developed for the Pixhawk® platforms, the single-frequency GNSS (L1) includes a processor and an IMU that is composed of a barometer, a compass, a gyroscope, and an accelerometer. The signal strength of the GNSS is 167dBm, and its navigational update rate is up to 10 Hz, factors

that allow the MAPM4 to be operated using autonomous features such as autonomous flight planning, position hold, auto-return home, auto takeoff/landing. The attainable position accuracy of this single-frequency GNSS (L1) is around 2.5 m. Additionally, a V-map® 20 Hz dual-frequency GNSS (L1/L2) lightweight receiver capable of the event marking was mounted on top of the UAS platform. The main advantages of this device are its capability to precisely capture the camera exposure positions at an accuracy of 0.05 m and eliminate the need for ground control points. Other advantages include its simple integration into any commercial or customized UAS.

UAS Data Communication and Collection: A radio transmitting system composed of a long-range telemetry radio bundle, a radio modem, and four RFdesign ® 9000 MHz antennas were relied upon to establish a maximum wireless link range of 1.5 km between the aerial platform and the ground control station. The radio controller used was a FrSky® Taranis Q X7, which is characterized by an operating voltage range of 6~15 V and a current of 210 mA. To acquire images and videos, a Sony® Alpha Camera 6000 was also mounted on the bottom of the MAPM4 platform using a 3D-printed camera mount system. This RGB imaging device has a 50 mm focal length, a resolution of 24.3 MP, video-recording capabilities at 11 FPS, and a total weight of 342 g. The camera was connected to both, autopilot and GNSS systems for the geotagging of the captured visuals and was also linked to a 600mW 5.8Ghz video transmitter with a first-person view monitor. Figure 19 shows the MAPM4 configuration along with the previously discussed components and sensors.

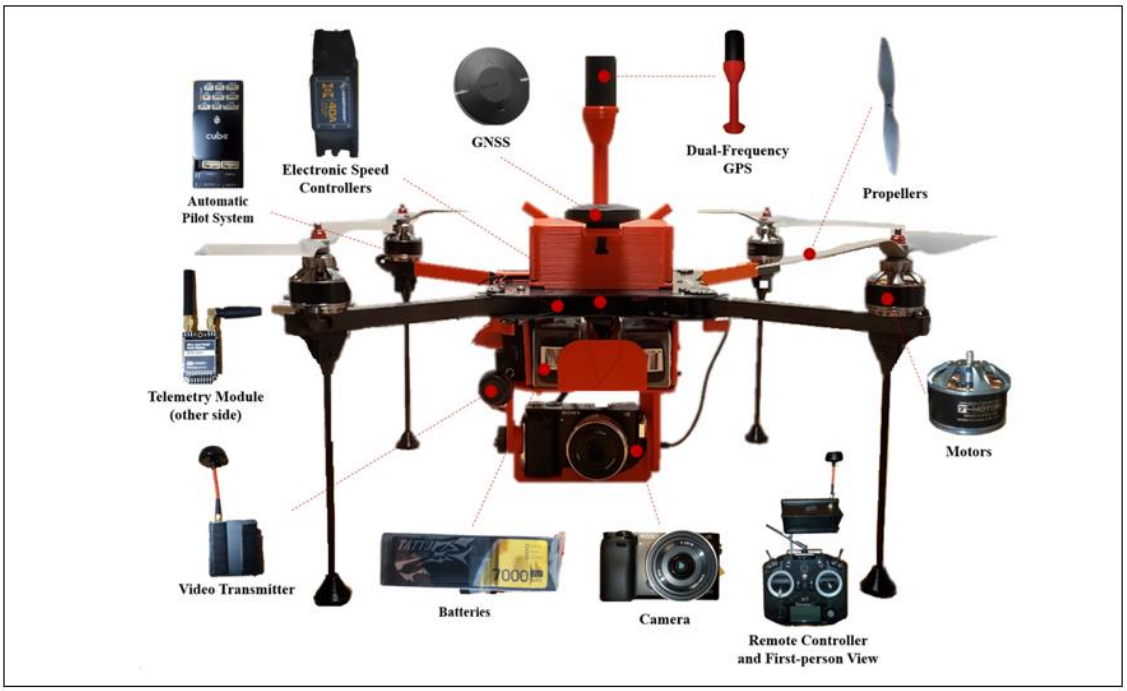

Figure 19. MAPM4 components

UAS Programming

In this step of UAS programming, the necessary firmware was installed to set up the automatic pilot using the ArduPilot Mission Planner software package. This software is a popular open-source unmanned vehicle autopilot suite that is capable of controlling vehicles such as UASs, rovers, boats, and submarines. (ArduPilot 2019).The specific ArduCopter V3.6.4 firmware was used, and then flight parameters such as takeoff altitude, maximum speed and acceleration, takeoff and landing speeds, maximum lean angle, telemetry, and flight modes were all transferred to the automatic pilot system. Finally, the UAS frame type was selected in the software, and the accelerometer, speed controllers, as well as the UAS compass were calibrated. It is important to note that the compass calibration should be accomplished in a location free from metal objects to avoid magnetic interferences (ArduPilot 2019).

4.3.2 Onsite data collection

The data collection process was conducted on a 924 m2 medium-sized building at the Energy Research and Education Park (29°37'38.8"N 82°21'37.9"W), located in Gainesville, FL (Figure 20). Reasons behind selecting this site include: (1) the ability to easily access the site; (2) the minimum amount of vegetation (e.g., trees) and building interferences around the site; (3) simple building shape; and (4) not being part of a Federal Aviation Administration (FAA) restricted or prohibited airspace zone. The FAA regulations might affect the proper implementation of UAS technology on construction jobsites, as acknowledged by several researchers (Gheisari and Esmaeili 2019; Martinez et al. 2020). For example, the FAA restricts UAS operation over active sites and populated areas (U.S. Department of transportation 2016), a factor that negatively affects the quality and resolution of the UAS-acquired images during data collection and, consequently, the generated PCDs. Besides, UASs cannot be operated at elevations higher than 400 feet above ground level and/or within restricted airspaces. These restrictions would limit the frequency and deployment of the UAS technology on the jobsites and the possibility of reaching certain areas, reducing the amount and quality of the captured data.

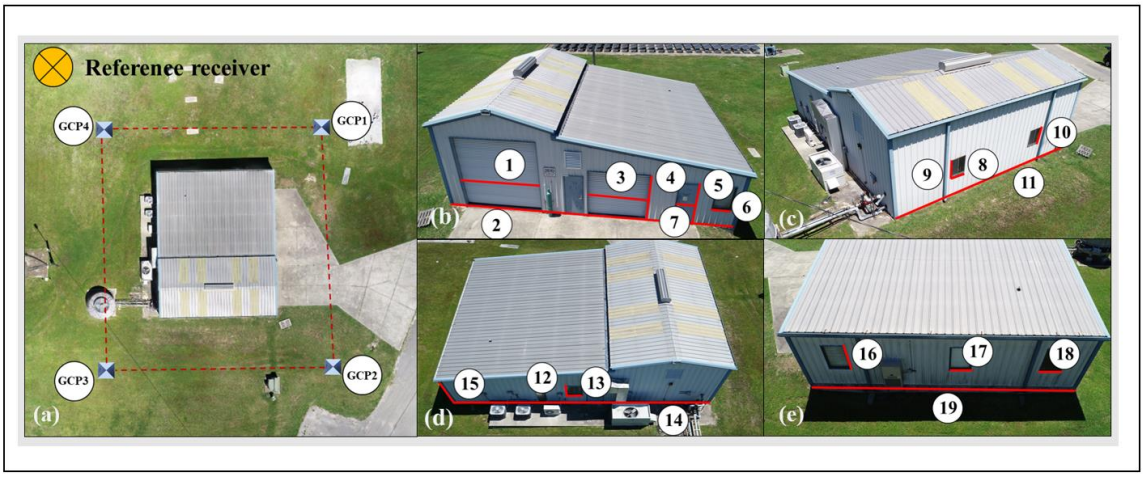

Figure 20. Surveyed building in the test area and: (a) Distribution of GCPs on the ground and reference receiver location; (b) East-side of the surveyed building; (c) South-side of the surveyed building; (d) West-

side of the surveyed building: and (e) North-side of the surveyed building. (Images by Jhonattan G. Martinez)

Data collections were performed using the previously developed MAPM4 with a dual-frequency GNSS (L1/L2) and a DJI® Phantom 4 Pro with a single-frequency GNSS (L1). The DJI® Phantom 4 Pro is a commercially available rotary-wing vehicle and was selected in this study to represent a UAS platform with a single-frequency GNSS (L1), which has also been a very popular platform in the AECO industry (Albeaino et al. 2019; Zhou and Gheisari 2018). This quadcopter has a 20-MP RGB sensor with a focal length of 8 mm/24 mm. The flight time of the platform is 30 minutes under optimal conditions and its total weight, including the propellers and the battery, is 1.34 kg (DJI 2017). The DJI® Phantom 4 Pro is equipped by two sets of redundant IMUs which include barometers, gyroscopes, and accelerometers, ensuring a stable and safe flight. Three steps were performed to collect the data on the above site location using the customized MAPM4 with a dual-frequency GNSS (L1/L2) and the DJI® Phantom 4 Pro with a single-frequency GNSS (L1): (1) surveying of the benchmark ground control points (GCP) using a dual-frequency terrestrial GNSS (L1/L2) ; (2) flight planning for the MAPM4 and the DJI® Phantom 4 Pro; and (3) initiating the flights and collecting the UAS-captured images. The following subsections further discuss these three steps.

Ground Control Points Surveying

Ground Control Points (GCPs) were strategically distributed and placed on the ground to be used as benchmark datasets later on in the PCDs assessment phase of the study. Several UAS-related mapping and surveying studies recommended the use of at least four GCPs to be placed homogeneously and with sufficient coverage and density over the area of interest (Benjamin et al. 2020; Bolkas 2019; Sanz-Ablanedo et al. 2018). In fact, Bolkas (2019) and Sanz-Ablanedo et al. (2018) concluded that the process of georeferencing UAS-acquired images requires the use of at least four GCPs to account for degrees of freedom in position, orientation, and scale of a single photo. In a more recent study, Benjamin et al. (2020) stated that the number and distribution pattern of the established GCPs play an important role in terms of accuracy of the reconstructed PCD,

and suggested that having more than four GCPs will only increase the accuracy level by a few centimeters. This slight increase does not seem to be of substantial benefit, especially with the amount of time and cost required to establish and survey additional GCPs onsite. Considering these recommendations, and to ensure that the GCPs are distributed with sufficient coverage over the surveyed 924 m^2 area, four GCPs were installed in a square-shaped manner to cover all four corners of the building (Figure 21-a). The GCPs consisted of lightweight 20 by 20 cm square-shaped targets that were spaced 23 m apart from each other.

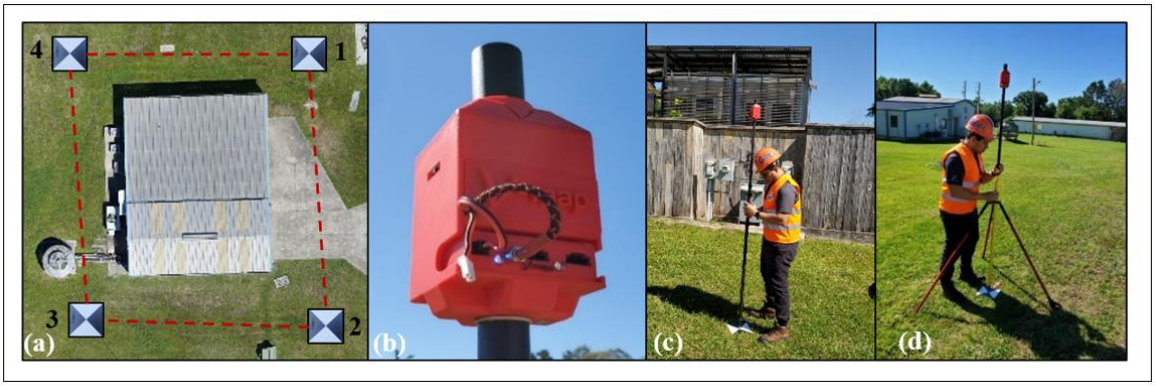

Figure 21. GCPs distribution: (a) Distribution of GCPs on the ground; (b) Dual-frequency terrestrial (L1/L2) GNSS; (c) Rover station; and (d) Reference station

The GCPs were surveyed using a dual-frequency terrestrial GNSS (L1/L2) (Figure 21-b) that is capable of event marking. This system included a rover station (GNSS receiver) and a 20 Hz reference receiver (dual-frequency 1217-1250 MHz L2 and 1565-1610MHz L1 GNSS) that was installed next to the building and acted as a reference station for which coordinate positions are known. See Figure 21-c and 21-d. The main advantages of this technique are its very high accuracy (<0.005 m) and fast and cost-efficient implementation process (Shouny et al. 2017). Besides, this system was equipped with a GNSS receiver, which eliminates the need for a direct line of sight between the rover station and the reference station (Carrivick et al. 2016). The coordinate system adopted was the WGS84 (World Geodetic System 1984), which allows localizing any point on the earth using given coordinates (X, Y, and Z) (Kumar 1988). After the benchmark data

collection, the coordinates were then corrected using the differential GNSS positioning technique based on PPK technology (See Table 13). This technique relies on the well-known positioning coordinates provided by the reference station receiver to correct the observed pseudoranges (raw GNSS data) collected using the mobile rover station (Tomaštík et al. 2019). In contrast to the stand-alone coordinates which are directly derived from GNSS satellite signals and have an estimated in the meter range (Datta-Barua et al. 2003), precise coordinates using differential GNSS technology can achieve a positioning accuracy of 0.5 cm to 30 cm (Carrivick et al. 2016). The process of coordinates correction was carried out using V-map® CamPos, free and stand-alone software that is compatible with the presented V-map system (Vmap 2016).

Table 13. GCPs precise coordinates

Target	Latitude (º)	Longitude (º)	Height (m)	X (m)	Y (m)	Z (m)
1	29.62755707	-82.36040174	24.223	807194.67	71507.592	24.223
2	29.62732135	-82.36037815	24.2655	807197.444	71481.511	24.265
3	29.62732161	-82.36062223	24.584	807173.81	71481.097	24.584
4	29.62755425	-82.36063659	24.673	807171.936	71506.853	24.673

Flight Planning

As previously discussed, data collections should be performed using the DJI® Phantom 4 Pro with a single-frequency GNSS (L1) and the customized MAPM4 with a dual-frequency GNSS (L1/L2). Pix4D® Capture was used to do the flight planning for the DJI® Phantom 4 Pro, and ArduPilot® Mission Planner was used for the MAPM4. Pix4D® Capture was chosen as the DJ1® Phantom 4 Pro flight mapping software due to its compatibility with the platform (Pix4D 2019). ArduPilot® Mission Planner is open-source software that was compatible with the autopilot flight controller that was mounted on the customized MAPM4 platform and provides a wide range of customized horizontal and vertical flight path types (ArduPilot 2019).

For each of the UAS platforms, two autonomous and one manual flight missions were performed. The autonomous flights were performed in two ground sampling distance

(GSD) of 0.05 cm/px (DJI® Phantom 4 Pro: 18 m above ground level (AGL) and MAPM4: 23 m (AGL) and 1 cm/px (DJI® Phantom 4 Pro: 36 m AGL and MAPM4: 41 m AGL) to acquire vertical or nadir images. Moreover, manual flights were performed using both platforms to acquire oblique images with a camera angle of 45º. Flights with different GSD and camera angles were performed to collect a variety type of images to study their effects on the overall PCD accuracy. Table 14 further discusses those flights and their related parameters.

Table 14. UAS flight missions, planning software, and flight parameters

UAS Platform (Camera Setting & Flight Speed)	Planning Software (Flight Style)	Flight Parameters
DJI® Phantom 4 Pro • Camera Setting: Shutter with exposure time 1/400 s; Resolution: 5472 x 3648 px; ISO-100 • Flight Speed: 3 m/s	Pix4D® Capture (Autonomous)	Image type: Nadir Height: 18 m AGL GSD: 0.05 cm/px Overlap: 80% front; 72% side Number of Waypoints: 10
	Pix4D® Capture (Autonomous)	Image type: Nadir Height: 36 m AGL GSD: 1 cm/px Overlap: 80% front; 72% side Number of Waypoints: 25
	Pix4D® Capture (Manual)	Image type: Oblique (45°) Height: 22 m AGL GSD: N/A Overlap: N/A Number of Waypoints: N/A
MAPM4 • Camera Settings: Shutter with exposure time 1/1250 s; Resolution: 6000 x 4000 px; ISO-100 • Flight Speed: 3 m/s	ArduPilot® Mission Planner (Autonomous)	Image type: Nadir Height: 23 m AGL GSD: 0.05 cm/px Overlap: 80% front; 72% side Number of Waypoints: 41
	ArduPilot® Mission Planner (Autonomous)	Image type: Nadir Height: 41 m AGL GSD: 1 cm/px Overlap: 80% front; 72% side Number of Waypoints: 45
	ArduPilot® Mission Planner (Manual)	Image type: Oblique (45°) Height: 22 m AGL GSD: N/A Overlap: N/A Number of Waypoints: N/A

In all flight missions, a double-grid flight mode was chosen, and the adopted image overlap percentage was 80% front and 72% side. The overlap percentages satisfy the minimum values required for the SfM-mediated image processing technique (Pix4D, 2019). The double-grid method enables the UASs to turn by 180º between two consecutive lines to capture images from multiple sides. All missions were accomplished using a UAS flight speed of 3 m/s. Figure 22 shows the UAS flight planning paths for both UAS platforms at 0.05 cm/px GSD and 1 cm/px GSD.

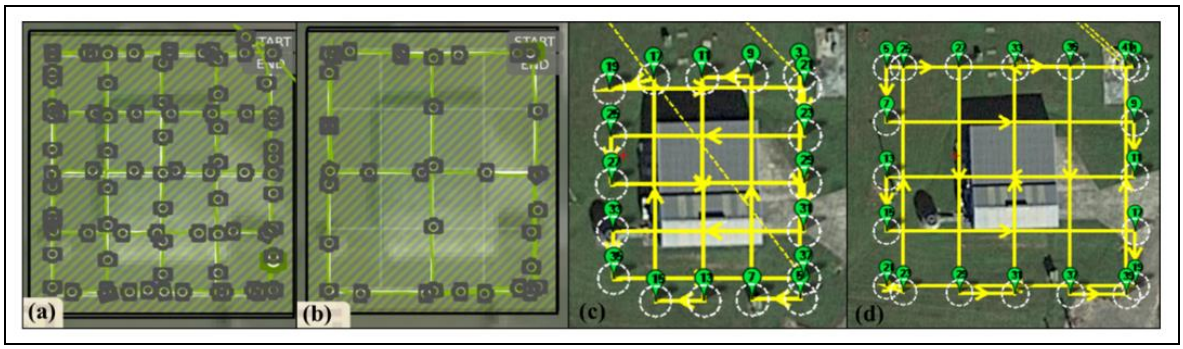

Figure 22. Pix4D® Capture flight planning paths for DJI® Phantom 4 Pro at (a) 0.05 cm/px GSD (b) 1 cm/px; ArduPilot® Mission Planner flight paths for MAPM4 at (c) 0.05 cm/px GSD (d) 1 cm/px.

Data Collection

The image acquisition process using both platforms was implemented on April 16th, 2019. The total flight time for each flight mission was approximately 15 minutes. The weather conditions during the period of the data collection (11 am – 1 pm) consisted of a clear and sunny sky with an outside temperature of 25° C (77° F). The data collection was conducted at this time to minimize the shadowing effects while processing the data and the total surveyed area was 924 m^2. The DJI® Phantom 4 Pro captured a total of 193 images with 1.5 GB data size (86 nadir images at 0.05 cm/px GSD, 37 nadir images at 1 cm/px GSD, and 70 Oblique (45°) images). MAPM4 captured a total of 308 images with 7.3 GB data size (107 nadir images at 0.05 cm/px GSD, 155 nadir images at 1 cm/px GSD, and 46 Oblique (45°) images).

4.3.3 PCD generation

The image-processing software adopted for the PCD generation was Agisoft® Methashape (Agisoft 2019). This SfM-based software has been widely applied in several surveying and mapping studies involving accuracy analyses (Bolkas 2019; Sanz-Ablanedo et al. 2018; Siebert and Teizer 2014; Tomaštík et al. 2019; Zekkos et al. 2018). The PCD generation process was accomplished using laptops that satisfy the minimum requirements recommended by the Agisoft® user manual (Agisoft 2019). Their specifications were:

Intel® Core i7 – 8086K CPU with a burst speed of 4.00 GHz and six processors; 64 gigabytes RAM; and NVIDIA® GeForce 1080 X GPU. The first step of the generation process consisted of producing the sparse PCD by aligning the images using the camera exposure positions and optimizing their orientation (Figure 23-a). Then, depth information was generated based on the estimated camera exposure positions, and images were combined to build a dense PCD (Figure 23-b). The dense PCD data was then used to reconstruct polygonal meshes (Figure 23-c) and subsequently produce textured models (Figure 6-d), tiled models (Figure 23-e), digital elevation models (DEMs) (Figure 6-f), and orthomosaics (Figure 23-g). The SfM workflow parameters, settings, and generated outcomes are presented in Figure 23. To achieve a PCD accuracy within a few centimeters range, the distance between the dual-frequency GNSS (L1/L2) antenna and the camera lens components in the MAPM4 was accurately measured before processing the images (Jóźków and Toth 2014). As a result, the offsets between the antenna center and the camera were estimated as: Δx= 0 m; Δy = 0 m; Δz = 0.344 m for the vertical or nadir images, and Δx = 0 m; Δy = -0.014 m; Δz = 0.356 m for the oblique (45° angle) images. These values were introduced in the Agisoft® Methashape under the camera calibration parameter. The DJI® Phantom 4 Pro did not require this offset measurement step since the GNSS receiver was already incorporated in the platform. It should be noted that all of the PCDs were processed while enabling the rolling shutter compensation option that is available in Agisoft® Methashape in order to avoid any possible distortions during PCD generation (Vautherin et al. 2016).

Figure 23. PCDs processing parameters and SfM-based workflow

A total of 21 PCDs were generated to conduct the comparative assessment, considering the following factors and conditions:

- Data captured by different UAS models and coordinate types:
  - DJI® Phantom 4 Pro with single-frequency GNSS (L1) and stand-alone coordinates (P4P-SAC)
  - MAPM4 with dual-frequency GNSS (L1/L2) and stand-alone coordinates (MP4-SAC)
  - MAPM4 with dual-frequency GNSS (L1/L2) and precise coordinates (MP4-PC)
- Data captures at different ground sampling distances (GSD) and angles:
  - High (H): Nadir images with 1 cm/px GSD
  - Low (L): Nadir images with 0.05 cm/px GSD

- Oblique (O): Images with a camera angle of 45º

Table 15 shows the characteristics of the generated PCDs and their processing information according to the seven image combinations for each of the three UAS platforms and coordinate types. Figure 24 shows the generated 21 PCDs. The precise coordinates were corrected using the differential GNSS positioning technique that is based on PPK technology, with the only exception that the raw GNSS data were collected from the dual-frequency GNSS (L1/L2) antenna that was mounted on the MAPM4 platform and not from the mobile rover station. On the other hand, the stand-alone coordinates were not corrected and were directly obtained from the GNSS satellite signals.

Table 15. PCDs characteristics and processing information

#	UAS Model[a]	Coordinate Type[b]	GNSS Type	PPK Correction?	Image Combination[c]	Processing Time (h:min)	Total Images
1	P4P	SAC	Single-frequency (L1)	No	H	1:36	37
2	P4P	SAC	Single-frequency (L1)	No	L	3:12	86
3	P4P	SAC	Single-frequency (L1)	No	O	3:12	70
4	P4P	SAC	Single-frequency (L1)	No	H + L	7 :36	123
5	P4P	SAC	Single-frequency (L1)	No	H + O	4:54	107
6	P4P	SAC	Single-frequency (L1)	No	L + O	6:24	156
7	P4P	SAC	Single-frequency (L1)	No	H + L + O	13:6	193
8	MP4	SAC	Dual-frequency (L1/L2)	No	H	29: 30	155
9	MP4	SAC	Dual-frequency (L1/L2)	No	L	9:42	107
10	MP4	SAC	Dual-frequency (L1/L2)	No	O	1:42	46
11	MP4	SAC	Dual-frequency (L1/L2)	No	H + L	33:6	262
12	MP4	SAC	Dual-frequency (L1/L2)	No	H + O	13:18	201
13	MP4	SAC	Dual-frequency (L1/L2)	No	L + O	12:18	153
14	MP4	SAC	Dual-frequency (L1/L2)	No	H + L + O	57:54	308
15	MP4	PC	Dual-frequency (L1/L2)	Yes	H	28:42	155
16	MP4	PC	Dual-frequency (L1/L2)	Yes	L	9:42	107
17	MP4	PC	Dual-frequency (L1/L2)	Yes	O	1:48	46
18	MP4	PC	Dual-frequency (L1/L2)	Yes	H + L	64:42	262
19	MP4	PC	Dual-frequency (L1/L2)	Yes	H + O	36:6	201
20	MP4	PC	Dual-frequency (L1/L2)	Yes	L + O	12:30	153
21	MP4	PC	Dual-frequency (L1/L2)	Yes	H + L + O	89:30	308

[a]DJI® Phantom 4 Pro (P4P); Customized MAPM4 (MP4)
[b]Stand-alone Coordinates (SAC); Precise Coordinates (PC)
[c]High (H); Low (L); Oblique (O)

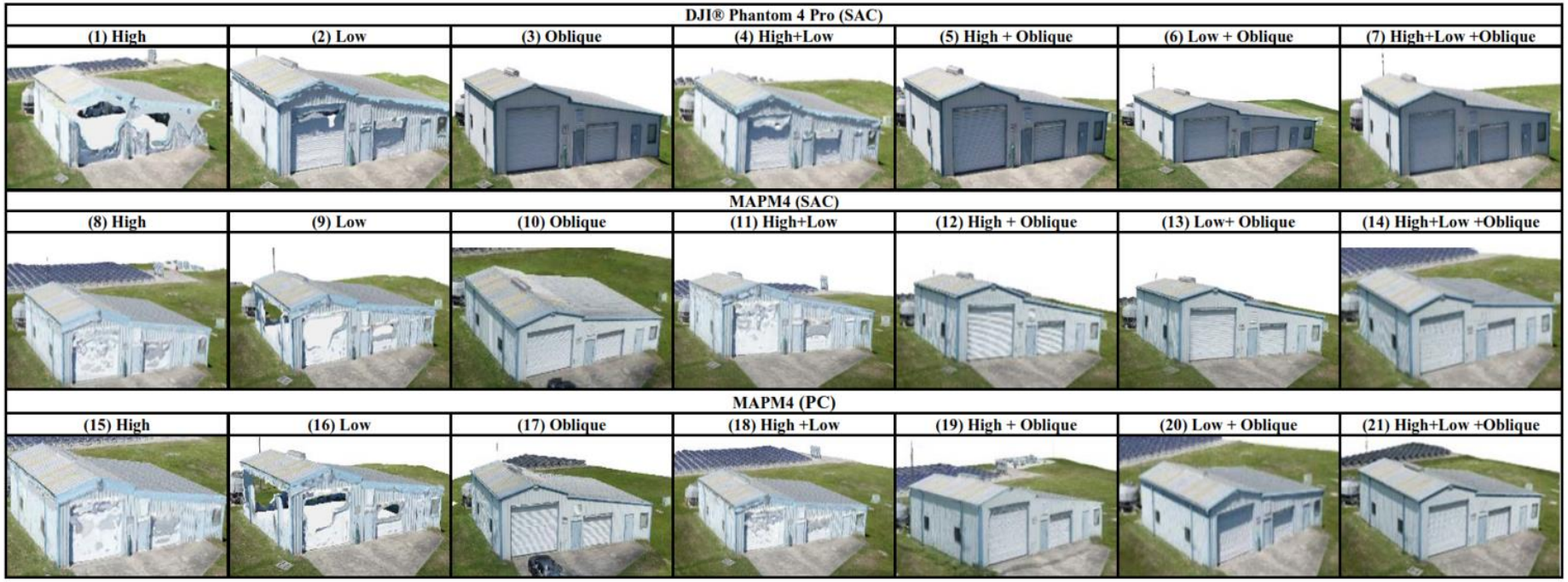

Figure 24. PCDs generated for each UAS model, coordination type, and image *combination*

4.3.4 PCD accuracy assessment

The PCD assessment was conducted using two approaches. The first method consisted of assessing the accuracy of the planimetric (X and Y) and altimetric (Z) positioning coordinates using GCP surveying. More specifically, the process was achieved by retrieving the coordinates positions of the 4 GCPs from the generated orthomosaics (X and Y) and the DEMs (Z) and comparing them to actual field positions of the GCPs which were surveyed using the dual-frequency terrestrial GNSS (L1/L2). The Global Mapper® software was used to measure the X, Y, and Z errors between the observed and the actual GCPs positions (Blue Marble Geographics 2017).

Due to the small size of the surveyed area and the limited number of GCPs or checkpoints, the comparative analysis was performed using Mean Absolute Error (MAE), Standard Deviation (SD), and Modular Error (ME) (Cuartero et al. 2010). MAE was calculated by the sum of the actual coordinate values of the GCPs surveyed (d_{ai}) minus the observed GCPs coordinate positions (d_{oi}) and then divided by the total number of the surveyed GCPs (n). The difference, or error, between the actual (d_{ai}) and observed (d_{oi}) GCPs coordinate positions is known as e_i. The Standard Deviation (SD) indicates the dispersion of observed GCP coordinate values concerning their actual positions. It was calculated by the square root of the sum of the square of e_i minus $\overline{e_i}$ (average of all the e_i) divided by total number of the surveyed GCPs (n) minus one. Finally, the ME was used for calculating the magnitude of the error, which is a vector with three Cartesian components (X, Y, and Z). This magnitude is equivalent to the square root of the sum of the square of MAE_x, MAE_y, and MAE_z, corresponding to the magnitude of the error along X, Y, and Z.

$$MAE = \frac{1}{n}\sum_{i=1}^{n}|d_{ai} - d_{oi}| = \frac{1}{n}\sum_{i=1}^{n}|e_i| \quad (1)$$

$$SD = \sqrt{\frac{\sum_{i=1}^{n}|e_i - \overline{e_i}|^2}{n-1}} \quad (2)$$

$$ME = \sqrt{(MAE_x)^2 + (MAE_y)^2 + (MAE_z)^2} \quad (3)$$

In order to further validate our results and assess the overall accuracy of the generated PCDs, 19 actual field measurements of several building components such as the heights and widths of windows, doors, and facades were measured in the field using a measuring tape. A comparative analysis between these measurements and the ones obtained from the generated PCDs was also performed using the MAE as well as the SD (Table 18). Figure 20-b, 20-c, 20-d, and 20-e shows the components that were measured manually in the field for this analysis.

4.4 PCD Accuracy Results and Discussion

PCD planimetric and altimetric accuracies were analyzed using the formulas discussed above. Table 16 shows the results of the accuracy assessment in Meter for the 21 generated PCDs, which are categorized and will be discussed based on their deployed UAS models, coordinate types, and image combinations: (UAS Model – Coordinates Type – Image Combination). It should be noted that it was not possible to survey the positions of the GCPs and hence assess the accuracy of the generated PCDs in #3 (P4P–SAC–O), #7 (P4P–SAC–HLO), #10 (MP4–SAC–O), and #17 (MP4–PC–O) due to the insufficient number of overlapped images.

Table 16. MAE (m), SD (m) and ME (m) results for the actual field measurement assessment.

#	UAS Model[a]	Coordinate Type[b]	Image Combination[c]	MAE_X (SD_X) (m)	MAE_Y (SD_Y) (m)	MAE_Z (SD_Z) (m)	ME (m)
1	P4P	SAC	H	1.34 (0.17)	1.47 (0.19)	96.59 (0.34)	96.61
2	P4P	SAC	L	0.53 (0.20)	0.57 (0.19)	98.68 (0.02)	98.68
3	P4P	SAC	O	N/A	N/A	N/A	N/A
4	P4P	SAC	H + L	0.25 (0.04)	0.53 (0.35)	98.70 (0.57)	98.70
5	P4P	SAC	H + O	2.23 (0.59)	1.80 (0.68)	94.27 (0.38)	94.32
6	P4P	SAC	L + O	2.37 (0.45)	1.54 (0.49)	95.57 (1.13)	96.53
7	P4P	SAC	H + L + O	N/A	N/A	N/A	N/A
8	MP4	SAC	H	1.09 (0.10)	6.29 (0.04)	30.41 (1.61)	31.07
9	MP4	SAC	L	1.11 (0.16)	0.80 (0.19)	31.17 (0.80)	31.20
10	MP4	SAC	O	N/A	N/A	N/A	N/A
11	MP4	SAC	H + L	1.49 (0.23)	2.10 (0.26)	31.43 (0.55)	31.61
12	MP4	SAC	H + O	1.00 (0.14)	0.80 (0.18)	30.17 (0.69)	30.20
13	MP4	SAC	L + O	0.40 (0.34)	0.35 (0.18)	32.75 (0.99)	32.76
14	MP4	SAC	H + L + O	0.90 (0.54)	1.35 (0.60)	32.48 (0.11)	32.52
15	MP4	PC	H	0.01 (0.01)	0.02 (0.01)	0.04 (0.01)	0.05
16	MP4	PC	L	0.02 (0.01)	0.01 (0.004)	0.03 (0.01)	0.03
17	MP4	PC	O	N/A	N/A	N/A	N/A
18	MP4	PC	H + L	0.01 (0.01)	0.01 (0.01)	0.03 (0.01)	0.03
19	MP4	PC	H + O	0.01 (0.01)	0.02 (0.01)	0.04 (0.01)	0.04
20	MP4	PC	L + O	0.07 (0.02)	0.07 (0.03)	0.16 (0.02)	0.18
21	MP4	PC	H + L + O	0.02 (0.01)	0.02 (0.01)	0.12 (0.01)	0.12

[a]DJI® Phantom 4 Pro (P4P); Customized MAPM4 (MP4)
[b]Stand-alone Coordinates (SAC); Precise Coordinates (PC)
[c]High (H); Low (L); Oblique (O)

The results of the comparative analysis (Table 16) revealed that the most accurate PCDs across all the accuracy measures (MAE_X, MAE_Y, MAE_Z, and ME) were the ones generated by the customized MAPM4 quadcopter with dual-frequency GNSS (L1/L2) and Precise Coordinates (PC) which were subject to PPK-technology coordinates correction (MP4–PC: #15, #16, #18, #19, #20, and #21). The least accurate PCDs were different under each specific accuracy measure. Analyzing the mean absolute error under the X-axis (MAEX) showed that the five least accurate PCDs were PCDs #6 (P4P–SAC–LO: 2.37 m ± 0.45 m), #5 (P4P–SAC–HO: 2.23 m ± 0.59 m), #11 (MP4–SAC–HL: 1.49 m ± 0.23 m), #1 (P4P–SAC–H: 1.34 m ± 0.17 m), and #9 (MP4–SAC–L: 1.11 m ± 0.16 m) (See Figure 25). The mean absolute error analysis under the Y-axis (MAEY) revealed that the five least accurate PCDs were PCDs #8 (MP4–SAC–H: 6.29 m ± 0.04 m), #11 (MP4–SAC–HL: 3.00 m ± 0.26 m), #5 (P4P–SAC–HO: 1.80 m ± 0.68 m), #1 (P4P–SAC–H: 1.47 m ± 0.19 m), and #14 (MP4–SAC–HLO: 1.35 m ± 0.60 m) (See Figure 26). The mean absolute error analysis under the Z-axis (MAEZ) showed that the five least accurate PCDs were PCDs # 4 (P4P–SAC–HL: 98.70 m ± 0.57 m), #2 (P4P–SAC–L: 98.68 m ± 0.02 m), #1 (P4P–SAC–H: 96.59 m ± 0.34 m), #6 (P4P–SAC–LO: 95.57 m ± 1.13 m), and #5 (P4P–SAC–HO: 94.27 m ± 0.38 m) (See Figure 27). Finally, the analysis of the Modular Error (ME) showed that the five least accurate PCDs were PCDs #4 (P4P–SAC–HL: 98.70 m), #2 (P4P–SAC–L: 98.68 m), PCD #1 (P4P–SAC–H: 96.61 m), and PCD #6 (P4P–SAC–LO: 96.53 m), and #5 (P4P–SAC–HO: 94.32 m) (See Figure 28). It should be noted that the least accurate PCDs analyzed by MAEZ and ME were the ones generated by the DJI® Phantom 4 Pro with single-frequency GNSS (L1) and Stand-alone Coordinates (SAC) which were not subject to PPK-technology coordinates correction (P4P–SAC PCDs: #4, #2, #1, #6, and #5). After reviewing the planimetric and altimetric error analysis, the following observations were noticed:

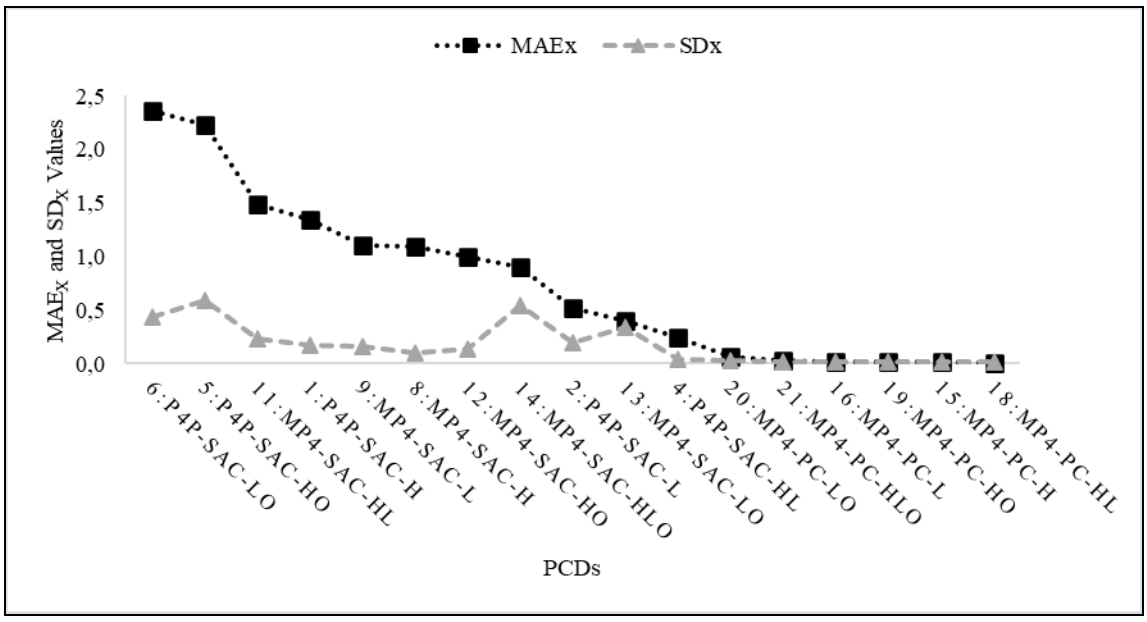

Figure 25. Planimetric error analysis under the X-axis: MAEX and SDX

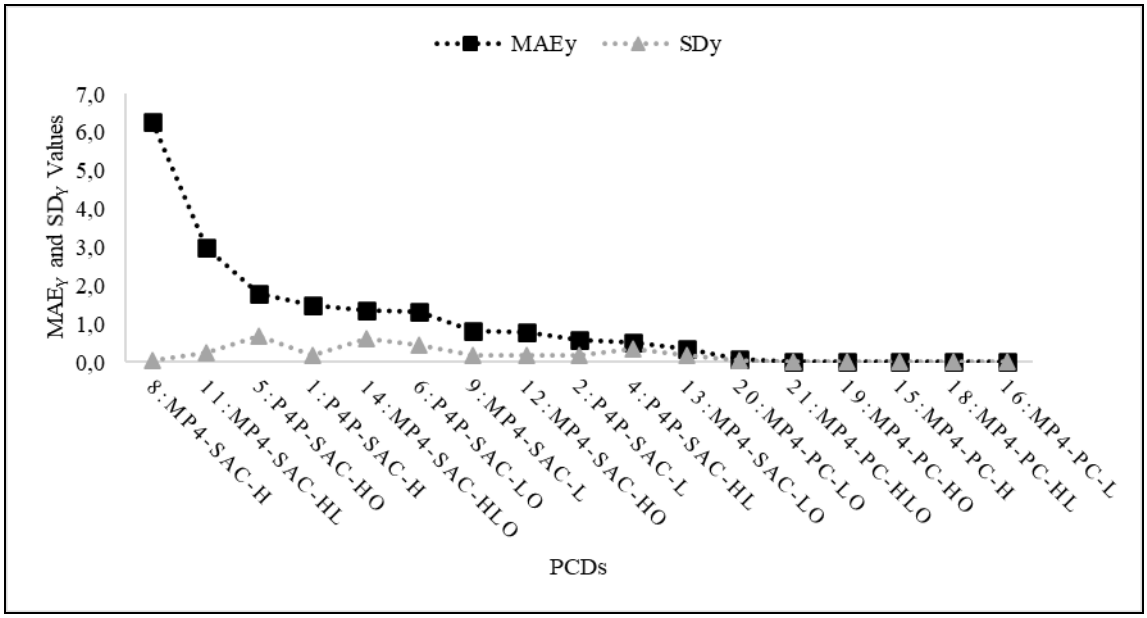

Figure 26. Planimetric error analysis under the Y-axis: MAEY and SDY

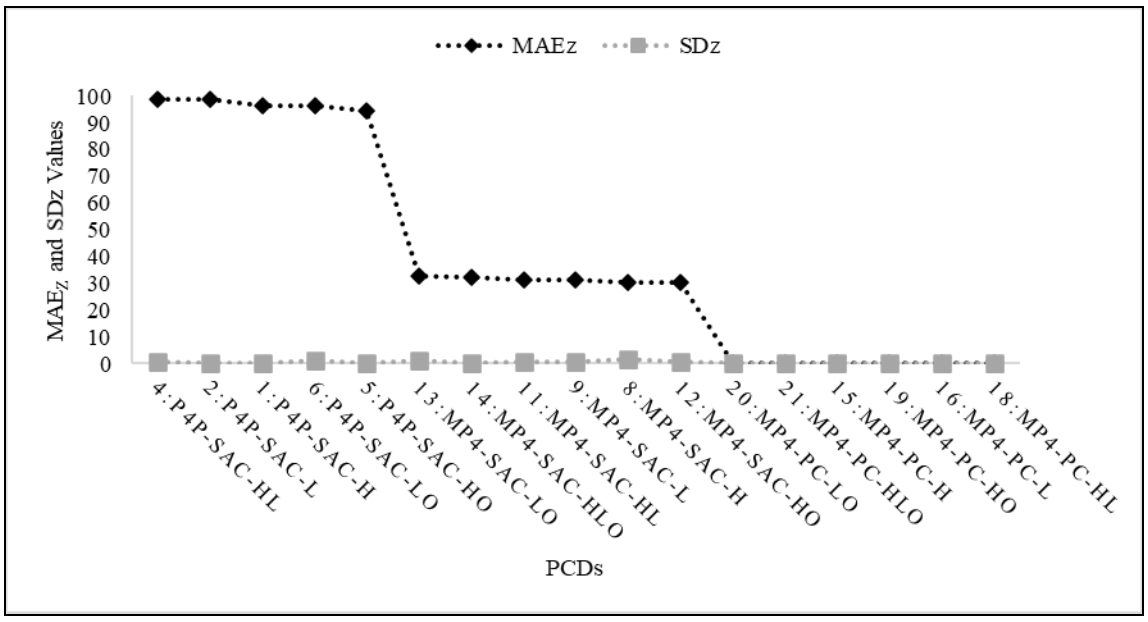

Figure 27.Altimetric error analysis under the Z-axis: MAEZ and SDZ

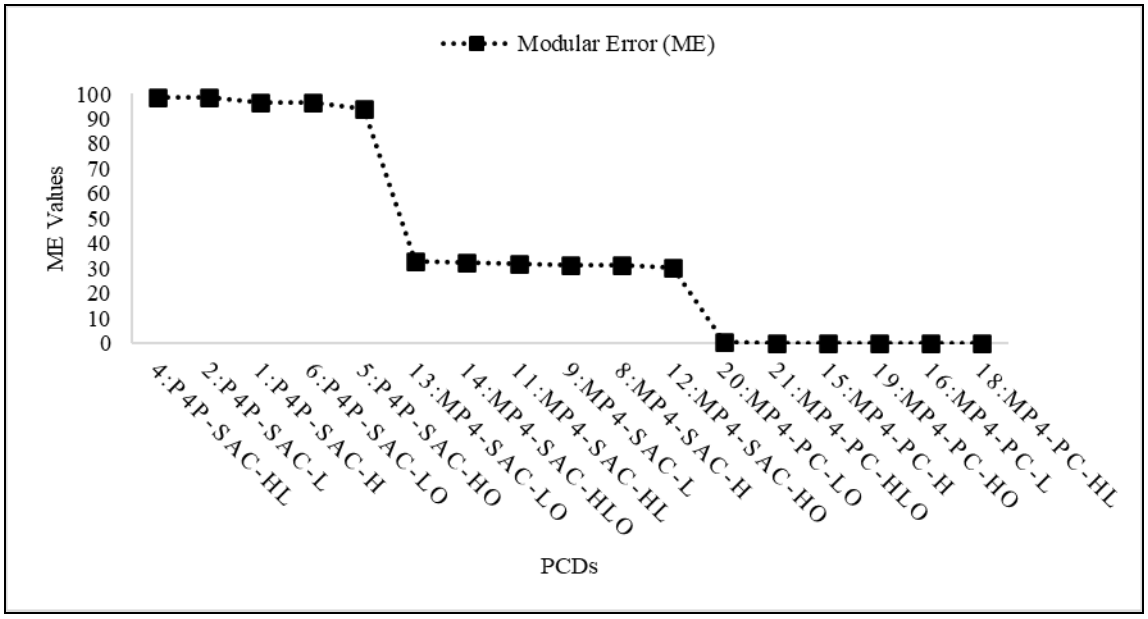

Figure 28. Modular error analysis: ME

After reviewing the planimetric and altimetric error analysis, the following observations were noticed:

- *PPK Correction:* The PCDs generated using PPK-corrected precise coordinates (MP4-PC) presented a high level of accuracy (MAE_X: 0.023, MAE_Y: 0.024, MAE_Z: 0.066, and ME: 0.075) compared to the ones processed using both customized and off-the-shelf platforms with stand-alone coordinates (MP4-SAC and P4P-SAC) (See Table 16). Not only would the use of PPK technology during post-flight enhance the generated PCD accuracies, but it reduces the prolonged and exhaustive amount of work associated with traditional georeferencing techniques through GCPs (Propeller 2019; Shouny et al. 2017).

- *GNSS Type:* It was noted that the dual-frequency GNSS (L1/L2) that was mounted on the MAPM4 platform enhanced the overall PCD accuracy. This enhanced accuracy was validated by the fact that on average, the ME results of the PCDs captured using the customized platform of MP4-SAC (ME: 31.560 m) and MP4-PC (ME: 0.075 m) coordinates with dual-frequency GNSS (L1/L2) were lower than the ones obtained from the commercially available off-the-shelf platform (P4P-SAC: 96.967 m) with single-frequency GNSS (L1). The dual-frequency GNSS (L1/L2) is capable of reducing the ionospheric interferences as well as the ambiguity resolution, factors that make this system a faster, more accurate, and more reliable positioning alternative as compared to the single-frequency GNSS (L1). It is worth noting that in terms of the planimetric error analysis, the PCDs captured using both the customized MP4-SAC with dual-frequency GNSS (L1/L2) (MAE_X: 0.998 m and MAE_Y: 2.097 m) and P4P-SAC with single-frequency GNSS (L1) (MAE_X: 1.342 m and MAE_Y: 1.180 m) did very similarly on average. However, in terms of altimetric analysis, MP4-SAC with dual-frequency GNSS (MAE_Z: 31.403 m) generated more accurate PCDs on average than the P4P-SAC with single-frequency GNSS (L1) (MAE_Z: 96.762 m).

- *Image Combination:* Although the results showed that the use of oblique images enhanced the completeness and visual quality of the processed PCDs, no specific pattern was identified between the types and combinations of the acquired images or camera resolution and the planimetric and altimetric accuracies of the processed PCDs.

It should also be noted that the general visual quality was not only influenced by the number of oblique images but was also negatively affected by the absence of a camera gimbal on the customized platform. The gimbal is responsible for reducing the blurring effects that are caused by inclement weather conditions such as high winds and turbulence during the data collection (Altan and Hacioglu 2017). Also, even with the use of similar GSD values on both platforms, higher resolution cameras such as the one mounted on the MAPM4 tend to increase the number of matching features between the UAS-acquired images, consequently improving the visual PCD quality. With respect to the camera angle, capturing oblique images, especially when visibility from the nadir-oriented camera was poor significantly improved the visual quality and completeness of the PCDs. This finding is expected since oblique image acquisition increases the matching features between the UAS-generated images and enhances the points density of the reconstructed PCDs. While this finding suggests an association between the PCD visual quality and oblique image usage, it also indicates that PCD feature positions and dimensions can be better measured because of the enhanced PCD visual quality definition. However, the results indicate neither that the use of oblique images or higher camera resolution improves the PCD positioning accuracy nor that the PCDs generated from sparser nadir imagery are less accurate than other types of image combinations.

- *Processing Time:* On average, the processing time for creating PCDs using the images captured by the MP4-PC (34:43) was higher than MP4-SAC (22:30) and P4P-SAC (5:43) (Table 15). It should be noted that the MAPM4-acquired images were not geotagged directly during the data collection process but had to be done manually prior to the PCD generation, which led to an increase in the processing time. Moreover, as a part of the coordinate correction process, more metadata were generated, which also led to increased processing time for the PCDs that included this type of coordinates. It is also worth noting that for each specific UAS model, the use of two or more image types increased the PCD processing time (See Table 15). By combining multiple images, the number of matching points required to recreate the dense PCD between the

acquired images increase, which will ultimately raise the SfM-mediated computational complexity and processing time (Qu et al. 2018).

Table 17. The average of the planimetric and altimetric PCD accuracy results for all image combinations

UAS Model	Combination #	GNSS Type	PPK Correction?	MAE_X (m)	MAE_Y (m)	MAE_Z (m)	ME (m)	Average Processing Time (h: min)
P4P-SAC	#1 to #7	L1	No	1.34	1.18	96.76	96.97	5:43
MP4-SAC	#8 to #14	L1/L2	No	1.00	2.10	31.40	31.56	22:30
MP4-PC	#15 to #21	L1/L2	Yes	0.02	0.02	0.07	0.08	34:43

- *Costs associated with PCDs generation:* The MAPM4 which was designed and developed using commercially available components has an estimated cost of USD 5,500, including four sets of batteries and a V-map® 20 Hz dual-frequency GNSS (L1/L2) lightweight receiver. To assembly and test this UAS, it is required at least 16-hour of specialized working hours. The cost of each working hour has an estimated cost of USD 100. Thus, the MAPM4 total cost is USD 7,100. Additionally, the Reference station which includes a V-map 1Hz dual-frequency (L1/L2) GNSS receiver costs USD 2,995. The DJI® Phantom 4 Pro equipped with a single-frequency GNSS (L1) receiver has a retail price of USD 2,000 (including additional propellers and batteries). Therefore, the additional equipment cost required to generate PCDs with accuracy similar the ones obtained in this analysis is approximated at USD 8,095.

As previously discussed, actual field measurements of several building components were conducted to validate the overall accuracy of the generated PCDs. Table 18 shows the results of the actual field measurement against the measurements conducted in the generated PCDs. It should be noted that it was not possible to perform measurements in nine PCDs due to their poor quality and a significant amount of distortions and gaps in them. And these nine PCDs (#1: P4P–SAC–H, #2:P4P–SAC–L, #4:P4P–SAC–HL, #8:MP4–SAC–H, #9:MP4–SAC–L, #11:MP4–SAC–HL, #15:MP4–PC–H, #1:MP4–PC–L, and #18:MP4–PC–HL) were the ones with no oblique images in their PCD generation process. This shows that the acquisition of oblique images plays a vital role in generating high-quality PCDs and avoiding significant visual gaps and inconsistencies in them. Overall, the field measurement validated the outcomes of the previous planimetric and

altimetric error analyses that the most accurate PCDs were the ones captured by the customized MAPM4 quadcopter with dual-frequency GNSS (L1/L2), and Precise Coordinates (PC) which were subject to PPK-technology coordinates correction (MP4–PC PCDs: #17, #19, #20, and #21).

Table 18. MAE (m) and SD (m) results for the actual field measurement assessment.

#	UAS Model[a]	Coordinate Type[b]	Image Combination[c]	MAE (SD)
1	P4P	SAC	H	N/A
2	P4P	SAC	L	N/A
3	P4P	SAC	O	0.11 (0.16)
4	P4P	SAC	H + L	N/A
5	P4P	SAC	H + O	0.14 (0.13)
6	P4P	SAC	L + O	0.08 (0.09)
7	P4P	SAC	H + L + O	0.07 (0.05)
8	MP4	SAC	H	N/A
9	MP4	SAC	L	N/A
10	MP4	SAC	O	0.06 (0.07)
11	MP4	SAC	H + L	N/A
12	MP4	SAC	H + O	0.20 (0.22)
13	MP4	SAC	L + O	0.16 (0.24)
14	MP4	SAC	H + L + O	0.21 (0.30)
15	MP4	PC	H	N/A
16	MP4	PC	L	N/A
17	MP4	PC	O	0.05 (0.05)
18	MP4	PC	H + L	N/A
19	MP4	PC	H + O	0.05 (0.05)
20	MP4	PC	L + O	0.03 (0.04)
21	MP4	PC	H + L + O	0.04 (0.06)

[a]DJI® Phantom 4 Pro (P4P); Customized MAPM4 (MP4)
[b]Stand-alone Coordinates (SAC); Precise Coordinates (PC)
[c]High (H); Low (L); Oblique (O)

4.5 Conclusion

This study evaluates the effects of the single-frequency GNSS (L1) and dual-frequency GNSS (L1/L2) together with post-processing kinematic (PPK) technique on the accuracy of the UAS-generated PCDs for building surveying types of applications. The main contribution of this study is to have a better understanding of the effects of various UAS technical configurations and flight parameters on the accuracy of the UAS-generated PCD data for building surveying applications.

First, a customized rotary UAS was developed and programmed using commercially available hardware and open-source software. On-site data collection was then conducted for a building surveying application using the customized platform with

and without PPK technique together with an off-the-shelf single-frequency GNSS (L1) UAS platform without PPK technology. Twenty-one PCDs were generated using these UAS configurations while considering different flight parameters and image combinations. Finally, the accuracy of those generated PCDs was assessed using planimetric, altimetric, and actual field measurement metrics. The results showed that the PCDs generated through the customized UAS platform with the dual-frequency GNSS (L1/L2) and PPK-corrected precise coordinates were the most accurate ones but required significant process time. Two different camera models could have possibly affected the accuracy of the generated PCDs. Despite using similar GSD values on both platforms during the analysis, the number of matching features between the UAS-acquired images tend to increase with the use of higher resolution cameras such as the one mounted on the MAPM4 platform. This in turn enhances the visual quality of the generated PCDs. On the other hand, outfitting a platform such as the DJI Phantom 4 Pro with a camera gimbal can reduce the blurring effects caused by inclement weather conditions during image data collection, factor that also enhances the visual quality of the reconstructed PCDs. Further research is warranted to assess, quantify, and better understand the effects of the camera configurations and resolutions on the PCD accuracy and visual quality.

The performed analyses led to the development of a PCD accuracy matrix, which categorized the levels of point cloud accuracy for different UAS configurations while considering their processing time (See Table 19). In this context, very high and high accuracy levels are usually necessary for applications such as structural and building inspections (e.g., crack width detection and quantification) or cadastral monitoring and surveying. Achieving such high accuracy levels usually require long processing time to generate the PCDs. Average accuracy levels could be used for applications such as earthwork volume calculations, safety management, or progress monitoring, whereas low and very low levels could be suitable for tasks such as marketing or project visualization. The outcome of this study would help the construction practitioners and researchers to better understand the use of UAS technology for generating PCDs with various levels of accuracy that could be used for different applications within the AECO industry.

Table 19. PCD Accuracy Matrix

			Level of PCD Accuracy[a]					PCD Processing Time[b]
			Planimetric and Altimetric Error Analyses				Actual Field Measurements	
UAS Model	GNSS Type	PPK Correction?	MAE_X	MAE_Y	MAE_Z	ME	ME	
P4P-SAC	L1	No	Very Low	Very Low	Very Low	Very Low	Low	Medium
MP4-SAC	L1/L2	No	Low	Very Low	Very Low	Very Low	Low	Long
MP4-PC	L1/L2	Yes	High	High	Average	Average	Average	Long

[a] Level of PCD Accuracy (m): Very High: <0.01, High: 0.01–0.05, Average: 0.05–0.25, Low: 0.25–1, Very Low: > 1
[b] PCD Processing Time: Short: <1 h, 1 h <Medium<10 h, Long>10 h

This research has some limitations that need to be stated. First, the experiment was performed on an isolated building with open sky, and the results obtained from this study cannot be generalized for other types of buildings. Further research is warranted to validate the adopted technique in other types of construction such as large size construction and high-rise buildings. As for the altimetric and planimetric error analyses, the small size of the surveyed area restricted the use of more than 20 GCPs or validation points, which constitute the minimum sample size required to conduct analyses based on the Root Mean Square Error (RMSE) (ASPRS 2015). The latter is one of the most common approaches used for assessing the planimetric and altimetric accuracy of the SfM-derived products (Rempel 2016). Future studies should also assess projects with larger surveying areas and conduct PCD accuracy assessment analyses based on the RMSE calculations.

4.6 Data Availability Statement

Some or all data, models, or code generated or used during the study are available from the corresponding author by request (PCDs and photos).

4.7 References

Adams, S. M., Levitan, M. L., and Friedland, C. J. (2014). "High resolution imagery collection for post-disaster studies utilizing unmanned aircraft systems (UAS)." *Photogrammetric Engineering and Remote Sensing*, 80(12), 1161–1168.

http://doi.org/10.14358/PERS.80.12.1161

Agisoft. (2019). “Agisoft Metashape User Manual.” Accessed September 17, 2019. https://www.agisoft.com/pdf/metashape-pro_1_5_en.pdf.

Albeaino, G., Gheisari, M., and Franz, B. W. (2019). “A systematic review of unmanned aerial vehicle application areas and technologies in the AEC domain.” *Journal of Information Technology in Construction*, 24(July), 381–405.

Altan, A., and Hacioglu, R. (2017). “Modeling of Three-Axis Gimbal System on Unmanned Air Vehicle (UAV) under External Disturbances.” *In 2017 25th Signal Processing and Communications Applications Conference, SIU 2017*, 3–6. http://doi.org/10.1109/SIU.2017.7960196

Álvares, J. S., Costa, D. B., and Melo, R. R. S. de. (2018). “Exploratory study of using unmanned aerial system imagery for construction site 3D mapping.” *Construction Innovation*, 18(3), 301–320. http://doi.org/10.1108/CI-05-2017-0049

ArduPilot. (2019). “The Cube User Manual V1 .0.” Accessed July 30, 2019. https://ardupilot.org/copter/index.html.

ASPRS. (2015). “ASPRS Positional Accuracy Standards for Digital Geospatial Data.” *Photogrammetric Engineering & Remote Sensing*, 81(3), 1–26. http://doi.org/10.14358/pers.81.3.a1-a26

Barbosa, A., Bastos, D., De, R. S., and Sampaio, J. (2017). “Uso de Veículo Aéreo não Tripulado (vant) para geração de produtos fotogramétricos aplicados à gestão de obras.” *1º Simpósio Brasileiro de Tecnologia da Informação e Comunicação na Construção*.

Benjamin, A. R., O’Brien, D., Barnes, G., Wilkinson, B. E., and Volkmann, W. (2020). “Improving Data Acquisition Efficiency: Systematic Accuracy Evaluation of GNSS-Assisted Aerial Triangulation in UAS Operations.” *Journal of Surveying Engineering*, 146(1): 05019006. http://doi.org/10.1061/(ASCE)SU.1943-5428.0000298

Blankenberg, L. E. (1992). “GPS-supported aerial triangulation - state of the art.” *The Photogrammetry Journal of Finland*, 13(1), 128–149.

Blue Marble Geographics. (2017). “Getting Started Guide.” Accessed Octuber 10, 2019. https://www.bluemarblegeo.com/docs/guides/global-mapper-v18-getting-started-

sp.pdf.

Bolkas, D. (2019). “Assessment of GCP Number and Separation Distance for Small UAS Surveys with and without GNSS-PPK Positioning.” *Journal of Surveying Engineering*, 145(3): 04019007. http://doi.org/10.1061/(ASCE)SU.1943-5428.0000283

Carlton, C. D., Mitchell, S., and Lewis, P. (2018). “Preliminary application of Structure from Motion and GIS to document decomposition and taphonomic processes.” *Forensic Science International*, 282, 41–45. http://doi.org/10.1016/j.forsciint.2017.10.023

Carrivick, J., Smith, M., and Quincey, D. (2016). *Structure from motion in the geosciencies*. (T. Atrium, ed.), Markono Print Media Pte ltd., Oxford.

Chao, H., Cao, Y., and Chen, Y. (2010). “Autopilots for small unmanned aerial vehicles: A survey.” *International Journal of Control, Automation and Systems*, 8(1), 36–44. http://doi.org/10.1007/s12555-010-0105-z

Costa, D., Melo, R., Alvares, J., and Bello, A. (2016). “Evaluating the Performance of Unmanned Aerial Vehicles for Safety Inspection.” *International Group for Lean Construction*, 23–32.

Cuartero, A., Armesto, J., Rodríguez, P. G., and Arias, P. (2010). “Error analysis of terrestrial laser scanning data by means of Spherical statistics and 3D graphs.” *Sensors (Switzerland)*, 10(11), 10128–10145. http://doi.org/10.3390/s101110128

Daftry, S., Hoppe, C., and Bischof, H. (2015). “Building with drones: Accurate 3D facade reconstruction using MAVs.” *2015 IEEE International Conference on Robotics and Automation (ICRA)*, IEEE, 3487–3494. http://doi.org/10.1109/ICRA.2015.7139681

Datta-Barua, S., Doherty, P. H., Delay, S. H., Dehel, T., and Klobuchar, J. A. (2003). “Ionospheric scintillation effects on single and dual frequency GPS positioning.” *Proceedings of the 16th International Technical Meeting of the Satellite Division of The Institute of Navigation (ION GPS/GNSS 2003)*, 336–346.

Deng, Z., Bender, M., Zus, F., Ge, M., Dick, G., Ramatschi, M., Wickert, J., Lhnert, U., and Schön, S. (2011). “Validation of tropospheric slant path delays derived from single and dual frequency GPS receivers.” *Radio Science*, 46(6), 1–11.

http://doi.org/10.1029/2011RS004687

DJI. (2017). “Phantom 4 Pro/Pro+ User Manual.” Accessed December 18, 2019. https://dl.djicdn.com/downloads/phantom_4_pro/Phantom+4+Pro+Pro+Plus+User+Manual+v1.0.pdf.

Eschmann, C., Kuo, C.-M., Kuo, C.-H., and Boller, C. (2013). “High-Resolution Multisensor Infrastructure Inspection With Unmanned Aircraft Systems.” *ISPRS - International Archives of the Photogrammetry, Remote Sensing and Spatial Information Sciences,* XL-1/W2(September), 125–129. http://doi.org/10.5194/isprsarchives-xl-1-w2-125-2013

Ezenne, G. I., Jupp, L., Mantel, S. K., and Tanner, J. L. (2019). “Current and potential capabilities of UAS for crop water productivity in precision agriculture.” *Agricultural Water Management*, Elsevier, 218(November 2018), 158–164. http://doi.org/10.1016/j.agwat.2019.03.034

Fazeli, H., Samadzadegan, F., and Dadrasjavan, F. (2016). “Evaluating the potential of RTK-UAV for automatic point cloud generation in 3D rapid mapping.” *International Archives of the Photogrammetry, Remote Sensing and Spatial Information Sciences - ISPRS Archives*, 41(July), 221–226. http://doi.org/10.5194/isprsarchives-XLI-B6-221-2016

Forlani, G., Dall’Asta, E., Diotri, F., di Cella, U. M., Roncella, R., and Santise, M. (2018). “Quality assessment of DSMs produced from UAV flights georeferenced with on-board RTK positioning.” *Remote Sensing*, 10(2), 1–23. http://doi.org/10.3390/rs10020311

Gende, M., Harris, E. M., Brunini, C., Radicella, S. M., and Herraiz, M. (2005). “Ionospheric biases correction for coordinates derived from GPS single point positioning.” *Annals of Geophysics*, 48(3), 439–444.

Ghaffarian, S., and Kerle, N. (2019). “Towards post-disaster debris identification for precise damage and recovery assessments from uav and satellite images.” *International Archives of the Photogrammetry,* Remote Sensing and Spatial Information Sciences - ISPRS Archives, 42(2/W13), 297–302. http://doi.org/10.5194/isprs-archives-XLII-2-W13-297-2019

Gheisari, M., and Esmaeili, B. (2019). “Applications and requirements of unmanned aerial systems (UASs) for construction safety.” *Safety Science*, 118(May), 230–240. https://doi.org/10.1016/j.ssci.2019.05.015

Gheisari, M., Rashidi, A., and Esmaeili, B. (2018). “Using Unmanned Aerial Systems for Automated Fall Hazard Monitoring.” *Proceeding of Construction Research Congress 2018*, (Janicak 1998), 148–157.

Harwin, S., and Lucieer, A. (2012). “Assessing the accuracy of georeferenced point clouds produced via multi-view stereopsis from Unmanned Aerial Vehicle (UAV) imagery.” *Remote Sensing*, 4(6), 1573–1599. https://doi.org/10.3390/rs4061573

Hubbard, B., Wand, H., Leasure, M., Ropp, T., Lofton, T., and Hubbard, S. (2015). “Feasibility Study of UAV use for RFID Material Tracking on Construction Sites.” *51st ASC Annual international conference proceedings*, (1995), 669–676.

Hugenholtz, C. H., Walker, J., Brown, O., and Myshak, S. (2015). “Earthwork volumetrics with an unmanned aerial vehicle and softcopy photogrammetry.” *Journal of Surveying Engineering*, 141(1): 06014003. https://doi.org/10.1061/(ASCE)SU.1943-5428.0000138

Iizuka, K., Itoh, M., Shiodera, S., Matsubara, T., Dohar, M., and Watanabe, K. (2018). “Advantages of unmanned aerial vehicle (UAV) photogrammetry for landscape analysis compared with satellite data: A case study of postmining sites in Indonesia.” *Cogent Geoscience*, Cogent, 4(1), 1–15. https://doi.org/10.1080/23312041.2018.1498180

Iqbal, U., Irtiza, S., Shah, A., Jamil, M., Gillani, S. O., and Ayaz, Y. (2015). “Selection of Unmanned Aerial System (Uas) for Disaster Relief Operations : a Comparison.” *Journal of Science International*, 27(4), 3199–3203.

Ishida, K. (2017). “Investigating the accuracy of 3D models created using SfM.” *ISARC 2017 - Proceedings of the 34th International Symposium on Automation and Robotics in Construction*, (Isarc), 834–839.

Jóźków, G., and Toth, C. (2014). “Georeferencing experiments with UAS imagery.” *ISPRS Annals of Photogrammetry, Remote Sensing and Spatial Information Sciences*, II–1(November), 25–29. https://doi.org/10.5194/isprsannals-ii-1-25-2014

Khosiawan, Y., Park, Y., Moon, I., Nilakantan, J. M., and Nielsen, I. (2018). "Task scheduling system for UAV operations in indoor environment." *Neural Computing and Applications*, Springer London, *31(9)*, 5431-5459. https://doi.org/10.1007/s00521-018-3373-9

Koutsoudis, A., Vidmar, B., Ioannakis, G., Arnaoutoglou, F., Pavlidis, G., and Chamzas, C. (2014). "Multi-image 3D reconstruction data evaluation." *Journal of Cultural Heritage*, 15(1), 73–79. https://doi.org/10.1016/j.culher.2012.12.003

Kumar, M. (1988). "World geodetic system 1984: a modern and accurate global reference frame." *Marine Geodesy*, 12(2), 117–126.

Liu, J., Jennesse, M. J., and Holley, P. (2016). "Utilizing Light Unmanned Aerial Vehicles for the Inspection of Curtain Walls: A Case Study." *Construction Research Congress 2016*, 2039–2049.

Luo, X., Li, S., and Xu, H. (2016). "Results of Real-Time Kinematic Positioning Based on Real GPS L5 Data." *IEEE* Geoscience and Remote Sensing Letters, IEEE, 13(8), 1193–1197. https://doi.org/ 10.1109/LGRS.2016.2575062

Mancini, F., Dubbini, M., Gattelli, M., Stecchi, F., Fabbri, S., and Gabbianelli, G. (2013). "Using unmanned aerial vehicles (UAV) for high-resolution reconstruction of topography: The structure from motion approach on coastal environments." *Remote Sensing*, 5(12), 6880–6898. https://doi.org/10.3390/rs5126880

Martínez-Carricondo, P., Agüera-Vega, F., Carvajal-Ramírez, F., Mesas-Carrascosa, F. J., García-Ferrer, A., and Pérez-Porras, F. J. (2018). "Assessment of UAV-photogrammetric mapping accuracy based on variation of ground control points." *International Journal of Applied Earth Observation and Geoinformation*, Elsevier, 72(June), 1–10. https://doi.org/10.1016/j.jag.2018.05.015

Martinez, J. G., Gheisari, M., and Alarcón, L. F. (2020). "UAV Integration in Current Construction Safety Planning and Monitoring Processes: Case Study of a High-Rise Building Construction Project in Chile." *Journal of Management in Engineering*, 36(3): 05020005. https://doi.org/10.1061/(ASCE)ME.1943-5479.0000761

Mian, O., Lutes, J., Lipa, G., Hutton, J. J., Gavelle, E., and Borghini, S. (2015). "Direct georeferencing on small unmanned aerial platforms for improved reliability and

accuracy of mapping without the need for ground control points." *International Archives of the Photogrammetry, Remote Sensing and Spatial Information Sciences - ISPRS Archives*, 40(1W4), 397–402. https://doi.org/ 10.5194/isprsarchives-XL-1-W4-397-2015

Mohammadi, M. E., and Wood, R. L. (2018). "Damage Assessment of Built-Up Areas Via UAS-SfM Derived Point Cloud Data." *11th U.S. National Conference on Earthquake Engineering*, 68503, 1–5.

Morgenthal, G., and Hallermann, N. (2014). "Quality Assessment of Unmanned Aerial Vehicle (UAV) Based Visual Inspection of Structures." *Advances in Structural Engineering*, SAGE PublicationsSage UK: London, England, 17(3), 289–302. https://doi.org/10.1260/1369-4332.17.3.289

Niethammer, U., James, M. R., Rothmund, S., Travelletti, J., and Joswig, M. (2012). "UAV-based remote sensing of the Super-Sauze landslide: Evaluation and results." *Engineering Geology*, Elsevier B.V., 128, 2–11. https://doi.org/10.1016/j.enggeo.2011.03.012

Papakonstantinou, A., Kavroudakis, D., Kourtzellis, Y., Chtenellis, M., Kopsachilis, V., Topouzelis, K., and Vaitis, M. (2019). "Mapping Cultural Heritage in Coastal Areas with UAS: The Case Study of Lesvos Island." *Heritage*, 2(2), 1404–1422. https://doi.org/10.3390/heritage2020089

Pix4D. (2019a). "Pix4Dcapture." Accessed April 29, 2019. https://www.pix4d.com/product/pix4dcapture/.

Pix4D. (2019b). "How to verify that there is enough overlap between the images." Accessed September 30, 2019. https://support.pix4d.com/hc/en-us/articles/203756125-How-to-verify-that-there-is-enough-overlap-between-the-images/.

Propeller. (2019). "Construction Industry: Trends and Predictions." Accessed April 23, 2019. https://www.propelleraero.com/blog/drones-in-construction-2019-industry-trends-and-predictions/.

Qu, Y., Huang, J., and Zhang, X. (2018). "Rapid 3D reconstruction for image sequence acquired from UAV camera." *Sensors (Switzerland)*, 18(1), 225.

https://doi.org/10.3390/s18010225

Remondino, F., Barazzetti, L., Nex, F., Scaioni, M., and Sarazzi, D. (2012). "UAV Photogrammetry for Mapping and 3D Modeling – Current Status and Future Perspectives." *ISPRS - International Archives of the Photogrammetry, Remote Sensing and Spatial Information Sciences*, XXXVIII-1/(June 2014), 25–31. https://doi.org/10.5194/isprsarchives-XXXVIII-1-C22-25-2011

Rempel, H. W. (2016). "Manual of Photogrammetry, 6th Edition." *Photogrammetric Engineering & Remote Sensing*, American Society for Photogrammetry and Remote Sensing, 82(4), 249–250.

Ruggles, S., Clark, J., Franke, K. W., Wolfe, D., Reimschiissel, B., Martin, R. A., Okeson, T. J., and Hedengren, J. D. (2016). "Comparison of SfM computer vision point clouds of a landslide derived from multiple small UAV platforms and sensors to a TLS-based model." *Journal of Unmanned Vehicle Systems*, 4(4), 246–265. https://doi.org/10.1139/juvs-2015-0043

Sanz-Ablanedo, E., Chandler, J. H., Rodríguez-Pérez, J. R., and Ordóñez, C. (2018). "Accuracy of Unmanned Aerial Vehicle (UAV) and SfM photogrammetry survey as a function of the number and location of ground control points used." *Remote Sensing*, 10(10). https://doi.org/10.1139/juvs-2015-0043

Scaioni, M., Barazzetti, L., and Brumana, R. (2009). "RC-Heli and structure & motion techniques for the 3-D reconstruction of a Milan Dome spire." *ISPRS - International Archives of the Photogrammetry, Remote Sensing and Spatial Information Sciences*.

Serrat, C., Banaszek, A., Cellmer, A., and Gibert, V. (2019). "Use of UAVs for Technical Inspection of Buildings within the BRAIN Massive Inspection Platform." *IOP Conference Series: Materials Science and Engineering*, 471(2). https://doi.org/10.1088/1757-899X/471/2/022008

Shouny, A. El, Yakoub, N., and Hosny, M. (2017). "Evaluating the Performance of Using PPK-GPS Technique in Producing Topographic Contour Map." *Marine Geodesy*, 40(4), 224–238. https://doi.org/10.1080/01490419.2017.1321594

Siebert, S., and Teizer, J. (2014). "Mobile 3D mapping for surveying earthwork projects using an Unmanned Aerial Vehicle (UAV) system." *Automation in Construction*,

Elsevier B.V., 41, 1–14. https://doi.org/10.1016/j.autcon.2014.01.004

Tomaštík, J., Mokroš, M., Surový, P., Grznárová, A., and Merganič, J. (2019). "UAV RTK/PPK Method—An Optimal Solution for Mapping Inaccessible Forested Areas" *Remote Sensing*, 11(6), 721. https://doi.org/10.3390/rs11060721

U.S. Department of transportation. (2016). "Small Unmanned Aircraft Systems (sUAS) - Part 017." Accessed September 2, 2019. https://www.faa.gov/documentlibrary/media/advisory_circular/ac_107-2.pdf.

UVS International. (2018). "UVS International – Remotely Piloted Systems : Promoting International Cooperation & Coordination." Accessed Nomberber 19, 2019. https://uvs-international.org/.

Vacanas, Y., Themistocleous, K., Agapiou, A., and Hadjimitsis, D. (2015). "Building Information Modelling (BIM) and Unmanned Aerial Vehicle (UAV) technologies in infrastructure construction project management and delay and disruption analysis." *Third International Conference on Remote Sensing and Geoinformation of the Environment (Rscy2015)*, 9535(September), 95350C. https://doi.org/10.1117/12.2192723

Vautherin, J., Rutishauser, S., Schneider-Zapp, K., Choi, H. F., Chovancova, V., Glass, A., and Strecha, C. (2016). "Photogrammetric Accuracy and Modeling of Rolling Shutter Cameras." *ISPRS Annals of Photogrammetry, Remote Sensing and Spatial Information Sciences*, III–3(June 2016), 139–146. https://doi.org/10.5194/isprsannals-iii-3-139-2016

Vmap. (2016). "Mapping without groud control points." Accessed Nomberber 19, 2019. http://v-map.net/white-paper/.

Westoby, M. J., Brasington, J., Glasser, N. F., Hambrey, M. J., and Reynolds, J. M. (2012). "Structure-from-Motion' photogrammetry: A low-cost, effective tool for geoscience applications." *Geomorphology*, Elsevier B.V., 179, 300–314. https://doi.org/10.1016/j.geomorph.2012.08.021

Xiang, T. Z., Xia, G. S., and Zhang, L. (2019). "Mini-Unmanned Aerial Vehicle-Based Remote Sensing: Techniques, applications, and prospects." *IEEE Geoscience and Remote Sensing Magazine*, 7(3), 29–63. https://doi.org/10.1109/MGRS.2019.2918840

Yao, H., and Clark, R. L. (2000). “Evaluation of sub-meter and 2 to 5 meter accuracy GPS receivers to develop digital elevation models.” *Precision Agriculture*, 2(2), 189–200. https://doi.org/10.1023/A:1011429815226

Zekkos, D., Greenwood, W., Lynch, J., Manousakis, J., Athanasopoulos-Zekkos, A., Clark, M., Cook, K. L., and Saroglou, C. (2018). “Lessons learned from the application of UAV-enabled structure-from-motion photogrammetry in geotechnical engineering.” *ISSMGE International Journal of Geoengineering Case Histories*, 4(4), 254–274. https://doi.org/10.4417/IJGCH-04-04-03

Zhou, S., and Gheisari, M. (2018). “Unmanned aerial system applications in construction: a systematic review.” *Construction Innovation*, 18(4), 453–468. https://doi.org/10.1108/CI-02-2018-0010

Zhou, Z., Irizarry, J., and Lu, Y. (2018). “A Multidimensional Framework for Unmanned Aerial System Applications in Construction Project Management.” *Journal of Management in Engineering*, 34(3): 04018004. https://doi.org/10.1061/(ASCE)ME.1943-5479.0000597

CHAPTER 5: iSafeUAS: DEVELOPMENT AND ASSESSMENT OF AN UNMANNED AERIAL SYSTEM FOR CONSTRUCTION SAFETY INSPECTION

Jhonattan G. Martinez[1]*, Gilles Albeaino[2], Masoud Gheisari, Ph.D., A.M. ASCE[3], Raja R. A. Issa, Ph.D., F. ASCE[4], and Luis F. Alarcón, Ph.D., M. ASCE[5]

5.1 Introduction

Construction is considered as one of the most dangerous industries for workers due to its dynamic, continuously changing, and diverse spatiotemporal environment (Pinto et al. 2011). The US Bureau of Labor Statistics reported that 971 (20.7%) out of 4,674 fatalities in the private sector occurred in the construction industry alone in 2017 (US Bureau of Labor Statistics 2018). More than half (59.9%) of these deaths were associated with the fatal four hazards, which include falls (39.2%), struck-by (8.2%), electrocution (7.3%), and caught-in or between (5.1%) (US Bureau of Labor Statistics 2017). During that same year, the construction industry was also ranked first in terms of the number of fatal work injuries compared to all other sectors (US Bureau of Labor Statistics 2018). Conventionally, safety managers and professionals used to walk and observe their jobsites in-person to mitigate unsafe situations and practices (Woodcock 2014). Based on their observations, preventative and corrective actions are implemented to prevent workers' injuries or even deaths (Perlman et al. 2014). However, the dynamic nature, complexity, and size of the jobsites, as well as the reduced number of safety managers within each site, might negatively affect the overall performance of the managers in fully identifying unsafe situations, which might potentially lead to injuries and fatalities among construction workers (Park et al. 2017).

As a result, researchers and practitioners are continuously exploring other safety management plans and technologies that would ultimately enhance safety inspection and monitoring on the jobsites. Recently, Unmanned Aerial Systems (UASs) have been utilized as an efficient safety inspection and monitoring tool that could potentially assist safety personnel on the construction jobsites (Gheisari and Esmaeili 2019). UASs, also known as

drones or Unmanned Aerial Vehicles (UAVs), are remotely-piloted aerial platforms that can be equipped with a variety of onboard sensors, depending on the nature of the applied tasks (Hassanalian and Abdelkefi 2017).

These vehicles have experienced enormous enhancements with respect to their software and hardware over the last few years, factors that promoted their incorporation in several construction-related tasks (Ham et al. 2016). In construction, UASs have been used for different applications, ranging from site mapping and surveying (Ham et al. 2016; Rakha and Gorodetsky 2018; Samad et al. 2013) and progress monitoring (Álvares et al. 2018; Ham et al. 2016; Irizarry and Costa 2016) to structural inspection (Ham et al. 2016; Wierzbicki et al. 2015) and post-disaster assessment (Adams et al. 2014; Ghaffarian and Kerle 2019; Iqbal et al. 2015). This adoption in construction stems from the operational flexibility of the aerial platforms, and their abilities to access hard-to-reach or dangerous areas (Albeaino et al. 2019). Besides, the use of UASs on jobsites is associated with reductions in time and costs while accomplishing tasks, as well as improvements in safety when compared to other more traditional techniques (Albeaino et al. 2019). UASs have also been applied for safety inspection and monitoring purposes on the construction jobsites. As an example, Alizadehsalehi et al. (2018) found that UAS technology is capable of identifying safety hazards on the jobsite and transmitting, in real-time, high-resolution videos and images to safety managers for safety inspection and assessment purposes. Tuttas et al. (2017) favored the use of UASs over handheld cameras due to the platforms' location independency, which allows a more comprehensive and accurate onsite safety evaluation by capturing images at different angles and heights. However, several limitations, such as weather conditions, mechanical failures, and flight regulations, were identified as factors that might limit the UAS's full implementation for construction safety applications (Martinez et al. 2020).

Such legal, safety, and human factors hinder the full deployment of UASs as reliable platforms for safety monitoring and inspection purposes on the construction jobsites. For example, the Federal Aviation Administration (FAA) flight regulations

restrict the use of aerial platforms over populated areas and active sites, an essential factor that might limit UAS operations near construction jobsites due to their potential safety risks. In addition, UAS-related deployment issues such as human or operational errors, software or hardware flaws, and signal losses could potentially result in hazardous situations such as struck-by, collision, and fall accidents. Besides, using UASs on the jobsites might distract workers, and affect their psychological status and situational awareness, potentially leading to hazardous situations. There is an increasing interest among researchers and practitioners to better integrate UAS technology for construction safety monitoring and inspection applications. However, no prior studies have investigated the development of methods in UAS design and development that might minimize the safety risks associated with the full deployment of UASs as safety monitoring and inspection platforms on construction jobsites. This study is an initial effort to develop and assess iSafeUAS, a UAS platform designed for safety inspection purposes with customized features that reduce the UAS flight-associated safety risks on the jobsite. To ensure a safe yet accurate visual data acquisition without the need to fly over populated areas, the iSafeUAS is equipped with an RGB Camera Sensor with super optical zoom capabilities and a Recovery System was designed, developed, and tested.

The RGB Camera Sensor with super optical zoom capabilities allows for capturing high-quality visual assets from farther distances, reducing the need for UAS operations over workers and active jobsites. Flying away from the jobsites and people, in turn, reduces the risks associated with workers distraction caused by UAS operation on the jobsites, signal interferences due to the presence of several onsite components (e.g., metallic structures, power lines), and jobsite obstacles which potentially lead to hazardous situations. The Recovery System significantly reduces the impact of struck-by or falling accidents caused by any technical, operational, or even weather-related challenges. Finally, the iSafeUAS was deployed on a real-world construction jobsite to validate its safety inspection capabilities. The outcomes of this study aid construction practitioners and researchers in providing a comprehensive overview and understanding of the technical design, development, assessment, and onsite implementation of a customized UAS

intended for safety inspection applications. The Architecture, Engineering, and Construction (AEC) industry and the academic field might benefit from the findings of this research in understanding how the use of a customized UAS would enhance the safety inspection process on construction sites and ensure a safe implementation in this setting.

5.2 Background

Over the past few years, there has been a growing interest among researchers to integrate UAS technology for construction safety management and monitoring tasks (See Table 20). UAS deployment for construction safety applications was first explored by Irizarry et al. (2012) and Gheisari et al. (2014), who conducted usability experiments through a heuristic approach to determine how UASs could assist safety managers on the jobsites. Both studies concluded that UASs provide managers the ability to communicate in real-time with construction workers in a faster and more efficient manner. Worker distraction due to the onsite use of the relatively new UAS technology and the potential struck-by accidents caused by UAS operation over workers on the active sites were two stated limitations that might hinder the full deployment of UASs on the construction jobsites. Later on, Irizarry and Costa (2016) conducted an exploratory study to determine the potential applications of UAS-acquired visual images for construction management tasks. Based on a database comprising UAS images and videos of several jobsites, the authors concluded that UAS adoption could be useful for several construction-related applications, including jobsite logistics, progress monitoring, safety condition evaluation, and quality inspection. However, the authors noted several challenges facing the use of UASs on the jobsites: (1) worker distraction due to the onsite utilization of UASs; (2) FAA flight regulations that prohibit flying over populated areas; and (3) potential struck-by hazards due to UAS operation near workers on the construction sites. Concurrently, Kim et al. (2016) developed a survey to identify the users' requirements and the challenges of integrating UASs into construction safety inspection tasks, as well as the factors that affect this technology's performance in this context. The authors recommended using high-quality UAS visualizations and user-friendly interfaces for a better implementation. They also indicated a few limitations of using UASs as safety monitoring tools, including the

FAA flight regulations that restrict UAS operation over workers, the presence of several obstacles on the jobsite (e.g., power lines, cranes, trees) which potentially cause hazardous situations, the limited technical capabilities of the UASs (e.g., short battery life), and the inclement weather conditions (e.g., high wind, rain). A more recent study assessed the feasibility of using UAS visuals to identify several onsite components (e.g., demarcation of material loading and unloading areas, personal protective equipment, warning signs, falling protection equipment, traffic routes) that do not comply with safety standards (de Melo et al. 2017). After establishing a guideline for UAS-mediated safety monitoring tasks, the study advocated the use of UASs and showed that this technology could enhance the visualization of the jobsite condition. Similar to the previous studies, authors mentioned a few implementation barriers to using UASs for safety monitoring, such as: (1) FAA flight regulations, which restrict the use of UASs over people; (2) lack of required training and skills among UAS pilots for safe flights on the jobsites; (3) severe weather conditions such as high wind and rain, which might affect UAS operation; (4) possible collision with several obstacles (i.e., cranes) present on the jobsite; and (5) low-quality visual sensors, which could affect the process of generating good quality visualizations of the site. At the same time, Roberts et al. (2017) applied a state-of-the-art object detector to a set of UAS-captured images and accurately monitored cranes and workers during crane payload activities, to reduce the safety hazards initially associated with this type of tasks. Although the object detector functioned properly, the authors considered the poor-quality images (e.g., blur or overexposed images) captured by UAS as one of the main barriers that might negatively affect the quality of the reconstructed point clouds and ultimately lead to improper identification of hazards on the jobsite.

More recently, Alizadehsalehi et al. (2018) integrated Building Information Modeling (BIM) and UASs to detect and monitor hazardous conditions on the jobsites. They showed that such integration helps with acquiring relevant information related to specific objects located onsite and identify hazardous conditions such as missing guardrails, unprotected openings, inadequate scaffoldings, lack of proper personal protective equipment, deficient safety signs, and the presence of hazardous wastes. The

authors also indicated a few factors limiting UAS implementation for construction safety, including lack of pilot training and skills, inclement weather and high winds, short battery life and radio-controller signal interference, as well as workers' distraction caused by the onsite UAS deployment. In another concurrent study, Gheisari et al. (2018) developed and tested an algorithm that relied upon UAS images to automate and ultimately simplify the safety inspection process by making it less time- and labor-intensive. The main objective of the algorithm was to detect openings and guardrails that did not meet the Occupational Safety and Health Administration (OSHA) standards. The authors found several limitations that might restrict the deployment of UASs for safety inspection applications, including: (1) workers' distraction associated with the onsite operation of UASs; (2) flight rules and regulations which restrict UAS usage over populated areas; and (3) technical factors such as short battery life, low quality onboard sensors, and radio-controller signal interferences. A similar study also developed and tested a pattern-recognition algorithm that relied on UAS images to automatically detect guardrails not meeting construction safety standards (Mendes et al. 2018). Despite mentioning several limitations such as environmental challenges (e.g., wind and sunlight reflectivity) and low quality of onboard sensors, the results revealed that this technique was efficient in detecting guardrails and accomplishing inspection tasks in a timely and effortless manner. Using UAS visualizations, Pratama et al. (2018) built a Virtual Reality (VR) environment of a post-disaster building zone for safety training purposes. The study concluded that the use of 3D models generated by UAS imagery is a more affordable, faster and safer alternative to recreate indoor environments of damaged buildings. Simultaneously, de Melo et al. (2018) conducted an exploratory case study on an existing building to understand the potential of integrating UAS point clouds and BIM for safety planning decision making and safety systems definition purposes. The authors advocated the UAS-BIM integration and concluded that this technique offers a low-cost solution for safety planning and improving the work conditions. Subsequently, de Melo and Costa (2019) developed a framework to better understand how UAS technology and resilience engineering can be integrated for safety planning and control purposes. After presenting a safety monitoring protocol using UASs, the authors advocated the use of this technology for safety monitoring tasks and concluded

that the aerial platforms are capable of enhancing workers' awareness through safety training and providing visual content for safety managers to assist them in the decision-making process. The authors noted that workers distraction due to the onsite deployment of UASs, possible struck-by accidents caused by UASs operation over workers and active sites, and limited UAS piloting skills and training were some limitations facing UAS adoption for construction safety inspection and monitoring. Gheisari and Esmaeili (2019) conducted a survey study on UAS applications for construction safety and addressed the challenges of using UAS as a construction safety monitoring and control tool on the jobsites. Based on the outcomes of that study, some of the most important barriers to UAS adoption in construction safety applications included liability and legal concerns (e.g., personal injuries and property damage caused by UAS or UAS pilot error, invasion of privacy and insurance issues) and safety challenges (e.g., struck-by or falling accidents, worker distraction due to the deployment of UASs over actives jobsites). Moreover, limited technical capabilities (e.g., short battery life, low sensors quality, and signal interferences) and extensive training requirements needed for UAS pilots to operate the UASs were some other important barriers that need to be considered for a better UAS deployment on the jobsites. More recently, Melo and Costa (2020) developed a UAS-based safety monitoring protocol to evaluate the potential of using UAS technology for construction safety monitoring applications. More specifically, the authors assessed the compliance of ongoing construction activities with the established safety standards using UAS imagery and a safety checklist. The results showed that UASs could help safety managers in the decision-making process by providing valuable jobsite information as well as improving workers' awareness through safety training. Martinez et al. (2020) investigated the impact of integrating UASs with current safety monitoring and planning methods for high-rise type of construction and concluded that this adoption might improve the identification and assessment of outdoor safety risks on the construction jobsites. Several legal (e.g., restricted flight regulations), technical (e.g., limited battery capacity, low visual sensor quality, signal interferences caused by nearby steel structures and power lines), environmental (e.g., strong winds), and safety-related (e.g., struck-by accidents, worker distraction, presence of several jobsite obstacles) challenges were stated as

limitations affecting the full deployment of UASs on jobsites. Finally, Kim et al. (2020) proposed a conceptual workflow integrating UAS technology for safety management applications on the construction jobsites. The authors indicated similar UAS-related limitations such as weather conditions, magnetic signal interferences, and worker distraction.

Table 20.UAS-related limitations

#	*References*	*Safety Inspection Aspect*	*Stated UAS Deployment Limitations*								
			FAA Flight Regulations	Low Quality Visual Sensors	Pilot Skills and Training Requirements	Struck-by Accidents	Workers Distraction	Signal Interferences	Short Battery Life	Weather Conditions	Jobsite Obstacles
1	Melo and Costa (2020)	General Inspection									
2	Martinez et al. (2020)	General Inspection	■			■	■	■	■	■	■
3	Kim et al. (2020)	General Inspection					■	■		■	
4	de Melo and Costa (2019)	General Inspection			■	■	■				
5	Gheisari and Esmaeili (2019)	General Inspection	■	■	■	■	■	■	■		
6	Pratama et al. (2018)	General Inspection									
7	Mendes et al. (2018)	Fall Hazards		■						■	
8	de Melo et al. (2018)	General Inspection									
9	Gheisari et al. (2018)	Fall Hazards	■	■			■	■	■		
10	Alizadehsalehi et al. (2018)	General Inspection			■		■	■	■	■	
11	Roberts et al. (2017)	Crane Inspection		■							
12	de Melo et al. (2017)	General Inspection	■	■	■					■	■
13	Kim et al. (2016)	General Inspection	■						■	■	■
14	Irizarry and Costa (2016)	General Inspection	■			■					
15	Gheisari et al. (2014)	General Inspection				■					
16	Irizarry et al. (2012)	Personal Protective Equipment				■					

As summarized in Table 20, several factors were noted in the literature that could affect the usage of UAS technology for safety monitoring and inspection tasks on construction jobsites. It was repeatedly indicated that the FAA regulations prohibit UAS operation over active sites and populated areas or over people who are not directly involved in the flight mission (US Department of Transportation 2016). The quality of the visual sensors mounted on the commercially available platforms that are commonly used in the construction domain is not yet sufficient to capture jobsite visual assets from farther distances. Therefore, UAS flight team members tend to compromise between the FAA regulations, which prevent UAS operation near active sites from one side, and the quality

of the UAS-acquired images and videos that would help identify onsite hazardous situations. Those limitations, together with the other ones indicated in the literature, including the high proficiency and training required for the UAS pilots to conduct the flight mission; high potentials for hazardous situations such as struck-by accidents or worker distraction due to the UAS flights on the jobsites and near or over people; technical limitations (e.g., signal interferences due to the presence of several obstacles and short battery life); the challenging environmental or weather conditions (e.g., snow, rain, wind, sunlight) as well as jobsite obstacles (e.g., building structure, trees, cranes) are considered as some of the critical barriers affecting the full usage of UASs for construction safety monitoring and inspection applications.

5.3 Research Problem and Objectives

This study aims to explore the methods in UAS technical design, development, and assessment that would improve the use of UASs as safety inspection and monitoring tools by minimizing the safety risks associated with their full deployment on construction jobsites. There is a need among construction researchers and practitioners to reduce the UAS-related limitations and safety challenges and improve the adoption of this technology on jobsites. No prior research has explored the UAS design and development methods that could minimize any of the challenges and safety risks shown in Table 20 to integrate UAS technology in construction safety management and monitoring tasks. In this study, a UAS platform, known as iSafeUAS, specifically designed, and developed for safety inspection purposes will be introduced. The iSafeUAS platform is specifically equipped with an RGB Camera Sensor with super optical zoom capabilities and a Recovery System. The combination of this RGB Camera Sensor and the Recovery System significantly reduce the challenges associated with the use of UASs as a safety inspection tool on the jobsites. More particularly, by equipping the iSafeUAS with an RGB Camera Sensor with super optical zoom capabilities, data collection can be accomplished from farther distances while providing significantly detailed visual data that can be used for safety assessment purposes. Data acquisition from farther distances might significantly reduce the number of flights required onsite or in close proximity to the buildings or other equipment on the jobsite and

minimize the hazardous situations these onsite or close UAS flights might cause (e.g., worker distraction, collision with the onsite equipment or jobsite obstacles, signal interferences due to the presence of several onsite obstacles). Furthermore, equipping the iSafeUAS with a Recovery System would minimize the potential safety risks of UAS crash over people or equipment and the ultimate struck-by accidents that might be caused due to various reasons such as technical challenges (e.g., hardware or software malfunction), operational issues (e.g., pilot mistakes), or inclement weather conditions. The use of this system would ensure that the impact of accidents due to struck-by and UAS crashes is significantly reduced, improving the system usefulness for safety monitoring and inspection applications in the construction domain. In this study, iSafeUAS, a customized aerial platform that is equipped with a high-quality RGB Camera Sensor with super optical zoom capabilities and a Recovery System was designed, developed, and its performance was assessed. iSafeUAS was then deployed on a real-world construction jobsite to validate its safety inspection capabilities. The main contribution of this study is to provide construction practitioners and researchers with a comprehensive overview and understanding of the adopted iSafeUAS technical design, development, assessment, and onsite implementation that would lead to the safe deployment of UASs as safety inspection tools on construction jobsites.

5.4 Research Method

iSafeUAS was designed to minimize the potential safety risks associated with UAS deployment for construction-safety related applications. A three-step process was implemented in this study (Figure 29):

(5) *iSafeUAS Design, Development, and Programming:* iSafeUAS was designed, developed and programmed using commercially available open-source software and hardware.
(6) *iSafeUAS Technical Performance Assessment:* Flight tests were conducted using iSafeUAS to evaluate the performance of its technical components

(7) *iSafeUAS Application for Safety Monitoring of a Real Jobsite:* iSafeUAS was deployed on a real-world construction jobsite to validate its safety inspection potential.

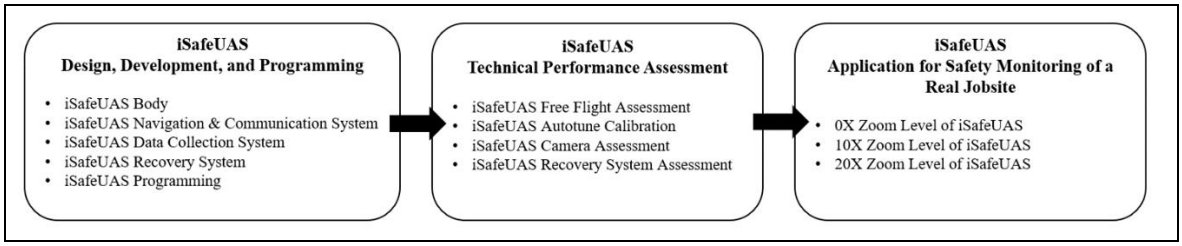

Figure 29. Research Steps

The following sections further discuss the three steps of iSafeUAS development, assessment, and system validation.

5.5 iSafeUAS Design, Development, And Programming

The first step in this study involves the design, development, and programming of iSafeUAS, using commercially available open-source software and hardware. The open-source design enables the customization of UASs based on the user's preferences and the specific tasks the platform is intended to accomplish. Besides, open sourcing allows the installation and modification of several types of sensors or spare parts in case of any required adjustments or hardware failure in the platform.

5.5.1 iSafeUAS design and development

The design of iSafeUAS is based on a rotary-wing hexacopter that is driven by six motors and characterized by a foldable design and an increased payload carrying capacity (Hassanalian and Abdelkefi 2017). Rotary-wing vehicles are characterized by their maneuverability, stability, vertical takeoff and landing capability, as well as their high payload capacity and mechanical simplicity (Albeaino et al. 2019) which would be ideal for conducting frequent safety inspections of the buildings and equipment on the jobsites. The hardware components used to build the iSafeUAS were selected based on their wide availability in the market as well as their ability to be integrated with open-source software (e.g., ArduPilot®). ArduPilot® is a popular fully-featured open-source autopilot software

that is designed specifically for remotely piloted vehicles (ArduPilot 2019). This software was specifically used because it allows performing tests both in real-time and during the post-flight setting through the use of the data-logging, analysis, and simulation features to better understand and control the effects of the flight parameters on the flight mission. Figure 30 shows the iSafeUAS platform with all the incorporated components which are as follows:

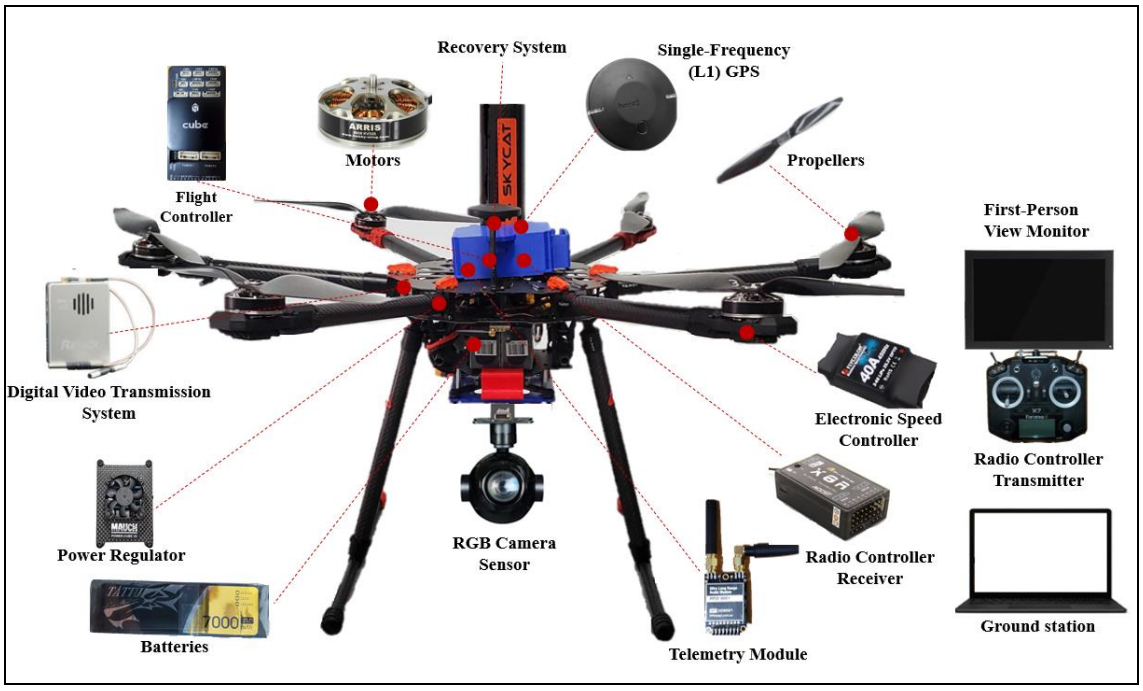

Figure 30. iSafeUAS assembled components

iSafeUAS Body: An aluminum and carbon fiber six-rotor airframe characterized by a lightweight and foldable design was used as the Vehicle Body of the iSafeUAS. The platform is powered by two Tattu® 6S1P 7000 mAh Lithium-Polymer Batteries, each composed of six cells. A total of six ARRIS® 5008 335KV Multi-Copter Outrunner Brushless Motors were mounted on the six arms of the platform. The Motors are connected to a Power Distribution Board that is embedded in the Platform Frame through six Flycolor® Weig Electronic Speed Controllers. Those controllers are responsible for regulating the speed of the Motors based on the instructions transmitted by the UAS Flight Controller. Additionally, six Tarot® 1855 Carbon Fiber Propellers were connected on top

of the Motors. A Power Regulator, Mauch Electronics® Power Cube-3, was also mounted on the platform to control the voltage and current levels required to operate the UAS, including its navigation, data collection, and Recovery System. Table 21 shows the UAS body components and their technical features.

Table 21. iSafeUAS Body components and their technical features

Components (×Quantities)	Manufacturer/ Model	Technical Features
Frame (×1)	Tarot® X6 960 Class Multirotor Airframe	Size: 960 mm diameter Arm legs (×6) length: 392 mm; ground clearance: 320 mm Operating temperature: -20 ~ +50 ℃ Suggested flight altitude: <1000m Weight: 2,700 g
Batteries (×2)	Tattu® 6S1P	Power: 7000 mA Cells: 6 in each Weight: 812 g each
Motors (×6)	ARRIS® 5008 335KV Multi-Copter Outrunner Brushless Motor	Power: 335 kV Diameter: 57.7 mm Weight:185.5 g each
Electronic Speed Controllers (×6)	Flycolor® Weig ESC	Current peak: 40 A Weight: 26 g each
Propellers (×6)	Tarot® 1855	Pitch size: 139.7 mm Diameter: 457.2 mm Weight: 37.3 g each
Power Regulator (×1)	Mauch Electronics® Power Cube-3	Size: 64 mm x 58 mm x 24 mm Input voltage: 4-14S Output voltage: 5.30V to 12.0 V Current: 200A Weight: 69 g each

iSafeUAS Navigation and Communication System: The UAS Navigation and Communication System relies on Inertial Navigation System (INS) sensors to determine the in-flight velocity, acceleration, altitude, as well as the position and angular orientation of the platform and the RGB Camera Sensor. These INS parameters are necessary for the autonomous flight control of the platform (Conte and Doherty 2011). The INS sensors, which were incorporated in the Automatic Pilot System or Flight Controller, consisted of three redundant sets of Inertial Measurement Units (IMUs) with multiple gyroscopes, and accelerometers, as well as several barometers and magnetometers. Such sensors will allow the platform to be controlled and operated autonomously (Chao et al. 2010). Pixhawk® 2.1 was used as the Flight Controller in the iSafeUAS due to its compatibility with ArduPilot open-source hardware and software (ArduPilot 2019). Besides, the iSafeUAS was also equipped with Hex Technology® Here-2 GNSS GPS, a single-frequency (L1) GPS,

mainly due to its compatibility with the Pixhawk® 2.1 Flight controller. A Telemetry Module was used to facilitate the communication between the platform and its ground station. Finally, a FrSky® Taranis Q X7 Radio Controller Transmitter and a FrSky® X8R Radio Controller Receiver were used for remote operation of the iSafeUAS. Table 22 summarizes the iSafeUAS Navigation and Communication System components and their technical features.

Table 22. iSafeUAS Navigation and Communication System components and their technical features

Components (×Quantities)	Manufacturer/ Model	Technical Features
Automatic Pilot System or Flight Controller (×1)	Pixhawk® 2.1 Series	Processor: 32bit STM32F427 Cortex-M4F® core with FPU RAM: 256 KB Flash memory: 2 MB Co-processor: 32-bit STM32F103 failsafe co-processor Weight: 250 g
Telemetry Module (×1)	RFDesign® 900	Air antenna 1: 900 MHZ 2 dBi Monopole Air antenna 2: 900 MHZ 2 dBi Right angle Monopole Ground antenna 1: 900 MHZ 3 dBi Dipole Ground antenna 2: 900 MHZ 3 dBi Dipole RFD air modem serie: RFD900 Plus Operating range: Up to 1.5 km Weight (total): 140 g
Single-Frequency (L1) GPS (×1)	Hex Technology® Here-2 GNSS GPS	Navigational update rate: 10 Hz Receiver type: L1 Tracking and navigation sensitivity: -167 dBm Positioning accuracy: up to 2.5 m INS included: Compass, Gyro, Accelerometer (ICM20948) and Barometer (MS561) Weight: 136 g each Size: 46.5 mm x 27 mm x 14.4 mm
Radio Controller Receiver (×1)	FrSky® X8R	Operating voltage range: 4V – 10.0V Operating current: 100mA at 5V Operating range: > 1.5 km Weight: 16.8 g
Radio Controller Transmitter (×1)	FrSky® Taranis Q X7	Operating voltage range: 6~15V Operating current: 210mA Number of channels: 16 Operating range: Up to 1.5 km Weight: 619 g

iSafeUAS Data Collection System: A Foxtech® Seeker-30 TR RGB Camera Sensor with super 30X optical zooming capabilities and a 3-axis gimbal was assembled on the iSafeUAS platform using a 3D-Printed Camera Mount System (Table 23). The main reasons behind choosing this specific visual sensor include: its lightweight and precise 3-axis gimbal, which ensures high camera sensor stability, particularly in unsteady weather environments; and its high zooming capabilities, capturing very detailed visual contents of

the jobsite from farther distances. DVL1® 5G, a Digital Video Transmission System, was also used to transmit the visual data from the RGB Camera Sensor to the First-Person View Monitor. A 10.1-inch large size Elecrow® First-Person View Monitor was used to provide an appropriate-size and high-quality visual data feed in real-time during the jobsite inspections (Irizarry et al. 2012).

Table 23. iSafeUAS data collection system components and their technical features

Components (×Quantities)	Manufacturer/ Model	Technical Features
RGB Camera Sensor (×1)	Foxtech ® Seeker-30 TR	Size: 144 mm x151 mm x158 mm Type of sensor: 1/2.8-inch 2.13 MP CMOS Focal length: 4.4 mm to 129 mm Maximum optical zoom: 30X Video output resolution: 1080-px 30 fps recording Voltage: 12 Volts Weight: 720 g
Digital Video Transmission System (×1)	DVL-1 ® 5G	Communication distance: Up to 2000 m Power: 200 mW Video resolution: Up to 1080- px 60 fps Weight: 284 g
First-Person View Monitor (×1)	Elecrow® HDMI Led Display	Size: 255 mm x 164 mm x 28 mm Screen size: 10.1 in Aspect ratio: 16:9 (width: height) Resolution: 1920 x 1080 px Weight: 450 g

iSafeUAS Recovery System: Skycat® Recovery Bundle, a Recovery System designed to accommodate UASs weighing between 5 and 10 kg, was added on the iSafeUAS platform using a 3D-Printed Mount System. This Recovery System was selected specifically due to its: (1) compatibility with the Pixhawk® 2.1 Flight Controller; (2) lightweight and small size design; and (3) programming capabilities which allow the Recovery System to be deployed both manually and automatically based on certain flight parameters that could be defined for the Recovery System (further discussed in Section iSafeUAS Programming). The Recovery System consists of a Carbon Fiber Launcher, a Servo Channel Trigger Switch, and a Blanket (Table 24).

Table 24. UAS Recovery system components and characteristics

Components	Model Manufacturer	Characteristics
Recovery System (×1)	Skycat® X55 PRO	Launcher: Length: 209 mm Diameter: 55 mm Weight: 157 g

	Servo trigger: Voltage: 45V Signal standard: RC PWM 50Hz Weight: 37 g Recovery System blanket: Diameter: 1.52 m Weight: 126 g

5.5.2 iSafeUAS programming

The ArduPilot® Mission Planner was used to program the iSafeUAS. This open-source navigation software is an autopilot suite that is compatible with a wide variety of unmanned vehicles, including UASs, rovers, boats, and submarines (ArduPilot 2019). First, the ArduCopter v4.0.1 Hexa firmware was installed by connecting the platform to the Ground Station (ASUS® VivoBook S510U) via the Flight Controller. Flight parameters such as maximum speed and acceleration, flight modes, takeoff and landing speeds, and maximum lean angle were then transferred from Ground Station to the Flight Controller. Then, some of the iSafeUAS navigation, communication, and speed-related components such as GPS Accelerometer, Radio Controller Receiver, Radio Controller Transmitter, and Electronic Speed Controller were calibrated, and the flight modes were configured. Three flight modes commonly used to program open-source platforms, were also adopted to program the iSafeUAS: (1) Stabilize Mode: maintaining a consistent altitude while self-leveling the roll and pitch axes; (2) Loiter Mode: using the GPS to automatically maintain the current platform altitude and position, allowing the pilot to manually fly the platform through the use of the remote controller; and (3) Auto Mode: executing pre-programmed mission scripts with waypoints and do commands. The GPS Compass was then calibrated to compensate for the effects of the magnetic fields, allowing the platform to operate in a pre-programmed path (Dinesh et al. 2018). Finally, the Recovery System of the iSafeUAS was programmed based on established automatic and manual deployment conditions retrieved from the Ardupilot user manual (ArduPilot 2019). The automatic and manual deployment conditions would cover the majority of the hazardous situations in case of any accidents and might minimize the impact of the iSafeUAS fall on the jobsites (Table 25). The automatic deployment mode would activate

without any human intervention, whereas the manual deployment mode would fully rely on the iSafeUAS pilot's judgment to deploy it.

Table 25. Automatic and manual Recovery System deployment conditions

Deployment Mode	Human Intervention	Conditions[a]
Automatic	None	The Motors need to be armed The UAS is not landed[b] The roll and/or pitch angle of the UAS is 20 degrees off from the target lean angle The UAS is not climbing The UAS is above the minimum deploy altitude (i.e., 5 m)
Manual	Full	The Motors need to be armed The Radio Channel 9 is set in the high position

[a]All the conditions pertaining to the automatic deployment mode need to be true for at least 2 seconds
[b]The UAS is considered landed if: (1) the output throttle is less than 25%; (2) the Motors have reached their lower limit; (3) the vehicle is not rotating by more than 20 degrees/seconds; and (4) the UAS pilot is not requesting a climb. The prior conditions need to be true for 1 second to consider the UAS as landed.

5.6 iSafeUAS Technical Performance Assessment

To assess the technical performance of the iSafeUAS, a widely open area in a community park located in Safety Harbor, FL was selected. This location was specifically selected because it was free from any obstacles, people, building interferences, and there were no FAA-restricted zones or controlled airspaces in place. The weather conditions during the UAS performance assessment period (10 am – 12 pm) consisted of a clear and sunny sky with light winds and an outside temperature of 30°C (86°F). Three onsite flight tests were conducted to assess the stability of the iSafeUAS and its adjustment, flight mode functionality, battery life, and camera assessment followed by two indoor flight simulations to evaluate the automatic and manual Recovery System deployments (Table 26).

Table 26. iSafeUAS assessment

Assessments	Assessment Description	Assessment Aspect	Flights
Free Flight Assessment	Flying the iSafeUAS using different flight modes to assess the platform's stability and its maximum battery life.	• Platform stability • Flight mode functionality (i.e., stabilize, loiter, and auto modes) • Maximum battery life	Onsite Flight Test #1
Autotune Calibration	Balancing iSafeUAS flight characteristics to get better inflight stability.	• Platform stability adjustment (i.e., roll, pitch)	Onsite Flight Test #2
Camera Assessment	Testing the camera response during pre-programmed flight missions.	• Functionality of the RGB Camera Sensor	Onsite Flight Test #3

Assessments	Assessment Description	Assessment Aspect	Flights
Recovery System Assessment	Testing the automatic deployment conditions of the Recovery System in a controlled environment.	• Automatic Recovery System deployment	Indoor Simulation #1
	Testing the manual deployment conditions of the Recovery System in a controlled environment.	• Manual Recovery System deployment	Indoor Simulation #2

Free Flight Assessment: A free flight was conducted at first to mainly assess, in a real-world outdoor environment, the stability of the customized platform, the functionality of its adopted flight modes, and the maximum UAS flight time and endurance with the addition of the payloads. It should be noted that prior to the initialization of the flight mission, the compass of the iSafeUAS was re-calibrated due to the change in the original location of the platform. During the free-flight test, the UAS was subject to different maneuvers, including roll, pitch, yaw, and pan to assess its stability in the air. In addition, the three adopted flight modes (i.e., Stabilize, Loiter, and Auto) that were performed and tested onsite showed that the platform was properly programmed and is capable of performing such types of flights. To safely operate the iSafeUAS without compromising the safety of the onsite construction personnel and avoid any damage caused by overheating, the platform battery reserve was set up to 20% (Imdoukh et al. 2017). This reduction resulted in a total flying time duration of 15.6 minutes when compared to the original 19.5 minutes flying capacity that was retrieved from the flight-generated logs. Future studies are needed to optimize the iSafeUAS hardware battery consumption to increase its flight duration.

Autotune Calibration: A second flight was performed using the autotune flight mode with the aim of improving the inflight iSafeUAS stability. The autotune calibration mainly consists of autonomously operating the platform and making several sharp maneuvers to automatically calibrate the UAS roll and pitch parameters, and achieve the highest level of response without significantly exceeding the capabilities of the platform (Kitchen et al. 2018). This step enhanced the maneuverability of the iSafeUAS during the autonomous flight and ensured its flight stability and accuracy.

Camera Assessment: An autonomous (Auto Mode) flight mission, generated using pre-defined GPS waypoints through the ArduPilot® Mission Planner, was performed to evaluate the functionality of the RGB Camera Sensor in automatically acquiring visuals based on the flight controller commands (Homola et al. 2016). The platform operated for a total duration of 9 min, at an elevation of 20 m AGL, covering an area of 230 m^2. Analyzing the flight logs, the results showed that the RGB Camera Sensor was capable of autonomously capturing visual assets based on the pre-planned instructions.

Recovery System Assessment: Two simulations were conducted in an indoor setting to assess the automatic and manual deployment of the Recovery System if any of the previously discussed programming conditions were not met (See Table 26). The minimum altitude value parameter was first disabled prior to any assessment given the indoor nature of the experiment. The connections between the Flight Controller and the Recovery System were also checked for proper installation. All previously defined programming conditions in both automatic and manual settings were simulated in the tests, and results indicated that the iSafeUAS was successfully programmed and is able to be deployed in case any of these conditions were not met. For example, in the automatic deployment mode, manually inclining the iSafeUAS by 20° relatively to its target lean angle for 2 seconds resulted in the indication of the Recovery System deployment in the Mission Planner (Figure 31). In the manual mode, the Radio Controller Channel 9 was exclusively programmed to deploy the Recovery System once set to the high position. This ultimately resulted in UAS motors stop, and a successful Recovery System deployment signal in the Mission Planner.

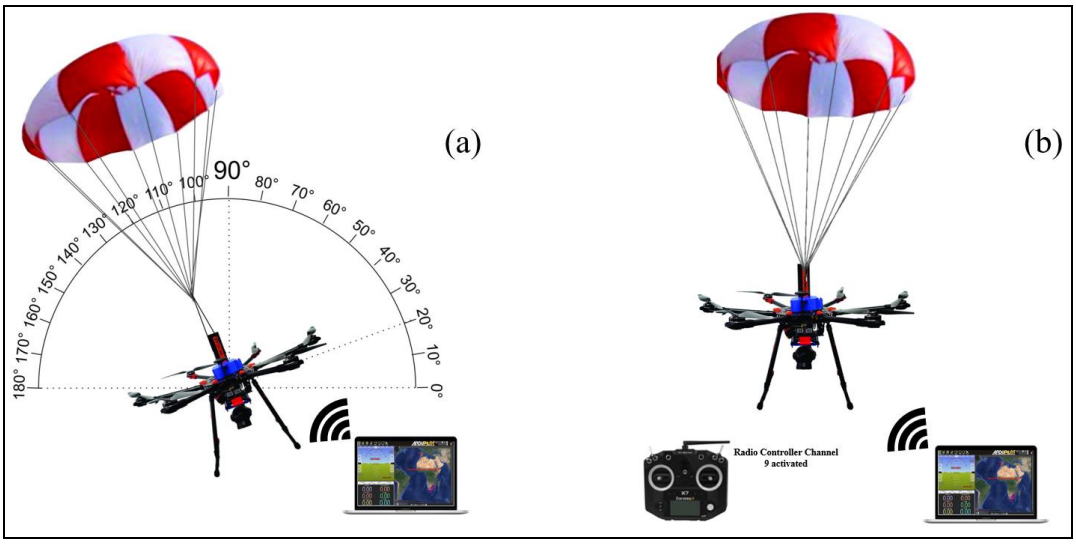

Figure 31. Recovery System Assessment: (a) Automatic Recovery System deployment; (b) Manual Recovery System deployment

To illustrate the safety potential of the Recovery System, the iSafeUAS falling accident (Figure 32) was analyzed under two conditions: (1) with Recovery System and (2) without Recovery System. An impact energy analysis and a probability of fatality assessment were used for analyzing the accident that could have resulted from any potential UAS collision with people and construction workers. Shelley (2016) has defined the impact energy as the energy of a falling UAS which could result in an injury or possible death to a person.

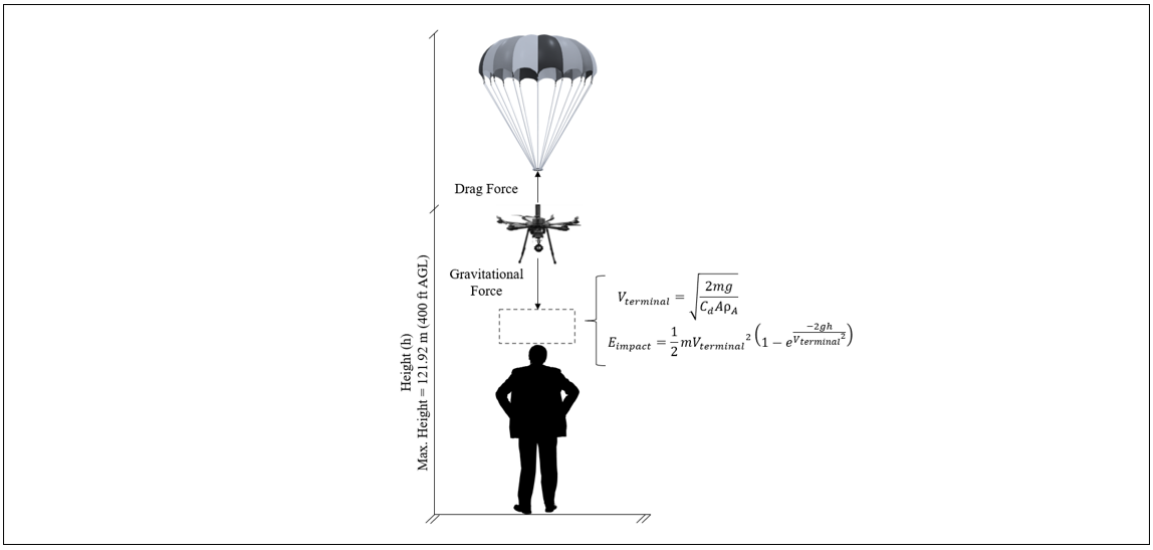

Figure 32. iSafeUAS falling accident

The following formulas were used to determine the impact energy of an object with free fall speed subject to a gravitational downward force while taking into consideration the upward drag force caused by air resistance (Low 2017; Shelley 2016). $V_{terminal}$ corresponds to the velocity at which the gravitational downward force and the upward drag force are both identical and the object stops accelerating, reaching terminal velocity. Table 27 summarizes the parameters used in this analysis for both conditions.

$$V_{terminal} = \sqrt{\frac{2mg}{C_D A \rho_A}} \quad (1)$$

$$E_{impact} = \frac{1}{2} m {V_{terminal}}^2 \left(1 - e^{\frac{-2gh}{{V_{terminal}}^2}}\right) \quad (2)$$

Table 27. Parameters used for the impact energy analysis

Variable	Symbol	Unit	Values	
			With the Recovery System	Without the Recovery System
Weight	m	Kg	7.8786	7.5586
Gravitational Acceleration	g	m/s^2	9.81	9.81
Drag Coefficient*	C_D	-	2.2**	0.3***
Platform Area****	A	m^2	1.814	0.2123
Air Density	ρ_A	Kg/m^3	1.225	1.225

* $\boldsymbol{C_D}$ *is determined experimentally depending on the object's surface roughness and shape (Shelley 2016).*
***Provided by the Recovery System manufacturer (Fruity Chutes 2020).*
****Provided in 2015 UAS Registration Task Force Committee final report (UAS Task Force 2015)*
*****Area of the platform* $\boldsymbol{A = [Core\ Area] + 0.2 \times ([Outer\ Area] - [Core\ Area])}$ *defined by Shelley (2016) where Core Area is the area of the central frame plate which includes all UAS hardware components; Outer Area is the total area of the UAS which is calculated using the motor to motor diameter of the UAS (0.96 m).*

Swisdak et al. (2007) graph was used to estimate the probability of fatality caused by UAS fall on people. This graph represents a cumulative lognormal distribution curve that relates the impact kinetic energy of an object to the fatality probability upon the object's potential impact with a person. The results of impact energy in Joules (J) and probability of fatality analyses for both conditions of: (1) with the Recovery System and (2) without the Recovery System are summarized in Figure 33. It should be noted that the falling height values (X-axis) ranged from 0 to 121.92 m, corresponding to the maximum allowable altitude of 400 ft that the iSafeUAS can attain based on the FAA regulations (US Department of Transportation 2016).

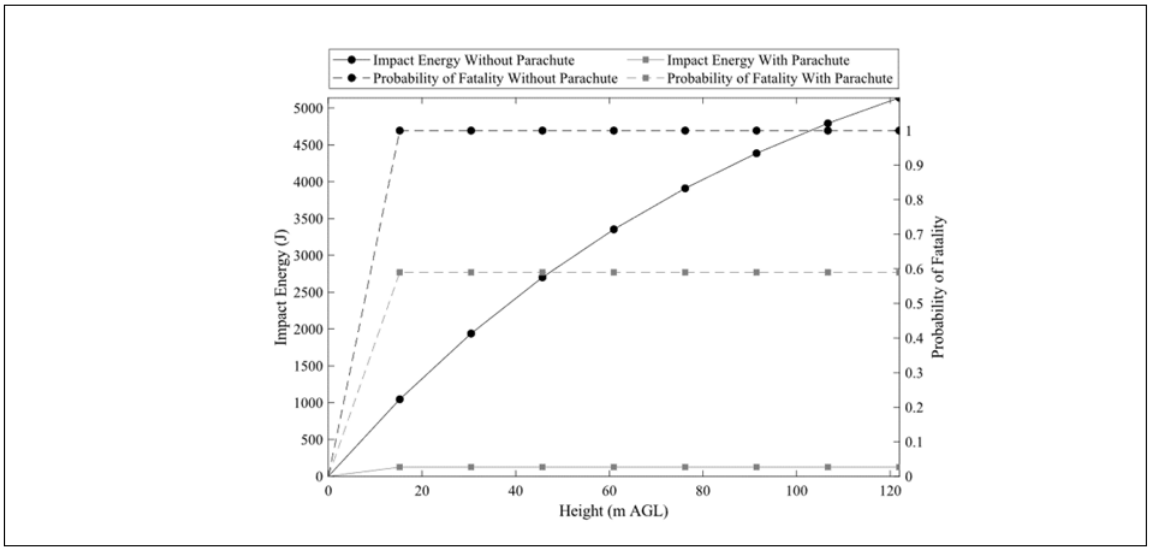

Figure 33. Impact energy (in Joules) and probability of fatality for iSafeUAS fall from different heights above the ground level (AGL) (in Meter) for both with and without the Recovery System conditions

A significant difference was noted in the impact energy values at different operational iSafeUAS heights between the two conditions of with and without the Recovery System. This difference is attributed to the use of the Recovery System, which tends to reduce and stabilize the velocity regardless of the operational iSafeUAS height. For example, an impact energy decrease of 88.1% at a 15.24 m fall or 97.6% at a 121.92 m fall occurs when using the Recovery System. In the same height range, the probability of fatality caused by iSafeUAS dropped from 100% to 59% when using the Recovery System. Since the probability of fatality was computed by considering that a worker without protection is directly impacted by the falling UAS on the head, it should be noted that this factor is expected to decrease even more when considering the sheltering parameter (Dalamagkidis et al. 2008). The sheltering parameter takes into consideration the ability of the people who are exposed to the UAS fall to take shelter in case of a possible impact. Moreover, using hardhats on the construction jobsites would reduce around 70% to 95% of the linear acceleration caused by a falling object (Suderman et al. 2014), which could ultimately reduce the fatality risk of a falling UAS on construction workers with hardhats. Additional studies are needed to quantitatively assess the energy impact of the iSafeUAS under such contexts.

5.7 iSafeUAS Application for Safety Monitoring of a Real Jobsite

The goal of this field assessment was to evaluate the potential of using the iSafeUAS for safety monitoring and inspection applications on a real construction jobsite. The main objective of this phase of the study was to assess, on a real-world construction jobsite, the iSafeUAS's super optical zoom capabilities for safety monitoring tasks, while minimizing the potential safety risk associated with the onsite iSafeUAS deployment by flying it outside of the active site boundary and at a significant distance from the building. The assessment was performed on a $65 million four-story (13,935 m^2) hospital building project located in Safety Harbor, Florida (Figure 34). The jobsite was not located in any FAA-restricted zone or controlled airspace, and was specifically selected due to its significant amount of activities occurring at elevations (e.g., formwork placement, concrete placement, steel erection) as well as on the site (e.g., crane operations, material storage). Data collection was conducted on April 12, 2020, around noon, under a clear and sunny sky and an outside temperature of 28°C (82.4°F).

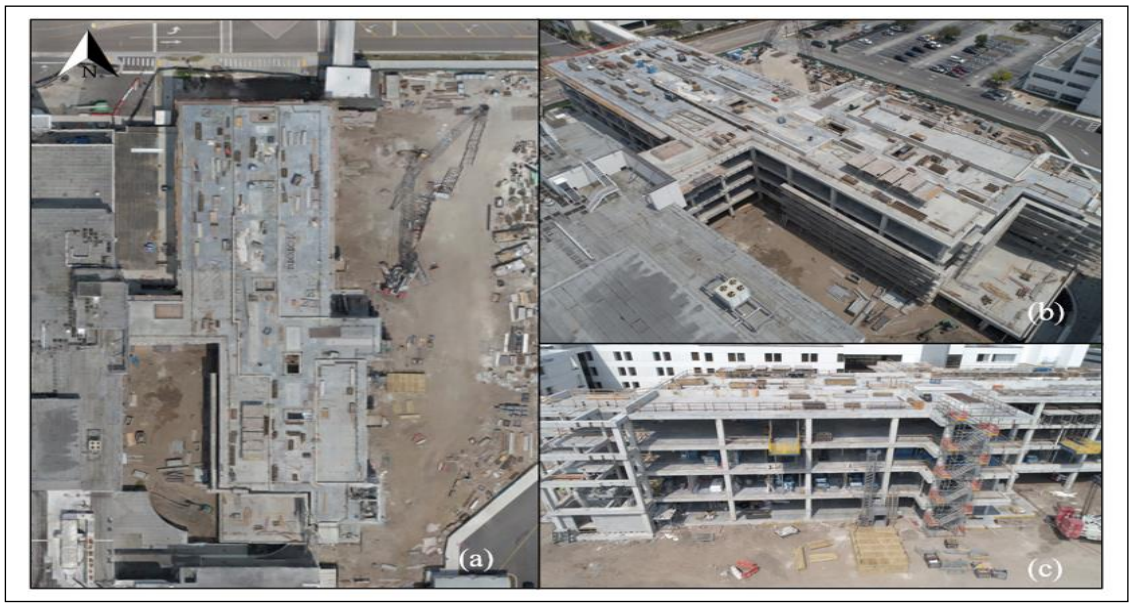

Figure 34. Data collection location: (a) Orthophoto of the area; (b) South-west side of the building; (c) East side of the building

Three optical zoom levels (0X, 10X, and 20X) were used to evaluate the optical zooming's ability in identifying hazardous situations on a construction site. From the location where the iSafeUAS was operating, the 30X zooming was even capable of detecting small elements (e.g., guardrail screws, scaffold joints) which were of minor importance in the context of this study, justifying the exclusion of this zooming level from further analysis. The east side of the building (Figure 34c) was selected for UAS visuals acquisition and data collection. A total of 65 images were acquired from the three flight missions that were conducted using the Ardupilot® Mission Planner v1.3.70. Table 28 summarizes the flight parameters and the zoom levels adopted in each of the three flights. To ensure consistency among the three flights and to minimize the potential safety risk of the iSafeUAS deployment, all visual assets were captured from a safe location outside of the jobsite with a 40 m distance from the building exterior. Then the collected visual data was shared with two safety managers, with more than 18 years of construction experience to review and identify any potential safety hazards at each zoom level. Figures 35 to 37 show a sample of the acquired visual data at each of the three optical zoom levels. The potential safety hazards identified pertaining to the 0X, 10X, and 20X levels were:

Table 28. iSafeUAS flight parameters at three optical zoom levels

iSafeUAS Flight Parameters	Zoom Levels	Frontal Images (#)
Flight Planning Software: ArduPilot® Mission Planner (Manual) Camera Settings: Shutter (1/1160 second exposure time) Image Resolution: 4608 x 2184 px; ISO-50 Flight Speed: 3 m/s Height: 23 m AGL Horizontal Distance: 40 m	None	15
	10X	20
	20X	30

0X Zoom Level of iSafeUAS: Analyzing the 0X optical zoom visual dataset showed that it mainly provided an overall, yet important, view of the outdoor jobsite safety conditions which is particularly useful in documenting the general conditions of the project site area, roof, and building exteriors. More specifically, safety managers reported several potential hazards including (See Figure 35): (1) fall hazards due to the lack of guardrails or safety nets in some of the unprotected edges and openings of the building exterior and roof; (2) tripping hazards due to the improper housekeeping on the project site; as well as

(3) caught-in/between and struck-by hazards due to the improper demarcation within the crane swing area and material handling area on the project site. However, the 0X dataset was not detailed and precise enough to properly visualize and accurately identify some of the potential hazards on the jobsite. As an example, the 0X optical zoom visual dataset could help in identifying some of the missing guardrails in a specific location (Figure 35); however, it could not provide detailed and precise visual information to check whether the guardrails are correctly installed, maintained, and used on the jobsite. To achieve that level of detail, closer views of the project needed to be captured using the other zooming levels of the RGB Camera Sensor (e.g., 10X, 20X).

10X Zoom Level of iSafeUAS: Safety managers also evaluated the 10X optical zoom visual dataset. All the potential safety hazards identified and discussed in the 0X optical zoom visual dataset were identified and visualized in more detail when the 10X optical zoom dataset was examined. In addition to those potential hazards, safety managers were able to report other possible hazards with the 10X closer zoom capability, such as (See Figure 36): (1) fall hazards due to the lack of guardrails or safety nets in some of the unprotected edges and openings of the building exterior and roof; (2) tripping hazards due to the improper waste storage on the project site; (3) caught-in/between and struck-by hazards due to the improper demarcation and more specifically, insufficient amount of warning signs around the crane; and (4) struck-by hazards due to the improper storage of material near the edges. The 10X zooming allowed for additional safety hazards to be identified with more details on each specific one, offering safety managers the ability to better understand and analyze the potential unsafe situations. Although the acquired visuals using the 10X optical zoom dataset effectively visualized the project site area, roof, and building exteriors, it did not accurately visualize and provide enough information on the unsafe conditions located inside the building that could be inspected from the outside. For this specific purpose, and to get more detailed visual data of the project site, closer views of the project were captured using the 20X RGB Camera Sensor zooming level.

20X Zoom Level of iSafeUAS: The 20X optical zoom dataset not only retrieved the potential hazards by the 10X zoom capability with better detail and accuracy but also facilitated the identification of specific hazards at outdoor and indoor locations. Some specific examples are as following (See Figure 37): (1) electrical hazards due to the improper warning signs around the electrical panel; (2) fall hazards due to the inappropriate guardrails of some indoor openings; (3) struck-by hazards due to the improper storage of material located in somewhat indoor areas of the building and improper demarcation of the material storage area; (4) tripping hazards due to the improper housekeeping of some indoor areas; (5) tripping hazards due to the uneven surfaces on the project site; and (6) caught-in/between hazards due to the insufficient warning signs and improper demarcation around the excavator. It should be noted that due to low light conditions and shadowing effects, the 20X optical zoom visual dataset could only illustrate the indoor areas that were located close to the building exterior. These very detailed visual data could also be used to monitor other smaller-in-size safety-related objects on the jobsite, such as improper fall protection systems (e.g., lifelines, full-body harnesses) or improper personal protective equipment (e.g., hardhats, safety glasses, gloves, safety-toed boots, earplugs/earmuffs, safety vests). Integrating such detailed visual datasets with indoor information acquired by other techniques (e.g., indoor robots or UAVs that are capable of operating in GPS-denied environments) could offer a comprehensive and automated construction safety monitoring and inspection medium for safety managers.

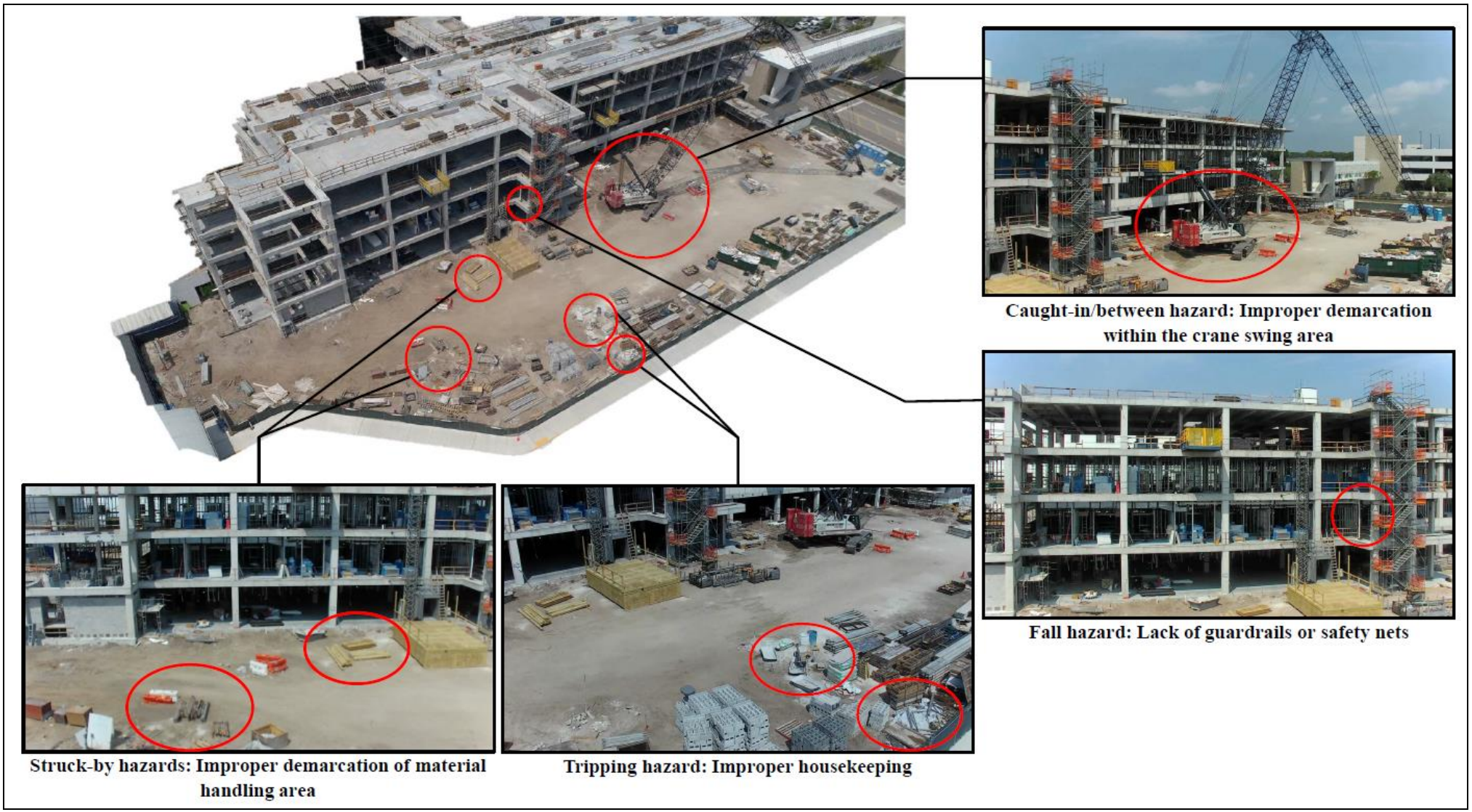

Figure 35. Potential safety hazards identified in visual data captured with 0X (no zooming) capability

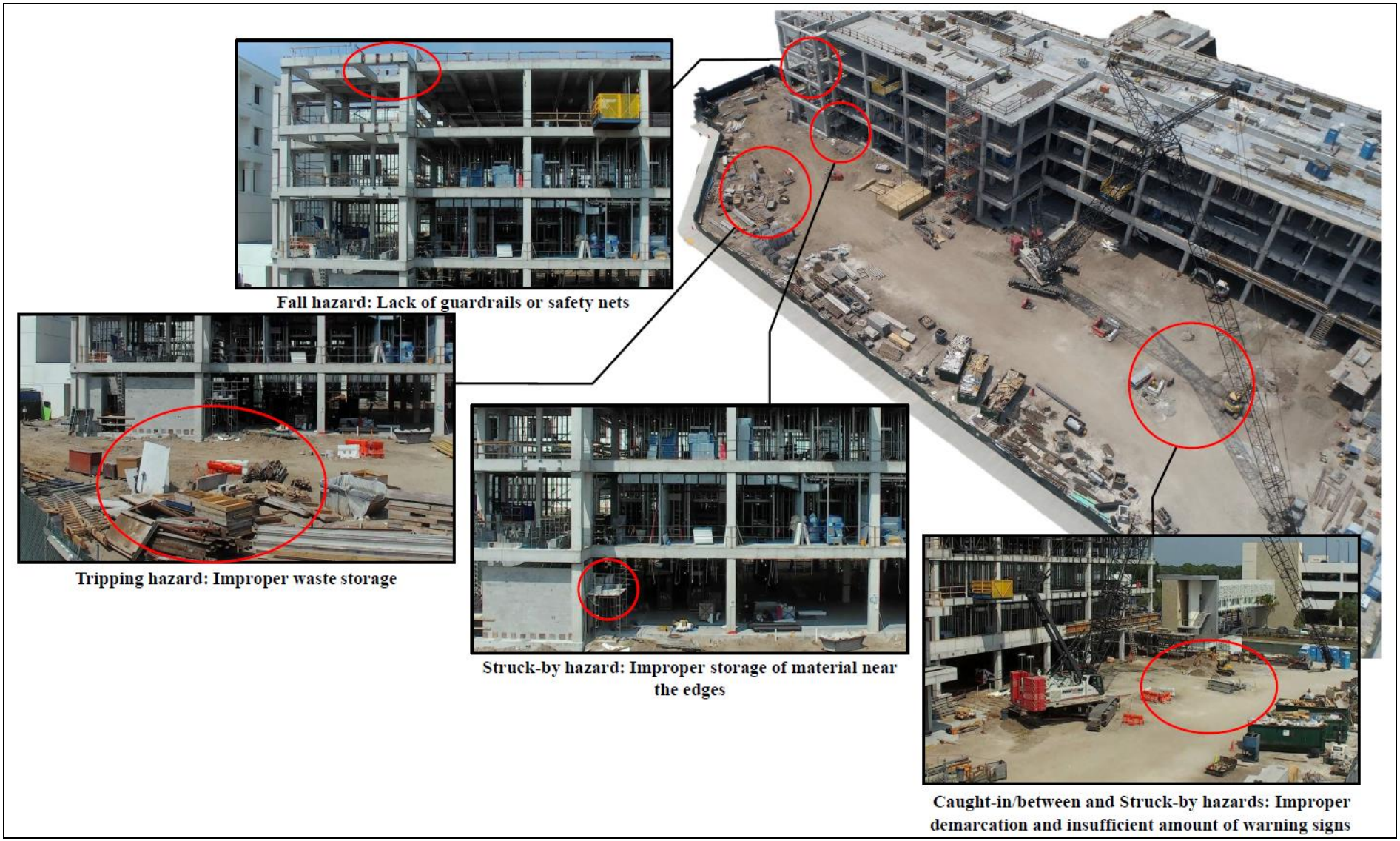

Figure 36. Potential safety hazards identified in the visual data captured with 10X zooming capability

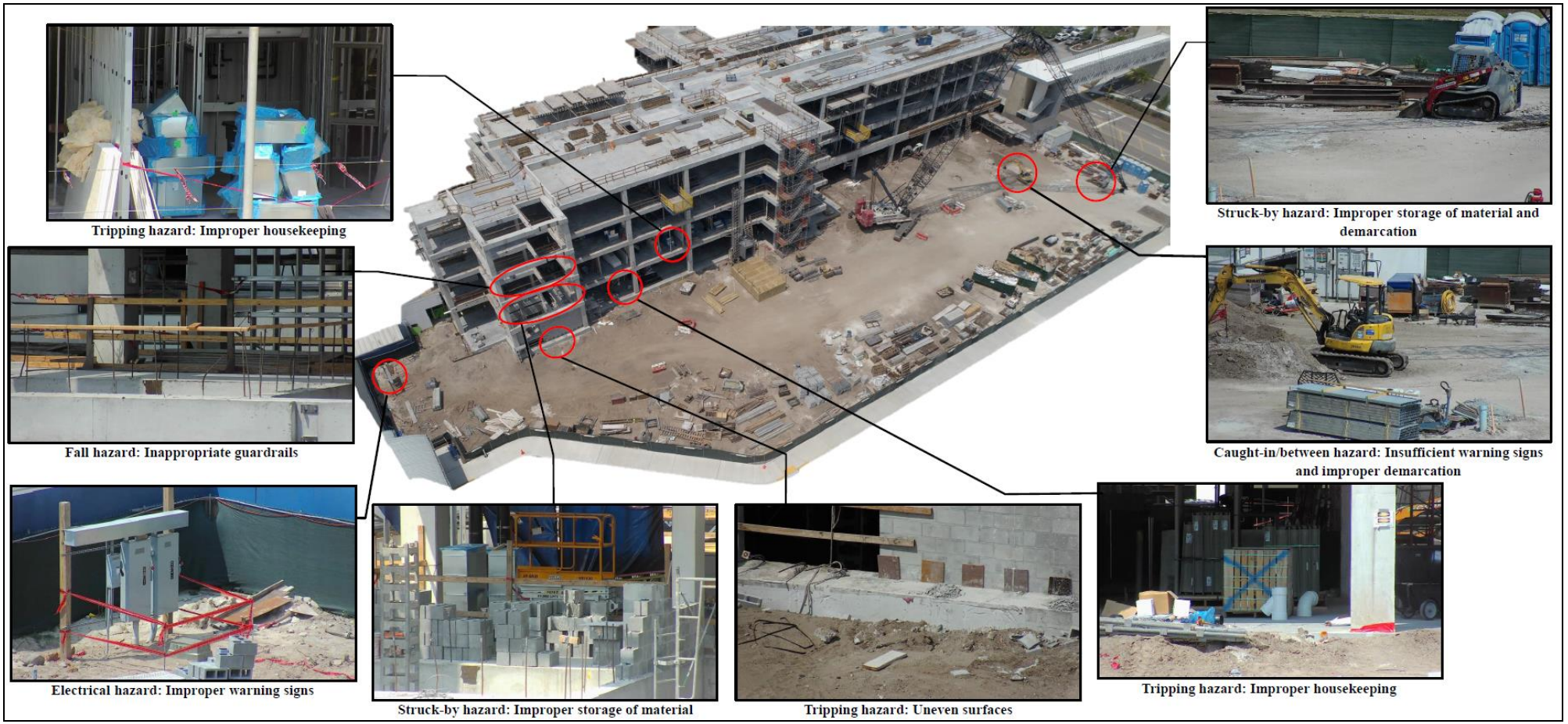

Figure 37. Potential safety hazards identified in the visual data captured with 20X zooming capability

5.8 Summary and Conclusion

In this study, iSafeUAS was introduced as an effective UAS platform that is designed and developed to capture detailed visual data for safety monitoring purposes using an RGB Camera Sensor with super optical zoom capabilities and a Recovery System to reduce the risks associated with its deployment over the jobsites. First, iSafeUAS was designed, developed, and programmed using commercially available open-source software and hardware. This development part included a detailed description of the technical assembly of the iSafeUAS platform's body, navigation and communication system, programming, data collection, and Recovery System. These details would provide construction researchers and professionals with an overall understanding of the required steps and procedures for the design, development and programming of customized UASs for construction safety monitoring and inspection applications. To assess the technical performance of the developed iSafeUAS, three onsite flight tests were then performed: free flight assessment, autotune calibration, and camera assessment. These tests were performed to ensure that the iSafeUAS is capable of accomplishing stable flights, with proper operation of flight modes, and at an appropriate amount of battery while automatically capturing visual data. This section provided a good understanding of general technical assessment procedures of a customized UAS platform before its deployment on an actual construction jobsite. Two indoor flight simulation assessments were also conducted to test the iSafeUAS Recovery System under automatic and manual deployment conditions. These assessments were followed by a detailed analysis of how using the Recovery System could affect the impact energy and probability of fatality in case of any potential iSafeUAS fall over people and construction workers. The indoor flight simulations illustrated the capability of iSafeUAS in triggering its Recovery System under both automatic and manual deployment procedures. Besides, the results of the impact energy and probability of fatality analyses showed that the integrated Recovery System in iSafeUAS could significantly reduce its energy and fatality in the case of any potential iSafeUAS fall over people. In the near future, flight Recovery Systems (e.g., parachutes,

airbags) might be an integral component of some UAS platforms in the construction domain to considerably minimize the potential safety risks of their flights over people or equipment on the jobsites. This part of the study reports initial efforts of integrating such Recovery Systems for an application in the construction domain and provides construction professionals and researchers with a good understanding of the technical integration and safety assessment of such systems. Finally, the iSafeUAS was used for the safety inspection of a real-world construction project under three zoom levels (i.e., 0X, 10X, and 20X). The outcomes of the case study showed that the enhanced iSafeUAS zoom level capabilities enabled capturing very detailed visual data without flying over the jobsite or close to the building and exposing anyone to UAS-associated fall hazards on the jobsite. Moreover, such detailed visual data helped the safety managers identify several types of hazards at outdoor and indoor building locations that could have been otherwise difficult or impossible to detect using visual datasets with lower zoom levels. iSafeUAS could reduce the risks associated with the onsite use of UASs and offer an efficient safety inspection of the construction jobsites. More specifically, by having the iSafeUAS fly at farther distances from the jobsite and workers, several common safety risks associated with UAS operation on the jobsites such as worker distraction, signal interferences, and UAS collision with jobsite obstacles could be avoided or minimized. Moreover, the Recovery System of iSafeUAS can considerably minimize the impact of struck-by accidents in case of any possible UAS fall on the jobsite.

Further research and development should be conducted to optimize the energy consumption of the iSafeUAS's components with the aim of enhancing the system's flight duration. Driven by its open-source design, it was noticed that operating the iSafeUAS requires more advanced piloting skills to effectively perform the intended flight missions. Further development and optimization should also be conducted to make the iSafeUAS more user-friendly while providing an easy-to-fly user experience. Construction practitioners and researchers might benefit from the outcomes of this study to better understand the adopted UAS system and its technical features that would lead to their safe

deployment as safety inspection tools on the construction jobsites. However, this research has some limitations. First, the iSafeUAS was deployed only on a multi-story building construction project, and its successful integration cannot be generalized to other types of construction projects, justifying the need to conduct further studies to achieve such generalization. Besides, iSafeUAS Recovery System was tested using indoor simulated flight assessments. Further controlled experimental assessments should be conducted on real sites to properly assess the Recovery System's potential in real-world conditions.

5.9 Acknowledgements

The authors would like to acknowledge Micro Aerial Projects L.L.C and Triad Drone L.L.C for their support with the iSafeUAS design, development, and assessment. This research did not receive any specific grant from funding agencies in the public, commercial, or not-for-profit sectors.

5.10 References

Adams, S. M., Levitan, M. L., and Friedland, C. J. (2014). "High Resolution Imagery Collection for Post-Disaster Studies Utilizing Unmanned Aircraft Systems (UAS)." *Photogrammetric Engineering & Remote Sensing*, 80(12), 1161–1168.

Albeaino, G., Gheisari, M., and Franz, B. W. (2019). "A systematic review of unmanned aerial vehicle application areas and technologies in the AEC domain." *Journal of Information Technology in Construction (ITcon)*, 24, 381–405.

Alizadehsalehi, S., Yitmen, I., Celik, T., and Arditi, D. (2018). "The effectiveness of an integrated BIM/UAV model in managing safety on construction sites." *International Journal of Occupational Safety and Ergonomics*, Taylor & Francis, 0(0), 1–16.

Álvares, J., Costa, D., and Melo, R. (2018). "Exploratory study of using unmanned aerial system imagery for construction site 3D mapping." *Construction Innovation*, 18(3), 301–320.

ArduPilot. (2019). *The Cube User Manual V1 .0*.

Chao, H., Cao, Y., and Chen, Y. (2010). "Autopilots for small unmanned aerial vehicles: A survey." *International Journal of Control, Automation and Systems*, 8(1), 36–44.

Conte, G., and Doherty, P. (2011). "A Visual Navigation System for UAS Based on Geo-referenced Imagery." *International Archives of the Photogrammetry, Remote Sensing and Spatial Information Sciences*, XXXVIII(4), 101–106.

Dalamagkidis, K., Valavanis, K. P., and Piegl, L. A. (2008). "Evaluating the risk of unmanned aircraft ground impacts." *2008 Mediterranean Conference on Control and Automation - Conference Proceedings, MED'08*, 709–716.

Fruity Chutes. (2020). "Parachute Descent Rate Calculator" <https://fruitychutes.com/help_for_parachutes/parachute-descent-rate-calculator?term=IFC-48-S&weight=11> (Jun. 5, 2020).

Ghaffarian, S., and Kerle, N. (2019). "Towards post-disaster debris identification for precise damage and recovery assessments from uav and satellite images." *International Archives of the Photogrammetry, Remote Sensing and Spatial Information Sciences - ISPRS Archives*, 42(2/W13), 297–302.

Gheisari, M., and Esmaeili, B. (2019). "Applications and requirements of unmanned aerial systems (UASs) for construction safety." *Safety Science*, 118, 230–240.

Gheisari, M., Irizarry, J., and Walker, B. N. (2014). "UAS4SAFETY: The Potential of Unmanned Aerial Systems for Construction Safety Applications." *Construction Research Congress 2014*, (2008), 1801–1810.

Gheisari, M., Rashidi, A., and Esmaeili, B. (2018). "Using Unmanned Aerial Systems for Automated Fall Hazard Monitoring." *Construction Research Congress 2018*, American Society of Civil Engineers, New Orleans, Louisiana, 62–72.

Ham, Y., Han, K. K., Lin, J. J., and Golparvar-Fard, M. (2016). "Visual monitoring of civil infrastructure systems via camera-equipped Unmanned Aerial Vehicles (UAVs): a review of related works." *Visualization in Engineering*, 4(1), 1.

Hassanalian, M., and Abdelkefi, A. (2017). "Classifications, applications, and design challenges of drones: A review." *Progress in Aerospace Sciences*, 91, 99–131.

Homola, J., Prevot, T., Mercer, J., Bienert, N., and Gabriel, C. (2016). "UAS traffic management (UTM) simulation capabilities and laboratory environment." *AIAA/IEEE Digital Avionics Systems Conference - Proceedings*, IEEE, 2016-Decem, 1–7.

Imdoukh, A., Shaker, A., Al-Toukhy, A., Kablaoui, D., and El-Abd, M. (2017). "Semi-autonomous indoor firefighting UAV." *2017 18th International Conference on Advanced Robotics, ICAR 2017*, (July), 310–315.

Iqbal, U., Irtiza, S., Shah, A., Jamil, M., Gillani, S. O., and Ayaz, Y. (2015). "Selection of Unmanned Aerial System (Uas) for Disaster Relief Operations : a Comparison." *Sci.Int.(Lahore)*, 27(4), 3199–3203.

Irizarry, J., and Costa, D. B. (2016). "Exploratory Study of Potential Applications of Unmanned Aerial Systems for Construction Management Tasks." *Journal of Management in*, 32(February), 1–8.

Irizarry, J., Gheisari, M., and Walker, B. N. (2012). "Usability assessment of drone technology as safety inspection tools." *Journal of Information Technology in Construction (ITcon)*, 17, 194–212.

Kim, S., Irizarry, J., and Costa, D. B. (2016). "Potential Factors Influencing the Performance of Unmanned Aerial System (UAS) Integrated Safety Control for Construction Worksites." *Construction Research Congress 2016*, American Society of Civil Engineers, San Juan, Puerto Rico, 2614–2623.

Kim, S., Irizarry, J., and Costa, D. B. (2020). "Field Test-Based UAS Operational Procedures and Considerations for Construction Safety Management: A Qualitative Exploratory Study." *International Journal of Civil Engineering*, Springer International Publishing, 9.

Kitchen, S., Breshears, K., Kitchen, S., and Mckinley, J. (2018). *Aerospace Systems Design I*. Missouri University of Science & Technolog.

Low, K. H. (2017). "An initial parametric study of weight and energy thresholds for falling unmanned aerial vehicles (UAVs)." *2017 Workshop on Research, Education and Development of Unmanned Aerial Systems, RED-UAS 2017*, 240–245.

Dinesh, M. A., Santhosh Kumar, S., Sanath, J., Akarsh, K. N., & Manoj Gowda, K. M. (2018). "Development of an Autonomous Drone for Surveillance Application." *Development of an Autonomous Drone for Surveillance Application*, 5(8), 331–333.

Martinez, J. G., Gheisari, M., and Alarcón, L. F. (2020). "UAV Integration in Current Construction Safety Planning and Monitoring Processes: Case Study of a High-Rise Building Construction Project in Chile." *Journal of Management in Engineering*, 36(3).

Melo, R., and Costa, D. (2020). “Reducing the gap between work as done and work as imagined on construction safety supported by UAS.” *8 th REA Symposium Embracing Resilience: Scaling up and Speeding up Kalmar, Sweden, June 24-27, 2019*.

de Melo, R. R. S., and Costa, D. B. (2019). “Integrating resilience engineering and UAS technology into construction safety planning and control.” *Engineering, Construction and Architectural Management*, Emerald Group Publishing Ltd., 26(11), 2705–2722.

de Melo, R. R. S., Costa, D. B., Álvares, J. S., and Irizarry, J. (2017). “Applicability of unmanned aerial system (UAS) for safety inspection on construction sites.” *Safety Science*, 98, 174–185.

de Melo, R. R. S., De Brito, B. L., Bastos, D., and Ferreira, E. A. (2018). “Analysis of the potential use of point cloud collected from UAS for BIM modeling and safety systems analysis.” *In 6th international workshop-When Social Sciences meets Lean and BIM*, 5–7.

Mendes, C., Costa, D., and Melo, R. (2018). “Evaluating Uas-Image Pattern Recognition System Application For Safety Guardrails Inspection.” (August), 1–3.

Park, J., Kim, K., and Cho, Y. K. (2017). “Framework of Automated Construction-Safety Monitoring Using Cloud-Enabled BIM and BLE Mobile Tracking Sensors.” *Journal of Construction Engineering and Management*, 143(2), 1–12.

Perlman, A., Sacks, R., and Barak, R. (2014). “Hazard recognition and risk perception in construction.” *Safety Science*, Elsevier Ltd, 64, 13–21.

Pinto, A., Nunes, I. L., and Ribeiro, R. A. (2011). “Occupational risk assessment in construction industry - Overview and reflection.” *Safety Science*, Elsevier Ltd, 49(5), 616–624.

Pratama, L. A., Fardhosseini, M. S., and Lin, K. Y. (2018). “An Overview of Generating VR Models for Disaster Zone Reconstruction Using Drone Footage.” *The University of Auckland, New Zealand*, (November), 336–344.

Rakha, T., and Gorodetsky, A. (2018). “Review of Unmanned Aerial System (UAS) applications in the built environment: Towards automated building inspection procedures using drones.” *Automation in Construction*, Elsevier, 93, 252–264.

Roberts, D., Bretl, T., and Golparvar-Fard, M. (2017). “Detecting and Classifying Cranes Using Camera-Equipped UAVs for Monitoring Crane-Related Safety Hazards.” *Computing in Civil Engineering 2017*, American Society of Civil Engineers, 442–449.

Samad, Abd. M., Kamarulzaman, N., Hamdani, M. A., Mastor, T. A., and Hashim, K. A. (2013). “The potential of Unmanned Aerial Vehicle (UAV) for civilian and mapping application.”

Proceedings - 2013 IEEE 3rd International Conference on System Engineering and Technology, ICSET 2013, IEEE, 313–318.

Shelley, A. V. (2016). "A model of human harm from a falling unmanned aircraft: Implications for UAS regulation." *International Journal of Aviation, Aeronautics, and Aerospace*, 3(3).

Suderman, B. L., Hoover, R. W., Ching, R. P., and Scher, I. S. (2014). "The effect of hardhats on head and neck response to vertical impacts from large construction objects." *Accident Analysis and Prevention*, 73, 116–124.

Swisdak Jr., M. M., Tatom, J. W., and Hoing, C. A. (2007). *Procedures for the Collection, Analysis, and Interpretation of Explosion Produced Debris – Revision 1*. *8th Australian Explosive Ordnance Symposium*, 1–14.

Tuttas, S., Braun, A., Borrmann, A., and Stilla, U. (2017). "Acquisition and Consecutive Registration of Photogrammetric Point Clouds for Construction Progress Monitoring Using a 4D BIM." *Photogrammetrie, Fernerkundung, Geoinformation*, Springer International Publishing, 85(1), 3–15.

UAS Task Force. (2015). *Unmanned Aircraft Systems (UAS) Registration Task Force (RTF) Aviation Rulemaking Committee (ARC): Task Force Recommendations Final Report*.

US Bureau of Labor Statistics. (2017). "Commonly Used Statistics | Occupational Safety and Health Administration." <https://www.osha.gov/oshstats/commonstats.html> (Sep. 20, 2018).

US Bureau of Labor Statistics. (2018). *National Census of Fatal Occupational Injuries in 2017*. 1–14.

US Department of Transportation. (2016). *Advisory Circular 107-2 - Small Unmanned Aircraft Systems (sUAS)*.

Wierzbicki, D., Kedzierski, M., and Fryskowska, A. (2015). "Assesment of the influence of UAV image quality on the orthophoto production." *International Archives of the Photogrammetry, Remote Sensing and Spatial Information Sciences - ISPRS Archives*, 1–8.

Woodcock, K. (2014). "Model of safety inspection." *Safety Science*, Elsevier, 62, 145–156.

CHAPTER 6: CONCLUSIONS, CONTRIBUTIONS, LIMITATIONS AND FUTURE RESEARCH

6. 1 Conclusions

This dissertation was developed with the aim of enhancing the current process of hazard identification and safety monitoring on construction sites through the implementation of UASs and positioning technologies. The main objective of the dissertation was addressed through four independent researches: (1) UAV Integration in Current Construction Safety Planning and Monitoring Processes: Case Study of a High-Rise Building Construction Project in Chile; (2) Development and Assessment of an Ultrasound-Base Positioning System for Measuring Hazard Exposure Time at Construction Jobsites; (3) UAS Point Cloud Accuracy Assessment Using SfM-Based Photogrammetry and PPK Georeferencing Technique for Building Surveying Applications, and (4) the Development and Assessment of an Unmanned Aerial System for Construction Safety Inspection.

Based on the finding of these researches and development efforts, it can be concluded that the use of UASs and positioning technologies demonstrated to be useful in obtaining a complete visualization of jobsites, that ultimately leads safety managers to better identify hazardous conditions on both indoor and outdoor environment. For instance, UAS-generated visual content aided safety managers to identify several types of hazards at outdoor building locations that could have been otherwise difficult or impossible to detect using another type of visual asset. Safety aspects such as missing guardrails or safety nets around unprotected edges or openings, loose or unsecured material at height, and lack of proper PPE or safety harnesses were better identified using UAS-generated visual content. The identification of such severe hazardous conditions led to a higher rating of severity assessment, probability of occurrence, and risk level by the safety managers, allowing to enhance their risk perception capabilities.

In addition, the systematic use of UASs on jobsites reduced the manual effort required to collect information, improved the quality and accuracy of its visual representation, and mitigated the risk associated with data collection. In fact, the use of the MAPM4 equipped with a dual-frequency GNSS (L1/L2) and subject to PPK-mediated coordinate correction significantly increased the accuracy of the UAS-generated point clouds when compared to commercially available platforms that are equipped with a single-frequency GNSS (L1). This factor led to enhance the visual quality and accuracy of the UAS-derived 3D jobsite representation and therefore increases its usefulness for safety monitoring and hazard identification. At the same time, the manual effort required to collect visual data of the jobsite was considerably lower when comparing with the traditional method. It can be demonstrated based on the time consumed (see Table 14) and the number of people employed during the data collection process.

On the other hand, the use of the iSafeUAS with a super optical zoom RGB camera and a parachute recovery system was useful as a safety inspection and monitoring tool by minimizing the safety risks associated with UAS full deployment on construction jobsites and reducing the manual effort required to collect information. The iSafeUAS offered UAS flight team members the operational flexibility in choosing a particular location on the jobsite to fly the UAS while limited the operational risks to that specific location, enabling enhanced control and risk reduction over the operation location. For instance, flying the customized UAS in a particular area on the jobsite, several common safety risks associated with UAS operation on the jobsites such as worker distraction, signal interferences, and UAS collision with jobsite obstacles could be avoided or minimized. Besides, the RGB camera sensor mounted on the customized UAS allowed safety managers to identify several types of hazards at outdoor and indoor building locations difficult to detect by the traditional safety inspection and monitoring approach.

Finally, by the implementation of positioning technologies, it was possible to achieve systematic and continuous safety monitoring and hazard identification on the

jobsite. This can be concluded thanks to the result obtained during the deployment of the ultrasound-based positioning system on a real construction jobsite. The result obtained showed that the ultrasound-based positioning system was capable of determining the position of workers during the entire workday. This indicates that the developed system had a reliability of 100% demonstrating that the deployment of this type of technology on actives jobsites allows determining worker positioning in an accurate and reliable manner compared with other commercially available technologies. This special attribute would be especially useful on construction sites location with an insufficient number of safety managers and where UAS cannot properly operate.

6.2 Contributions

This research contributes to the body of knowledge by providing construction practitioners and researchers with a comprehensive overview and understanding of technical development, assessment, and onsite implementation of customized UASs and positioning sensors intended to enhance safety monitoring and hazard identification process on construction jobsites. Besides, the four independent research developed in this dissertation resulted in the theoretical and practical contribution to the body of knowledge. These contributions are presented in Table 29 and described in detail in Section 6.2.1 and 6.2.2.

Table 29. Dissertation Contributions

Chapter	Theorical contributions	Practical contributions
(1) UAV Integration in Current Construction Safety Planning and Monitoring Processes: Case Study of a High-Rise Building Construction Project in Chile	Provide a comprehensive analysis of the current construction safety planning and monitoring process and UAS-related implementation barriers	Propose in details new steps required to integrate UAS within the current safety planning and monitoring process in construction projects.
(2) Development and Assessment of an Ultrasound-Based Positioning System for Measuring Hazard Exposure Time at Construction Jobsites	Provide a method for the successful deployment of an ultrasound-based positioning system on building interiors	Propose a guideline intended for the technical development and assessment of an ultrasound-based positioning system
(3) UAS Point Cloud Accuracy Assessment Using SfM-Based Photogrammetry and PPK Georeferencing Technique for Building Surveying Applications	Contribute with a complete analysis of the ideals UAS flight parameters to enhance UAS-derived 3D visual jobsite representation.	Propose a guideline to aid researches and professionals in determining what UAS technical configurations would be ideal to improve the accuracy and visual quality of UAS-derived 3D

Chapter	Theorical contributions	Practical contributions
		models
(4) Development and Assessment of an Unmanned Aerial System for Construction Safety Inspection	Contribute with a detailed overview and understanding of how UAS-derived images captured from different zoom levels lead safety managers to identify several types of hazardous conditions	Provide a comprehensive overview and understanding of the design, development, assessment, and onsite implementation of a customized UAS intended for safety inspection applications

6.2.1 Contributions to theory

This dissertation contributes to the theory of safety monitoring and hazard identification by providing a comprehensive analysis of the factors that affect the proper implementation of UASs and positioning technologies in the construction industry. Besides, the dissertation analyzes different technologies used for construction safety-related tasks through an extensive literature review. The result of this analysis contributed to determinate the advantages and disadvantages of the application of such technologies for safety monitoring and hazard identification, offering a theoretical framework for future research on the AECO .

In addition to the theoretical contribution of the dissertation, each chapter presents specific contributions to the theory.

Chapter 2 provides a comprehensive analysis of the current construction safety planning and monitoring process and its implementation barriers. This analysis complements the studies carried out by authors such as Irizarry et al. (2012), Gheisari et al. (2014), Irizarry and Costa (2016), de Melo (2017) and de Melo and Costa (2019), who did not considering these barriers for the successful integration of UAS technologies in the construction project

Chapter 3 analyzed in detail the reasons that affect the ultrasound-based positioning systems deployment on actives jobsites. Factor such as signal interference, short communication range and low positioning accuracy were overcome during the implementation of the proposed solution, contributing to the theory of how positioning

technologies can be used as a reliable and accurate mean for indoor data collection. Besides, chapter 3 proposed a method to successfully deploy the ultrasound-based positioning system considering aspects such as distance and height of sensors installation for building interiors. Previous researches have implemented different types of positioning technologies including Ergen and Akinci (2007), Lu et al. (2011), Ergen and Akinci (2007), Costin et al. (2015) and Awolusi et al. (2018), however, none of these studies proposed a method to overcome the limitation that faces positioning technologies in real actives jobsites.

Chapter 4 studied the effects of various UAS flight parameters on the accuracy of the visual quality and accuracy of the UAS-derived 3D jobsite representation. This chapter presented a series of ideal flight parameters such as Ground sampling distance (GSD) and camera angle that led to enhance the accuracy and visual quality of the UAS-derived 3D models. Previous researches tested different UAS flight parameters to enhance the accuracy of the UAS-derived point clouds, however, none of these studies provided the optimal parameters to increase their visual quality. The findings of this chapter complement the studies conducted by author such as Bolkas (2019), Fazeli et al. (2016), Martínez-Carricondo et al. (2018) and Sanz-Ablanedo et al. (2018), who did not consider the ideal flight parameters to obtain a better 3D jobsite visual representation.

Finally, chapter 5 provided an overview and understanding of how UAS-derived images captured from different zoom levels led to identify several types of hazardous conditions that could be difficult to detect by the traditional-based safety inspection method. The chapter contributed to the theory by providing the type of hazardous conditions that safety managers can identify using each type of RGB camera zoom level and how UAS-derived images visual quality impact their hazard identification skills. The aforementioned analysis developed in this chapter complement UAS-related studies such as Irizarry et al. (2012), Gheisari et al. (2014), Irizarry and Costa (2016), de Melo (2017), Gheisari et al. (2018), de Melo and Costa (2019), Gheisari and Esmaeli (2019) and Melo

and Costa (2020) which don’t analyze in deep how the quality of the visual data can affect safety managers’ hazard identification process on construction jobsites.

6.2.2 Contributions to practice

This dissertation contributes to practice by providing a comprehensive understanding of technical development, assessment, and onsite implementation of customized UASs and positioning sensors on construction jobsite. The outcome of this dissertation could benefit the AECO industry and the academic field in understanding how the technical development, assessment, and onsite implementation of customized UASs and positioning technology would enhance the construction safety monitoring and hazard identification process.

Chapter 2 proposed the details of new steps required in construction projects to integrate UASs within the current safety planning and monitoring process. The main added steps were related to designing, conducting UAS flights and collecting and processing visual data. The aerial visual contents and 3D models generated in the UAS-based method provided a detailed and comprehensive view of the site and its associated safety challenges and consequently enhanced safety managers' risk perception skills. Besides, UAS-derived images would primarily integrated into the earliest stages of the safety planning and monitoring process to facilitate the hazard identification and assessment of the construction projects.

Chapter 3 proposed a guideline intended for the technical development and assessment of an ultrasound-based positioning system. The practical contribution of this chapter is to provide a step -by-step of how the developed system should be installed and tested before and during its deployment in real construction environments. In addition, the chapter provided a general description of the technical components required to obtain a

centimeter-level of accuracy, as well as, how the data collected can be systematized and transformed into the hazard exposure time indexes.

Chapter 4 presented a guideline to aid practitioners and researchers to determine the UAS technical configurations that would be ideal for improving the accuracy and visual quality of the UAS-derived 3D jobsite representation. UAS technical aspects such as the type of GNSS and coordinates correction techniques (PPK and RTK) are presented and compared in detail to understand how these aspects could contribute to the better visualization and accuracy of the UAS-derived 3D models intended for hazard identification.

Finally, chapter 5 showed the technical design, development, assessment, and onsite implementation of a customized UAS intended for safety inspection applications. The chapter contributes to the practice by providing construction researchers and professionals with an overall understanding of the required steps and procedures for the development and integration of customized UASs for construction safety monitoring and inspection applications.

6. 3 Limitations and future researches

This section summarizes the research limitations and future research lines that could address these limitations.

Since UAS and positioning technologies were implemented in a limited number of construction projects, it is necessary to conduct further studies to assess the effectiveness and reliability of the proposed technologies on different types of projects such as residential building construction, industrial construction as well as heavy civil construction.

An important limitation of this dissertation refers to the non-implementation of the proposed technologies in the same construction project. This fact could limit the understanding of the real impact of those technologies on construction safety applications. Therefore, further studies that integrate both technologies in the same construction project and analyze their impact on safety-related tasks are necessary.

Despite both UAS and positioning technologies were deployed on a real construction environment to determine their usefulness for safety monitoring, only UASs technology was integrated into the current construction safety monitoring and hazard identification process. Further studies are required to integrate positioning technologies into the current safety monitoring and hazard identification process and evaluate its effectiveness.

Despite the multiples advantages of using UAS technologies for safety monitoring purposes on jobsites, limitations such as the difficulty of flying UAS indoors would affect the complete visualization of safety conditions as well as their assessment. Further studies are required to consider the use of other types of visualization technologies capable of obtaining a detailed visual representation of the indoor safety conditions.

Ultrasound-positioning system deployment could be affected by construction processes (e.g. demolition of walls or ceiling) that affect the physical integrity of the beacons. Further studies are necessary to understand the practical implications of using ultrasound-based location systems related to work-in-progress development in the construction site.

The parachute recovery system demonstrated to be a vital tool to reduce the risks associated with the UAS deployment over actives jobsites. Nevertheless, adverse weather condition including strong rain and wind could affect the parachute recovery system

capabilities to perform its intended tasks. Further studies are required to explore the risks associated with the use of such systems in real construction environments.

UAS-derived images were analyzed by safety managers to identify jobsite safety conditions. It means that the hazard identification process relies on the safety managers' experience in identifying such types of conditions. Further studies can be conducted to implement an automated hazard identification process using the UAS-derived visual assets to reduce the manual effort associate with this process

UASs and positioning technologies were implemented from the perspective of the traditional safety management approach, which consists of identifying safety nonconformities and deviations throughout the construction site. Thus, this approach doesn't consider the full usage of these technologies during the early stages of the construction project and workers' training. Further studies are required to combine UAS and positioning technologies with recent safety management approaches such as Resilience Engineering (RE) and Lean Proactive Indicators.

The dissertation presents two well-known technologies intended to enhance the current construction safety monitoring and hazard identification process. From one side, UASs offer a detailed visualization of the outdoor safety aspects. However, the complete visualization of indoor safety aspects is not possible to achieve using these vehicles together with positioning technologies. Therefore, it is necessary to perform further studies that integrate other types of technologies such as AR and VR to overcome such limitation.

6.4 References

Awolusi, I., Marks, E., Hallowell, M., Ibukun Awolusi, Eric Marks, and Matthew Hallowell. (2018). “Automation in Construction Wearable technology for personalized construction safety monitoring and trending : Review of applicable

devices.” *Automation in Construction*, Elsevier, 85(July 2016), 96–106.

Bolkas, D. (2019). “Assessment of GCP Number and Separation Distance for Small UAS Surveys with and without GNSS-PPK Positioning.” *Journal of Surveying Engineering*, 145(3), : 04019007.

Costin, A. M., Teizer, J., and Schoner, B. (2015). “RFID and BIM-enabled worker location tracking to support real-time building protocol control and data visualization.” *Journal of Information Technology in Construction*, 20(January), 495–517.

Ergen, E., and Akinci, B. (2007). “An Overview of Approaches for Utilizing RFID in Construction Industry.” *2007 1st Annual RFID Eurasia*, IEEE, 1–5.

Fazeli, H., Samadzadegan, F., and Dadrasjavan, F. (2016). “Evaluating the Potential of Rtk-Uav for Automatic Point Cloud Generation in 3d Rapid Mapping.” *ISPRS - International Archives of the Photogrammetry, Remote Sensing and Spatial Information Sciences*, 41B6, 221–226.

Gheisari, M., and Esmaeili, B. (2019). “Applications and requirements of unmanned aerial systems (UASs) for construction safety.” *Safety Science*, 118(May), 230–240.

Gheisari, M., Rashidi, A., and Esmaeili, B. (2018). “Using Unmanned Aerial Systems for Automated Fall Hazard Monitoring.” *Proceeding of Construction Research Congress 2018*, (Janicak 1998), 148–157.

Ghueisari, M., Irizarry, J., and Walker, B. N. (2014a). “UAS4SAFETY: The Potential of Unmanned Aerial Systems for Construction Safety Applications.” *Construction Research Congress 2014*, (2008), 140–149.

Ghueisari, M., Irizarry, J., Walker, B. N., Jalaei, F., Jrade, A., Gheisari, M., Irizarry, J., and Walker, B. N. (2014b). “UAS4SAFETY: The Potential of Unmanned Aerial Systems for Construction Safety Applications.” *Construction Research Congress 2014*, (2008), 140–149.

Irizarry, J., Gheisari, M., and Walker, B. N. (2012). “Usability Assessment of Drone Technology As Safety Inspection Tools.” *Journal of Information Technology in Construction (ITcon)*, 17(17), 194–212.

Irizarry, J., and Bastos, D. (2016). “Exploratory Study of Potential Applications of Unmanned Aerial Systems for Construction Management Tasks.” *Journal of Management in Engi-*

neering, 28(January), 1–10.

De Melo, R. R. S., Costa, D. B., Álvares, J., and Irizarry, J. (2017). "Applicability of unmanned aerial system (UAS) for safety inspection on construction sites." *Safety Science*, Elsevier Ltd, 98, 174–185.

De Melo, R. R. S., and Costa, D. B. (2019). "Integrating resilience engineering and UAS technology into construction safety planning and control." *Engineering, Construction and Architectural Management*, 26(11), 2705–2722.

Martínez-Carricondo, P., Agüera-Vega, F., Carvajal-Ramírez, F., Mesas-Carrascosa, F. J., García-Ferrer, A., and Pérez-Porras, F. J. (2018). "Assessment of UAV-photogrammetric mapping accuracy based on variation of ground control points." *International Journal of Applied Earth Observation and Geoinformation*, Elsevier, 72(June), 1–10.

Melo, R., and Costa, D. (2020). "Reducing the gap between work as done and work as imagined on construction safety supported by UAS." *8 th REA Symposium Embracing Resilience: Scaling up and Speeding up Kalmar, Sweden, June 24-27, 2019*.

Sanz-Ablanedo, E., Chandler, J. H., Rodríguez-Pérez, J. R., and Ordóñez, C. (2018). "Accuracy of Unmanned Aerial Vehicle (UAV) and SfM photogrammetry survey as a function of the number and location of ground control points used." *Remote Sensing*, 10(10).